The Synthesis and Characterization of Semicrystalline Polyimides

by

M. Heather Brink

Dissertation Submitted to the Faculty of Virginia Polytechnic Institute and State University in Partial Fulfillment of the Requirements for the Degree of

Doctor of Philosophy
in
Chemistry

Approved By:

James E. McGrath, Chair

R. G. Kander

H. Marand

J. S. Riffle

J. M. Tanko

April 1994
Blacksburg, Virginia

c.2

LD
5655
V856
1994
B757
c.2

The Synthesis and Characterization of Semicrystalline Polyimides

by

M. Heather Brink

Committee Chairman: James E. McGrath

Chemistry

(ABSTRACT)

Polyimides derived from 2,2-bis[4-(4-aminophenoxy)phenyl]-hexafluoropropane (BDAF) and pyromellitic dianhydride (PMDA) displayed a glass transition temperature (Tg) at 306°C and a melting point (Tm) near 470°C as measured by differential scanning calorimetry (DSC) with a heating rate of 10°C/min. The degree of crystallinity increased with decreasing molecular weight. The incorporation of 20 mole percent of the comonomer, hexafluoroisopropylidene-2,2-bisphthalic acid anhydride (6FDA), gave a Tm of 440°C that appeared to be stable 20°C above the melt.

A fluorinated diamine, 1,1-bis[4-(4-aminophenoxy) phenyl]-1-phenyl-2,2,2-trifluoroethane (3FEDAM), was synthesized in 80% yield from trifluoroacetophenone with a melting point of 169-170°C. The 3FEDAM-PMDA polyimide controlled to 30,000 g/mol with phthalic anhydride exhibited by DSC a Tg of 308°C and a Tm of 476°C. Similar to the BDAF based copolymer, the 3FEDAM-20%6FDA/80%PMDA-PA polyimide had a Tg of 286°C and a Tm of 440°C which appeared to show short term thermal stability above the Tm.

Three 1,4-bis(4-aminophenoxy)benzene (TPEQ) homopolyimides were synthesized with 3,3',4,4'-benzophenonetetracarboxylic dianhydride (BTDA), 3,3',4,4'-biphenylcarboxylic dianhydride (BPDA), and 4,4'-oxydiphthalic anhydride (ODPA). The Tg values were 255°C, 251°C, and 239°C for the TPEQ-BPDA-PA, TPEQ-BTDA-PA, and TPEQ-ODPA-PA polyimides, respectively. The TPEQ-ODPA-PA polyimide displayed the lowest Tm of 411°C. A series of TPEQ-ODPA polyimides of different molecular weights were synthesized using the Carother's equation and the monofunctional reagent, phthalic anhydride. The Tg values ranged from 214°C to 239°C for the 7.5K to the 30K polyimides. All the TPEQ-ODPA polyimides displayed an endotherm on the first heat of the DSC analysis. However, the 7.5K, 10K, and 15K polyimide also recrystallized upon heating.

Polyimide powders were directly synthesized via preparation of the poly(amic acid) followed by cyclodehydration by solution imidization. One requirement is the polyimide must be crystalline so that as the polyimide is formed it will crystallize and precipitate from solution as small particles in the range of 2-16 μm. The particle size may be controlled by the concentration of the solution, temperature, and drying process.

Dedicated to:

George A. Woodard, my grandfather

ACKNOWLEDGEMENTS

I would like to thank Dr. J. E. McGrath, Chairman of my program committee, for his patience, guidance, and support but most of all for having faith in me.

I would like to sincerely thank my committee members, Drs. J. S. Riffle, J. Tanko, H. Marand, and R. Kander, for their valuable suggestions and help throughout my education. In addition, Dr. Riffle provided me with insight and comfort during my graduate education. A special thanks goes to Dr. Marand for organizing my interview trip and arranging for Andy to pick me up at the airport. I would also like to thank Dr. T. Pickering for his patience while I worked on the patent disclosure and for taking time from his busy schedule to attend my dissertation defense.

Several people in my past have played an important role in my career in chemistry and deserve recognition. Mr. G. Thompson, my high school chemistry teacher, introduced me to the world of chemistry. Dr. M. Zerner, my honors general chemistry professor, for inviting me to participate in undergraduate chemistry research in his group. Dr. K. B. Wagener who both allowed me to join his research group and discover the wonders of polymer chemistry and also helped me select a graduate school. Dr. D. Schiraldi, my mentor during my internship at Hoechst Celanese, who helped to expand my knowledge in polymer chemistry as well as in life.

I wish to thank Andy Brink for being a loving husband and for his devotion, encouragement, and confidence in me.

I wish to extend my gratitude to:

Martin Rogers- For teaching me the fundamentals of polyimide synthesis and characterization and being the best labmate.

Don Brandom- For many discussions and help with the WAXS studies.

Tom Glass- For his friendly personality and willingness to help and guidance in NMR analysis.

Rick Bucher- For electrostatic prepregging.

Joel Lee- For discussions and help in mechanical testing.

Dr. Wilkes- For many discussions on my project and guidance on the characterization of semicrystalline polyimides.

Dr. Davis- For discussions on powders and use of the particle size analyzer.

TABLE OF CONTENTS

CHAPTER 1: SCOPE OF DISSERTATION 1

CHAPTER 2: LITERATURE REVIEW 3

2.1 Introduction 3

2.2 POLYIMIDE SYNTHESIS 4

2.2.1 Poly(amic acid) Synthesis 4
2.2.2 Bulk Imidization 13
2.2.3 Solution Imidization 16
2.2.4 Chemical Imidization 17

2.4 Molecular Weight Control Of Polyimides 21

2.5.1 Properties of Fluorinated Polyimides 26
2.5.2 Properties of Semicrystalline Polyimides 35

2.6 Composites and Processing 50

CHAPTER 3: EXPERIMENTAL 54

3.1 Solvents and Reagents 54

3.1.1 Solvents 54

3.1.1.1 1-Methyl -2-Pyrrolidone 54
3.1.1.2 Dimethyl Acetamide 54
3.1.1.3 o-Dichlorobenzene 54
3.1.1.4 Toluene 55
3.1.1.5 Deuterated Dimethyl Sulfoxide 55
3.1.1.6 Absolute Ethanol 56
3.1.1.7 Tetrahydrofuran 56
3.1.1.9 Glacial Acetic Acid 56

3.1.2 Monomers and Reagents 56

3.1.2.1 Pyromellitic dianhydride 56
3.1.2.2 Hexafluoroisopropylidene-2,2-bisphthalic acid anhydride 57
3.1.2.3 4,4'-Oxydiphthalic anhydride 57
3.1.2.4 3,3',4,4'-benzophenonetetracarboxylic dianhydride 58
3.1.2.5 3,3',4,4'-biphenylcarboxylic dianhydride 58
3.1.2.6 Phthalic anhydride 59

3.1.2.7 1,1-Bis(4-aminophenyl)-1-phenyl-2,2,2-trifluoroethane 60
3.1.2.8 1,4-Bis(4-aminophenoxy)benzene 60
3.1.2.9 2,2,2-Trifluoracetophenone 61
3.1.2.10 Phenol 61
3.1.2.11 1-Fluoro-4-nitrobenzene 62
3.1.2.12 Trifluoromethanesulfonic acid (triflic acid) 62
3.1.2.13 Potassium Carbonate 63
3.1.2.14 2,2-bis[4-(4-aminophenoxy)phenyl] hexafluoropropane 63
3.1.2.15 LaRC TPI Polyamic Acid 63
3.1.2.16 Triton X-100 64

3.2.1 Two Step Procedure to the 1,1-bis[4-(4-nitrophenoxy)phenyl]-1-phenyl-2,2,2-trifluoroethane (3F-Dinitro) Precusor 65

3.2.1.1 Step 1 Preparation of bis(4-hydroxyphenyl) phenyl-2,2,2-trifluoroethane (3F-bisphenol) 65
3.2.1.2 Step 2 Formation of (1,1-bis[4-(4 nitrophenoxy)phenyl]-1-phenyl-2,2,2-trifluoroethane) (3F-Dinitro) Precursor Via a Nucleophilic Aromatic Substitution Reaction With the 3F-Bisphenol 66

3.2.2 One Step Procedure to (1,1-bis[4-(4-nitrophenoxy)phenyl]-1-phenyl-2,2,2-trifluoroethane) (3F-Dinitro) Precursor 67

3.2.2.1 Hydroxyalkylation Reaction With Nitrophenyl phenyl ether 67

3.2.3 Preparation of 1,1-bis[4-(4-aminophenoxy)phenyl]-1-phenyl-2,2,2- trifluoroethane (3FEDAM) Via Hydrogenation of the 3F-Dinitro Precursor 68

3.3 Polymer Synthesis 69

3.3.1 Molecular Weight and Endgroup Control for Step Growth Polymerizations 69
3.3.2 Formation of Poly(amic acid) 74
3.3.3 Cyclodehydration 76

3.3.3.1 Bulk Imidization 76
3.3.3.2 Solution Imidization 77

3.4 Preparation of Polyimide Powders 77

3.5 Characterization 78

3.5.1 High Performance Liquid Chromatography 78
3.5.2 Nuclear Magnetic Resonance Spectroscopy 78
3.5.3 Fourier Transform Infrared (FTIR) Spectroscopy 78
3.5.4 Potentiometric Titration 78
3.5.5 Intrinsic and Inherent Viscosities 79
3.5.6 Gel Permeation Chromatography 79
3.5.7 Thermal Analysis 79
3.5.8 Wide Angle X-ray Scattering 81
3.5.9 Solubility Tests 81
3.5.10 Particle Size Analysis 81
3.5.11 Polymer Density 82
3.5.12 Environmental Scanning Electron Microscopy 82
3.5.13 Sintering of Polyimide Powders 83
3.5.14 Mechanical Testing 83

CHAPTER 4: RESULTS AND DISCUSSION 84

4.1 Synthesis of the Fluorine Containing Monomers 84

4.1.1 Two Step Procedure to the 1,1-bis[4-(4-nitrophenoxy)phenyl]-2,2,2-trifluoroethane (3F-Dinitro) Precursor 85

4.1.1.1 Step 1 Preparation of 1,1-bis[4-(4-hydroxyphenyl)phenyl]-2,2,2-trifluoroethane (3F-Bisphenol) 87
4.1.1.2 Step 2 Formation of the 3F-Dinitro Precursor Via a Nucleophilic Aromatic Substitution Reaction 93

4.1.2 One Step Procedure to the 1,1-bis[4-(4-nitrophenoxy) phenyl]-1-phenyl-2,2,2-trifluoroethane (3F-Dinitro) Precursor 100

4.1.2.1 Hydroxyalkylation Reaction of Trifluoroacetophenone With 4-Nitrophenyl Phenyl Ether 100

4.1.3 Preparation of 1,1-bis[4-(4-aminophenoxy)phenyl]-1-phenyl-2,2,2-trifluoroethane (3FEDAM) Via Hydrogenation of the 3F-Dinitro Precursor 100

4.2 Polyimide Characterization 108

4.2.1 Synthesis of Polyimides 108
4.2.2 Molecular Weight and Endgroup Control 111

4.2.3 3FEDAM Based Polyimides....120

4.2.3.1 Homopolyimides Derived From 3FEDAM....120
4.2.3.2 Copolyimides Derived From 3FEDAM....127
4.2.3.3 Thermooxidative Stability of 3FEDAM Polyimides....131
4.2.3.4 Solvent Resistance of 3FEDAM Polyimides....131

4.2.4 BDAF Based Polyimides....136

4.2.4.1 Homopolyimides Derived From BDAF....136
4.2.4.2 Copolyimides Derived From BDAF....137
4.2.4.3 Other Polyimides Derived From BDAF....146
4.2.4.4 Solvent Resistance of BDAF Polyimides....146
4.2.4.5 Thermooxidative Stability of Polyimides....150

4.2.4.5.1 Short Term Thermooxidative Stability Studies of BDAF Polyimides....150
4.2.4.5.2 Long Term Thermooxidative Stability Studies of Polyimides....150

4.2.5 TPEQ (1,4-bis(4-aminophenoxy)benzene) Based Polyimides....154

4.2.5.1 Various Homopolyimides Derived From TPEQ....154
4.2.5.2 TPEQ-ODPA-PA Polyimide....157

4.2.5.2.1 Influence of Molecular Weight on Properties....157

4.3 Polyimide Powders....168

4.3.1 Preparation of Polyimide Powders....168
4.3.2 Particle Size Analysis....170

4.3.2.1 Density Measurements....170
4.3.2.2 Environmental Scanning Electron Microscopy....171

4.3.3 Parameters Influencing Polyimide Particle Size....171

4.3.3.1 Concentration of the Solution....171
4.3.3.2 Temperature....173
4.3.3.3 Polymer Molecular Weight....173
4.3.3.4 Particle Stabilization....176

4.3.3.4.1 Self Stabilization 176
4.3.3.4.2 Particles Stabilized by Ammonium Salts of Poly(amic acid) 178

4.3.3.5 Drying and Imidization of Particles 180

4.3.3.5.1 Percent Imidization of Particles 180
4.3.3.5.2 Drying of Particles 181

4.3.3.6 Suspension Concentration 185

4.3.3.7 Suspension Shelf-Life 186

4.3.4 Sintering 189

CHAPTER 5: CONCLUSIONS 194

CHAPTER 6: REFERENCES 198

LIST OF FIGURES

Figure 2.1: The Conventional Two-Step Method For the Preparation of Polyimides....5

Figure 2.2: A Mechanism For the Formation of the Poly(amic acid) 6

Figure 2.3: The Complexation and Decomplexation Process Proposed For Poly(amic acid)s In the Presence of NMP Solvent 8

Figure 2.4: Possible Reaction Mechanism for the Solution Imidization Process 18

Figure 2.5: The Residual Amic Acid Content and Intrinsic Viscosity As a Function of Reaction Time At 180°C 19

Figure 2.6: A Proposed Mechanism for Chemical Imidization 20

Figure 2.7: Dependence of Mechanical Strength on the Polymer Molecular Weight 22

Figure 2.8: Chemical Structure of Kapton (ODA-PMDA)....27

Figure 2.9: Chemical Structure of BDAF-PMDA 27

Figure 2.10: Repeat Units For 6F-PD (Avimid-N) and 3F-PD Polyimides 32

Figure 2.11: BTDA-3,3'-DDS Repeat Unit 36

Figure 2.12: The Repeat Unit of LARC-TPI 36

Figure 2.13: DSC Thermograms of the As-Received LARC-TPI....38

Figure 2.14: The Chemical Structure of NEW TPI 40

Figure 2.15: X-Ray Diffractograms of Polyimide Films....42

Figure 2.16: The Chemical Structure Representing ODPA (n=x) Polyimides....44

Figure 2.17: DSC Heat Capacity Curves Measured During Heating At 10K/min For ODPA (n=1) Polyimide After The Samples Had Been Annealed At 440K For Various Times....47

Figure 2.18: Repeat Unit of BTDA-DMDA Semicrystalline Polyimide 48

Figure 2.19: DSC Thermogram of BTDA-DMDA Polymer Sample After Quenching From 400°C 49

Figure 4.1: General Reaction Pathways to 1,1-bis[4-(4-aminophenoxy)phenyl]-1-phenyl-2,2,2-trifluoroethane (3FEDAM)....86

Figure 4.2: Proposed Mechanism for the Hydroxyalkylation Reaction of Trilfluoroacetophenone With Phenol 88

Figure 4.3: A Proposed Mechanism for the Hydroxyalkylation Reaction of Trifluoroacetophenone in the Presence of Triflic and Mercapto Acids....91

Figure 4.4: The 400 MHz Proton NMR Spectrum of 3F-Bisphenol....92

Figure 4.5: The FTIR Spectrum of 3F-Bispenol....94

Figure 4.6: Mass Spectrogram of 3F-Bisphenol 95

Figure 4.7: Synthesis of 1,1-bis[4-(4-nitrophenoxy)phenyl]-2,2,2-trifluoroethane (3F-Dinitro) Via Nucleophilic Aromatic Substitution Reaction....97

Figure 4.8: The 400 MHz Proton NMR Spectrum of 1,1-bis[4-(4-nitrophenoxy)phenyl]-2,2,2-trifluoroethane (3F-Dinitro)....98

Figure 4.9: The FTIR Spectrum of 1,1-bis[4-(4-nitrophenoxy)phenyl]-2,2,2-trifluoroethane (3F-Dinitro) 99

Figure 4.10: The Synthesis of 3F-Dinitro Via Hydroxyalkylation of Trifluoroacetophenone With 4-Nitrophenyl Phenyl Ether 101

Figure 4.11: The Synthesis of 3FEDAM Via Catalytic Hydrogenation of 3F-Dinitro....102

Figure 4.12: The 400 MHz Proton NMR Spectrum of the Partial Hydrogenation of 3F-Dinitro to the 3FEDAM Compound....104

Figure 4.13: The 400 MHz Proton NMR Spectrum of 1,1-bis[4-(4-aminophenoxy)phenyl]-1-phenyl-2,2,2-trifluoroethane (3FEDAM): The Quantitative Hydrogenation of 3F-Dinitro Compound 105

Figure 4.14: The FTIR Spectrum of 1,1-bis[4-(4-aminophenoxy)phenyl]-1-phenyl-2,2,2-trifluoroethane (3FEDAM)....106

Figure 4.15: The 19Fluorine NMR Spectrum of 1,1-bis[4-(4-aminophenoxy)phenyl]-1-phenyl-2,2,2-trifluoroethane (3FEDAM)....107

Figure 4.16: The Synthetic Scheme For Fully Cyclized Polyimides 110

Figure 4.17: FTIR Spectrum of Fully Cyclized t-Butyl Phthalamide Endcapped 3FDAM-PMDA Polyimide 112

Figure 4.18: The 400 MHz Proton NMR Spectrum of the 20,000 g/mol 3FDAM-PMDA Polyimide Endcapped With t-Butyl Phthalimide 113

Figure 4.19: The 400 MHz Proton NMR Spectrum of 3FDAM 116

Figure 4.20: WAXS Analysis of 3FEDAM-PMDA Polyimide 122

Figure 4.21: The First Heat Thermogram of 3FEDAM-PMDA-PA (30K) 123

Figure 4.22: The Second Heat Thermogram of 3FEDAM-PMDA-PA (30K) 125

Figure 4.23: WAXS of 3FEDAM-PMDA-PA (30K) 126

Figure 4.24: DSC Analysis of 3FEDAM-20% 6FDA/80% PMDA-PA (30K) 129

Figure 4.25: WAXS Analysis of 3FEDAM-6FDA/PMDA-PA Copolyimides: The Influence of Comonomer Concentration on Crystalline Order 130

Figure 4.26: Dynamic TGA of 3FEDAM-PMDA-PA (30K) Polyimide 133

Figure 4.27: Short Term (24 hours) Isothermal TGA at 371°C of 3FEDAM-PMDA-PA (30K) Polyimide 134

Figure 4.28: First Heat DSC Thermogram of BDAF-PMDA-PA (30K) Polyimide 138

Figure 4.29: First Heat DSC Thermogram of Different Molecular Weight BDAF-PMDA Polyimides 139

Figure 4.30: TMA Analysis of BDAF-PMDA-PA (30K) Polyimide 140

Figure 4.31: DSC Thermogram of BDAF-20% 6FDA/80% PMDA-PA (30K) 144

Figure 4.32: WAXS Analysis of BDAF-PMDA-PA Polyimides: The Effect of Molecular Weight on Crystalline Order 145

Figure 4.33: WAXS Analysis of Uncontrolled Molecular Weight BDAF-PMDA Polyimide 147

Figure 4.34: Typical Dynamic TGA of BDAF-PMDA-PA (30K) Polyimide 151

Figure 4.35: Isothermal TGA of BDAF-PMDA-PA (30K) Polyimide for 24 Hours at 371°C in Air 152

Figure 4.36: Thermooxidative Stability Study of Polyimides at 316°C (600°F) 153

Figure 4.37: Thermooxidative Stability Study of Polyimides at 371°C (700°F) 155

Figure 4.38: DSC Analysis of TPEQ-BPDA-PA (30K) Polyimide.....158

Figure 4.39: DSC Analysis of Three Lower Molecular Weight.....161

Figure 4.40: WAXS Analysis of 15K TPEQ-ODPA-PA Polyimide.....162

Figure 4.41: First Heat DSC Thermograms of TPEQ-ODPA-PA Polyimides.....163

Figure 4.42: DSC Analysis of TPEQ-ODPA-PA (15K) Polyimide At Various Times in the Melt.....167

Figure 4.43: ESEM of BDAF-PMDA-PA (30K) Polyimide Powder.....172

Figure 4.44: TGA Analysis of TPEQ-ODPA-PA (30K) Powders Synthesized at Different Temperatures.....182

Figure 4.45: Sample Preparation For Sintering and Mechanical Testing 190

LIST OF TABLES

Table 2.1: Electron Affinity (EA) Values For Several Commercially Available Dianhydrides 10

Table 2.2: 15N NMR Chemical Shifts of Several Diamines 11

Table 2.3: The Molecular Weight of the Poly(amic acid)s and the Tensile Properties of the Corresponding ODA/mPD-BTDA Polyimide Copolymers 23

Table 2.4: The Dielectric Properties of Polyimides Prepared From BDAF 29

Table 2.5: Thermal Stability (10% Wt. Loss) of Polymers Prepared From DABTF....34

Table 2.6: The Thermodynamic Properties of ODPA (n=x) Polyimides 45

Table 4.1: The Influence of the Type of Acid and the Concentration of Acid on the Percent Yield of 3F-Bisphenol at Ambient Temperature For 12 Hours....89

Table 4.2: Elemental Analysis of the 3F Monomers....96

Table 4.3: Summary of the 3F Monomer Properties....109

Table 4.4: Molecular Weight Evaluation of 3FDAM-PMDA-tBuPa Polyimides Via NMR and Solution Viscosity 115

Table 4.5: Determination of Absolute Molecular Weights Via GPC With Universal Calibration of Soluble Polyimides....117

Table 4.6: Intrinsic Viscosity Values of Several Soluble Fluorinated Polyimides In NMP and Chloroform....117

Table 4.7: Intrinsic Viscosity Values of TPEQ-ODPA-PA Poly(amic acid)s....119

Table 4.8: Thermal Analysis Results of 3FEDAM-PMDA Homopolyimides....121

Table 4.9: Results of the Thermal Analysis of 3FEDAM-6FDA/PMDA-PA Copolyimides....128

Table 4.10: Thermal Treatment Study of 3FEDAM-6FDA/PMDA-PA (30K) Copolymers....132

Table 4.11: Solubility Study of 3FEDAM Based Polyimides 135

Table 4.12: Thermal Analysis Results of BDAF-6FDA/PMDA-PA (30K) Copolymers....141

Table 4.13: Thermal Analysis Results of BDAF/3FDAM-PMDA-PA (30K) Copolymers....143

Table 4.14: Thermal Analysis Results of BDAF-PMDA/ODPA Polyimides....148

Table 4.15: Solubility Study of BDAF Based Polyimides....149

Table 4.16: Thermal Analysis Results of TPEQ Based Polyimides....156

Table 4.17: Thermal Analysis Results of the TPEQ-ODPA-PA Polyimides-Second Heat Values....159

Table 4.18: Comparison of First and Second Heat Values for the Tm of TPEQ-ODPA-PA Polyimides....164

Table 4.19: The Relationship Between the Thermal Behavior of TPEQ-ODPA-PA (15K) Polyimide and Time in the Melt....166

Table 4.20: Crystallization Behavior of TPEQ-ODPA-PA (30K) Polyimide Powders....169

Table 4.21: The Influence of the Solution Concentration on the Size of BDAF-PMDA-PA (30K) Polyimide Particles....174

Table 4.22: The Effect of the Solution Imidization Temperature on the BDAF-PMDA-PA (30K) Particle Size....174

Table 4.23: The Relationship of Molecular Weight and Particle Size....175

Table 4.24: BDAF-PMDA-PA (30K) Particles Isolated in NEUTRAL Water....177

Table 4.25: BDAF-PMDA-PA (30K) Particles Isolated in BASIC Water....177

Table 4.26: The Influence of the Stabilizer on the Size of BDAF-PMDA-PA (30K) Particles....179

Table 4.27: The Effect of the Solution Imidization Temperature on the Percent Imidization of the TPEQ-ODPA-PA (30K) Powders....183

Table 4.28:The Effect of Drying on the Particle Size....184

Table 4.29: The Influence of the Suspension concentration on the BDAF-PMDA-PA (30K) Particle Stabilization With Triton X-100 187

Table 4.30: The Shelf-Life of BDAF-PMDA-PA (30K) Particles Stabilized With Triton X-100 188

Table 4.31: The Shelf-Life of BDAF-PMDA-PA (30K) Particles Stabilized With The Ammonium Salt of the LARC TPI Poly(amic acid) 188

Table 4.32: Conditions for the Sintering Experiments of the TPEQ-ODPA-PA (30K) Particles 191

Table 4.33: The Moduli Values for the Sintered TPEQ-ODPA-PA (30K) Particles 191

Table 4.34: TGA Results of the Sintered TPEQ-ODPA-PA (30K) Particles 192

Table 4.35: DSC Analysis Results of the Sintered TPEQ-ODPA-PA (30K) Particles 192

CHAPTER 1: SCOPE OF DISSERTATION

This research has focused on three separate areas which include monomer synthesis, polymer synthesis and characterization, and powder preparation. A novel fluorinated diamine, 1,1-bis[4-(4-aminophenoxy)phenyl]-1-phenyl-2,2,2-trifluoroethane (3FEDAM), was developed in this research. This diamine which was based on trifluoroacetophenone which contains one trifluoromethyl group; therefore, it has been coined as a "3F" monomer. Two methods were utilized to synthesize the 3F monomer which will be discussed in the Experimental Section (Chapter 3). The Experimental chapter will also include the description of the various monomers and reagents used in this research along with the analytical procedures. Many common analytical techniques were utilized to fully characterize the novel diamine and its precursors and will be presented in the Results and Discussion Section (Chapter 4).

The second major area of focus was the synthesis and characterization of semicrystalline wholly aromatic polyimides. The most conventional method to prepare polyimides was employed in this research which consists of a two step procedure. The first step involves the synthesis of the poly(amic acid) from aromatic dianhydrides and aromatic diamines and subsequent cyclodehydration to form the polyimide which is described in the Experimental Section. Three different polyimide systems were investigated with the pertinent diamines being 2,2-bis[4-(4-aminophenoxy)phenyl]hexafluoropropane (BDAF), 1,4-bis(4-aminophenoxy)benzene (TPEQ), and 3FEDAM. The homopolyimides and copolyimides were characterized by various techniques and the results are discussed in the Results and Discussion.

Polyimide powder preparation was the third major thrust of this research which is a project in its infancy. A relatively facile method to directly prepare polyimide powders was developed during the latter stages of this thesis which is detailed in the Experimental Section. Several studies have been conducted to determine the ability to control particle size and the results are outlined in the Results and Discussion Section.

The dissertation begins with a review of the literature (Chapter 2) with particular emphasis on the topics pertaining to this research. The first part of the review describes the preparation of polyimides and the factors influencing the synthesis. The next section introduces the topic of molecular weight control. A section describing the properties of fluorinated and semicrystalline polyimides and a brief survey of composites and processing are included in the review.

CHAPTER 2: LITERATURE REVIEW

2.1 Introduction

In the last several decades, there has been a great interest in the use of polyimides for a variety of applications in many different areas. Aromatic polyimides are considered high performance materials due to their many outstanding properties which include high thermal and thermooxidative stability, excellent mechanical and electrical properties, and chemical resistance. Polyimides have been thoroughly investigated and there now a number of good books and reviews available (1-6).

It has been reported that polyimides may be synthesized by numerous procedures. Common methods are formation of the poly(amic acid) in solution from aromatic dianhydrides and aromatic diamines (7) or from esters of aromatic tetracarboxylic acids with aromatic diamines (8, 9) and subsequently cyclodehydrate chemically or thermally (7), melt polymerization of aromatic dianhydrides and aromatic diamines (10), and a direct (one step) synthesis of polyimides from aromatic dianhydrides or tetracarboxylic acids and aromatic diamines in high boiling solvents such as n-methylpyrrolidinone or m-cresol (11). Polyimides have also been synthesized from aromatic dianhydrides and aromatic diisocyanates (12), aromatic tetracarboxylic acid ester chlorides with aromatic diamines (13), displacement of an activated nitro group with a phenoxide anion (14), and transimidization (amine-imide interchange) (15-17). This review will concentrate on the most common synthetic route to polyimides which is the two step synthesis of polyimides via the precursor poly(amic acid) from aromatic dianhydrides and aromatic diamines. The next section will describe the importance of molecular weight and end group control followed by

the properties of fluorinated and semicrystalline polyimides. The last section will briefly introduce composites and processing.

2.2 POLYIMIDE SYNTHESIS

2.2.1 Poly(amic acid) Synthesis

Early workers (8, 18) synthesized aliphatic/aromatic polyimides by fusion of salts from aliphatic diamines and tetra-acids or diacid/diesters, which is similar to the well-known polyamide-salt technique. However, this method was unsuccessful for the preparation of wholly aromatic polyimides because the polyimides were infusible and the reduced basicity of the aromatic diamines precluded the formation of salts with tetra-acids. A more general method (7) was developed to prepare wholly aromatic polyimides via direct polymerization of an aromatic dianhydride and an aromatic diamine in solvent to form high molecular weight poly(amic acid). The poly(amic acid) was subsequently cyclodehydrated to afford the polyimide as shown in Figure 2.1.

The formation of poly(amic acid)s from diamines and dianhydrides proceeds via nucleophilic substitution on the anhydride carbonyl carbon atom with the amine acting as the nucleophile as depicted in Figure 2.2. This is an equilibrium reaction in which the existence of the equilibrium between the amic acid groups and the diamine and dianhydride was proposed in 1908 (19). The reaction proceeds by a S_N2 mechanism in which the carboxylate group is eliminated. Unfortunately, this condensation by-product remains chemically attached to the product; therefore, it cannot be removed to drive the equilibrium reaction to completion. The reverse reaction can occur by the donation of the carboxyl proton to the amide. However, this reversal can be virtually eliminated

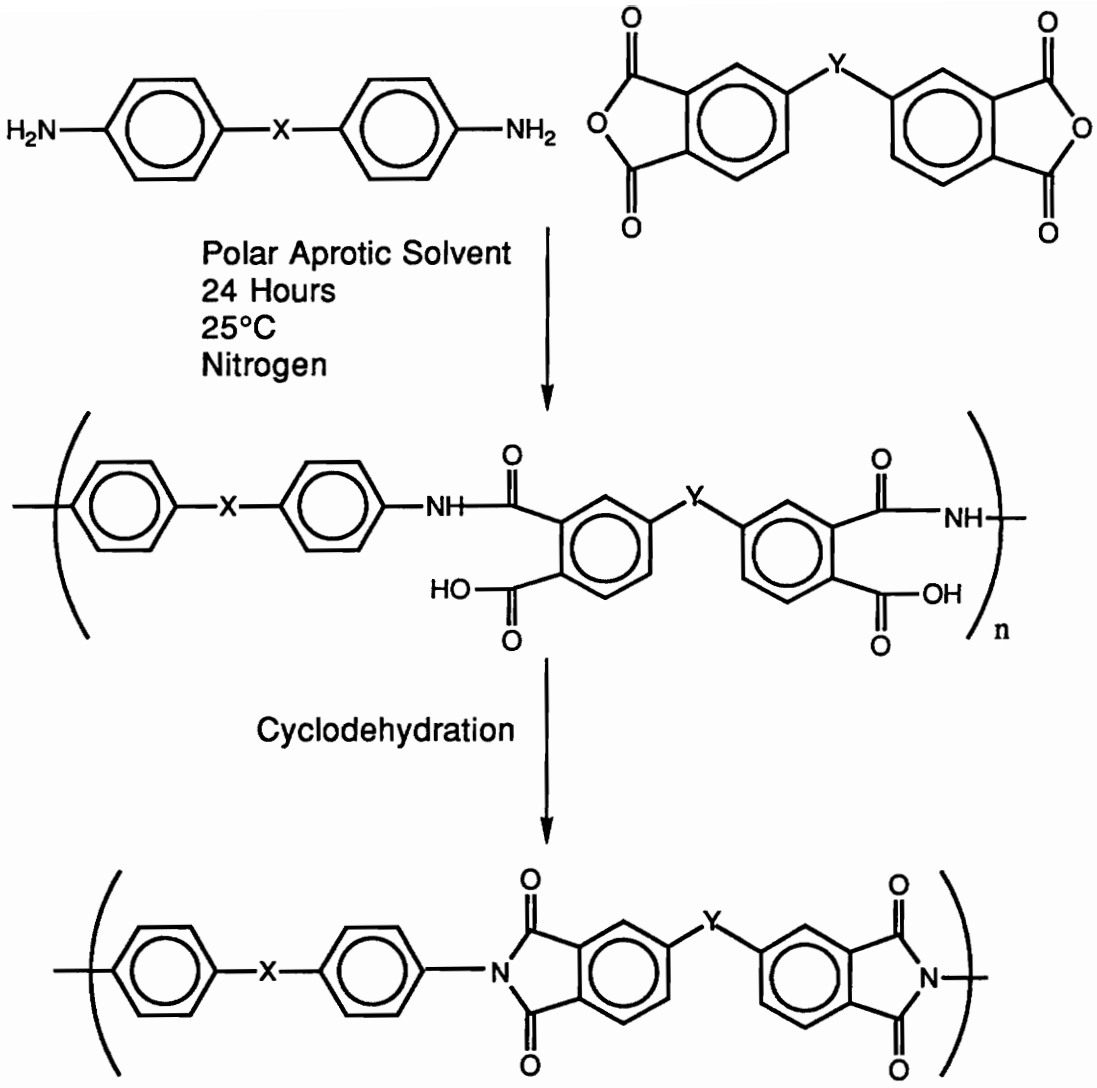

Figure 2.1: The Conventional Two-Step Method For the Preparation of Polyimides

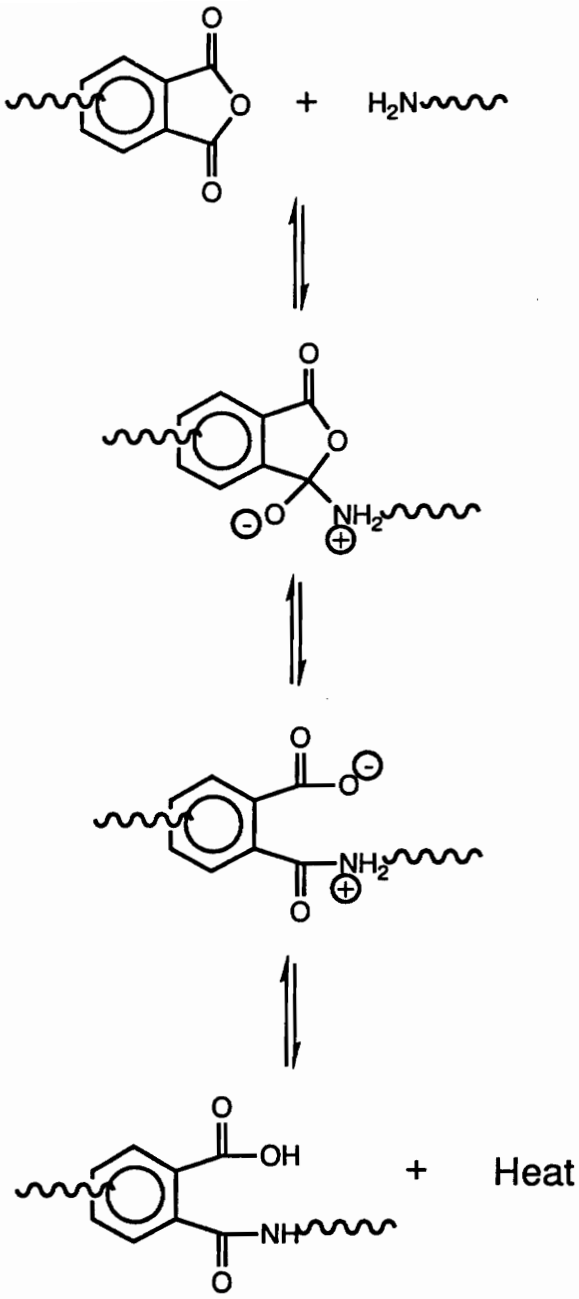

Figure 2.2: A Mechanism For the Formation of the Poly(amic acid) (2)

by complexation of the carboxyl proton, thereby, chemically removing the carboxylate group from the system. This has been shown to be the case in the presence of polar aprotic solvents such as 1-methyl pyrrolidone (NMP). Brekner and Feger (20, 21) have shown that poly(amic acid)s form complexes with polar aprotic solvents as shown in Figure 2.3. The complexes are due to strong hydrogen-bonding of the NMP with the acid and the amide yielding two types of complexes which have characteristic stoichiometric ratios of 1:4 and 1:2. Also, early workers (7) cited that the solvent, dimethyl acetamide (DMAC), was interacting with the carboxyl groups. The equilibrium constants of the formation of poly(amic acid)s in polar aprotic solvents at ambient temperature are in the range of 10^5 l/mol (22); therefore, it is possible to prepare high molecular weight poly(amic acid)s.

The reactivity of the monomers influences the equilibrium constant. Koton at al (23) investigated the kinetics of acylation of aromatic diamines by dianhydrides in amide solvents. The reaction rate constants for dianhydrides were compared to their electron acceptor properties. The reaction rate increases with increasing affinity for the electron by the dianhydride. The spectra of charge transfer complexes were used to evaluate the electron affinity (E_A) values of aromatic dianhydrides. The data showed that as the E_A increased the acylation rate was accelerated. The E_A of several dianhydrides are provided in Table 2.1 (2). PMDA displays the highest E_A of the commercially available dianhydrides and is highly reactive toward nucleophilic substitution.

The nature of the bridging group (23-25) of the aromatic dianhydrides affects the isomeric composition of the poly(amic acid). The percentage of

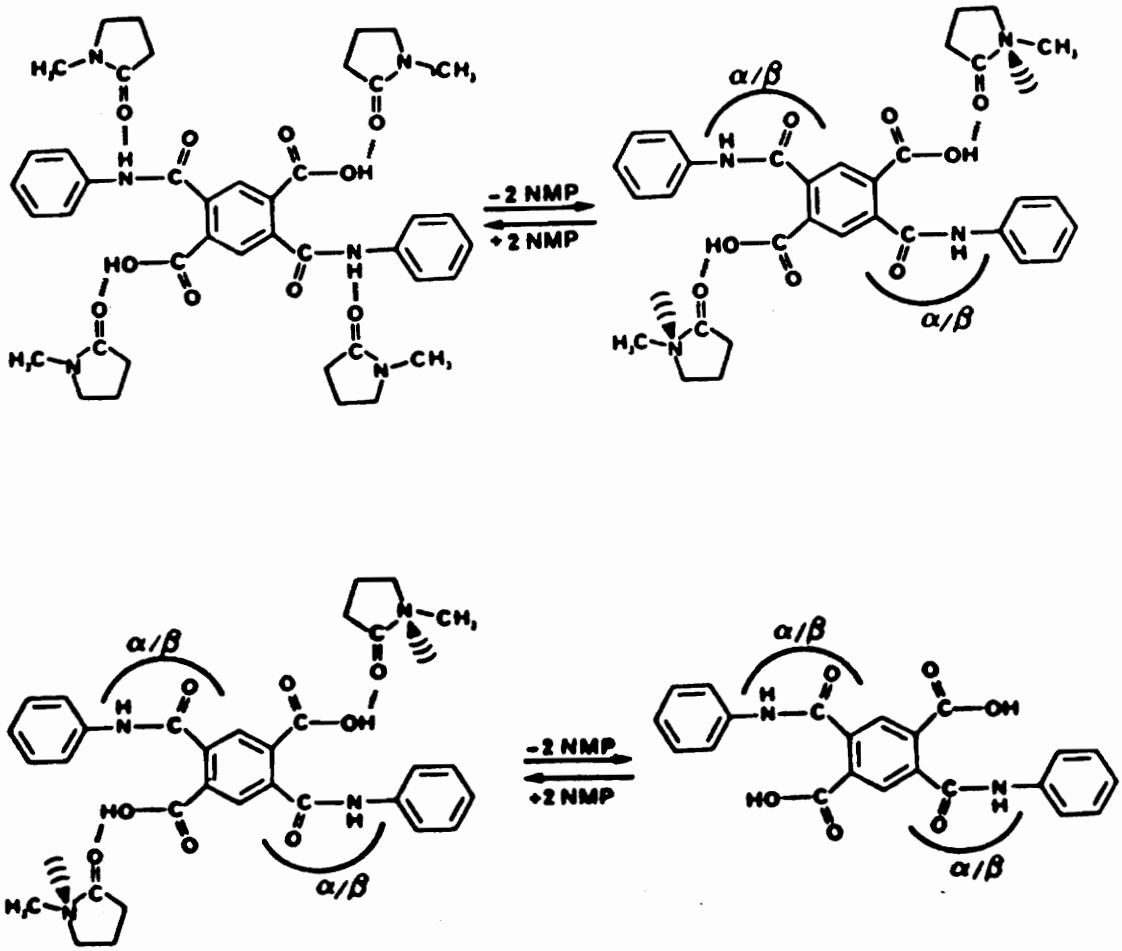

Figure 2.3: The Complexation and Decomplexation Process Observed For Poly(amic acid)s In the Presence of NMP Solvent (20, 21)

meta- and para- isomers has been calculated by ^{13}C NMR (25-27). The ratio of units with para- and meta- amide bonds increases with increasing electron acceptor character of the bridge.

The reaction rate constants for diamines were compared with their electron donor and basic properties (23). A linear relationship exists between the pKa values for diamines and the logarithm of the acylation rate constants indicating that the rate constants increase as the diamine becomes more basic. Ando and coworkers (26) used ^{15}N NMR chemical shifts to estimate the electronic properties of aromatic diamines. The NMR chemical shifts of the aromatic diamines are displaced according to their electron donor and electron acceptor properties which reflect their acylation rate constants. Table 2.2 (26) summarizes the ^{15}N NMR shifts of several aromatic diamines.

Heteroatom functional groups in the diamine and the dianhydride influence the imidization kinetics. Kim et al (25) investigated the effects of heteroatom electron-donating and -withdrawing bridging groups such as the ether link and sulfone link in the diamines and the dianhydrides on the imidization rate. They demonstrated that an electron-donating group (-O-) in the diamine component accelerated the rate of imidization due to the direct electronic effects on the amide nitrogen group effectively making it more basic. However, the effects of the dianhydride on the rate of imidization was relatively small as compared to those of the diamine component. Zubkov et al (28) also showed that the structural changes in the diamine affect the reaction rate more significantly than changes in the dianhydride.

Table 2.1: Electron Affinity (E_A) Values For Several Commercially Available Dianhydrides (2)

Dianhydride	Abbreviation	E_A (eV)
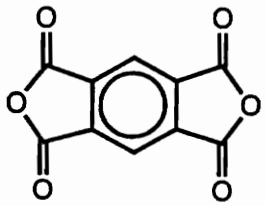	PMDA	1.90
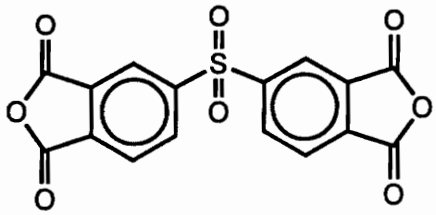	DSDA	1.57
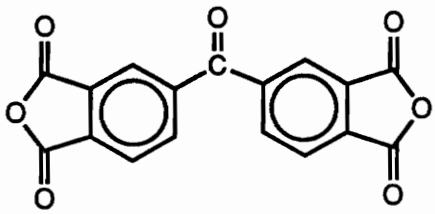	BTDA	1.55
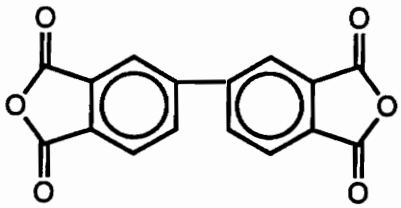	BPDA	1.38
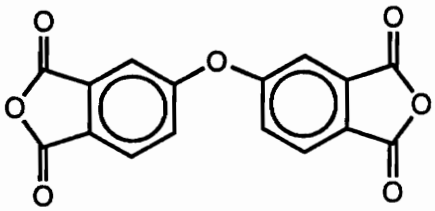	ODPA	1.30

Table 2.2: ^{15}N NMR Chemical Shifts of Several Diamines (26)

Diamine	Abbreviation	^{15}N Chemical Shift (ppm)
	pPD	53.8
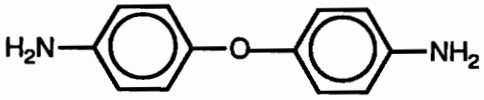	4,4'-ODA	57.9
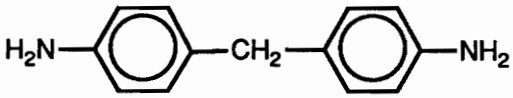	MDA	59.4
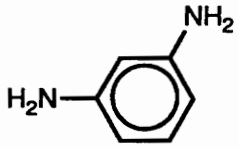	mPD	60.8
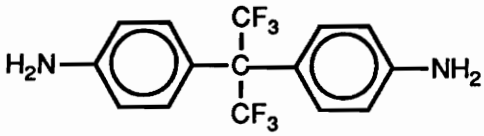	6F diamine	64.0
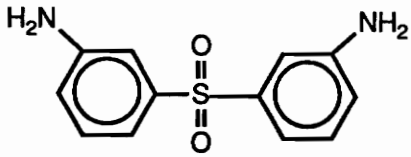	mDDS	65.7

The formation of the poly(amic acid) is an exothermic reaction at ambient temperature (22) as shown in Figure 2.2. Therefore, the equilibrium is shifted to the left with increasing temperature resulting in a lower molecular weight of the poly(amic acid) (18). High molecular weight can be achieved when the reaction temperature is lowered. However, as mentioned previously, basic aprotic solvents favor the formation of the poly(amic acid); therefore, decreasing the temperature does not show a significant change in molecular weight.

Traditionally, poly(amic acid)s were prepared by the addition of powdered dianhydride to a solution of diamine because the diamines are usually highly soluble and the dianhydride solutions are extremely sensitive toward hydrolytic degradation. Bower and Frost (7) reported that high molecular weight poly(amic acid) could only be achieved when the solid dianhydride was added to the solution of the diamine. The reverse order only resulted in low molecular weight species. However, Volksen and Cotts (19) found that the addition of the dianhydride first had no effect on the ultimate molecular weight probably because they rigorously purified reactants and solvents being sure to exclude moisture from the polymerizing system.

The most probable mechanism for the drop in weight average molecular weight (Mw) in solution is the cleavage of the amide link due to the catalytic effect of the carboxyl group in the ortho position followed by hydrolysis of the terminal anhydride group due to the presence of water in the system which is known as the amide interchange reaction (29). It was reported that direct hydrolysis of the amide bond does not readily occur. The molecular weight of an esterified poly(amic acid) does not significantly change in the solution during

storage which was attributed to the absence of the carboxyl proton. Hasegawa and coworkers (29) concluded from these results that the hydrolysis does not occur through direct hydrolysis of the amide linkages but through the acid catalyzed formation of the anhydride end groups. Bender et al (30) measured the rate constants of hydrolysis of phthalamic acid and benzamide in dilute acid. They found that the hydrolysis rate of phthalamic acid is faster than for benzamide by a factor of about 10^5. Therefore, they concluded that the mechanism of anhydride formation was predominant. Poly(amic acid) solutions were stored for long periods below 0°C without any apparent degradation (8). The stability of the poly(amic acid)s in solution at 23°C was dependent upon the polymer concentration. Dilute polymer solutions decreased in viscosity much more rapidly than the concentrated solutions (18). Elevated storage temperatures accelerated the decrease in viscosity and Mw (29).

2.2.2 Bulk Imidization

The most common method of cyclodehydration to convert poly(amic acid)s to polyimides is bulk or thermal imidization (5, 7, 18, 21, 31-33). First, the poly(amic acid) solutions are usually cast as a film, formed as a coating, or spun into a fiber (34-36). The processed poly(amic acid)s are thermally imidized by heating in the solid state to 250-400°C (22). The cyclodehydration is accomplished through nucleophilic attack on the acid carbonyl carbon by the free electron pair of the amide nitrogen with elimination of water. Bell et al (37) reported one of the most popular heating cycles which consists of one hour each at 100°C, 200°C, and 300°C. Bower and Frost (7) used a similar heating cycle in which 300°C was the maximum temperature.

The reaction kinetics and mechanism of the thermal imidization process is very complex and is still under extensive investigation. Many techniques have been utilized to study the thermal imidization process which include FTIR (31, 32, 38), thermogravimetric analysis and differential scanning calorimetry (32, 33), ^{1}H and ^{13}C NMR (39), viscosity (21), microdielectrometry (40), HPLC (41), UV-VIS (39), and FT-Raman spectroscopy (42). Numata and coworkers (33) followed imidization by measuring the weight losses via thermogravimetric analysis (TGA) that occurred during dehydrocyclization. The amount of imide cyclization and dehydrocondensation are stoichiometrically equal. Therefore, it was crucial to eliminate all factors that might contribute to weight loss. Numata developed a stringent procedure to remove the solvent from the poly(amic acid). The procedure involved casting a poly(amic acid) film followed by precipitation in distilled water. The film was cleaned 5 times in distilled water with an ultrasonic cleaner for 30 minutes each. The material was dried for 2 hours at 80°C under vacuum. Thermal decomposition gas chromatography showed the NMP content was less than 0.01%. FTIR analysis showed that only an extremely small amount of imidization had occurred. Most of the imidization occurred in the range of 150-250°C but the reaction was not complete until the temperature exceeded 250°C. The temperature at which the reaction was complete varied with the structure of the polyimides and likely correlated with the glass transition temperature.

The kinetics of solid-phase imidizations have been characterized by a "physicochemical process". Laius and Tsapovetsky (43) suggest that the physicochemical process consists of two stages. The first is a the physical stage which includes the diffusion of the amic acid groups into various

conformational states. The chemical stage is the second stage which involves the closure of the imide ring. The bulk imidization process is affected by many factors such as residual amount of solvent (44), film thickness (44), molecular mobility (33, 45), the physical state of the poly(amic acid) (43), the degree of imidization (31), and the occurrence of side reactions (21, 46-48).

Some researchers (48, 49) consider polyimides to be crosslinked which is responsible for insolubility rather than essentially linear materials. Kim et al (25) provided evidence for network formation involving imine branching and crosslinking for polyimide systems containing benzophenonetetracarboxylic dianhydride. Others (48) support the idea that diamidation causes branching and crosslinking producing insoluble polymers. Snyder et al (46) reported that the thermal curing of poly(amic acid)s to polyimides at low temperatures (150-200°C) resulted in the formation of cyclic imides and intermolecular (acyclic) imide linkages. However, the author was unable to provide convincing evidence from the infrared study to support the speculation of the formation of intermolecular imide linkages. Critchley et al (10) have attributed the insolubility of polyimides to the rigidity and the highly aromatic nature of the backbone. In the study of perfluoroalkylene-linked aromatic polyimides, the authors (10) cited that increasing incorporation of pyromellitimide units (PMDA) produced more rigid copolyimides which resulted in decreasing solubility. There is strong evidence (50) that PMDA units tend to form strong intermolecular bonds consistent with the presence of charge transfer complexes. The authors describe these strong interchain forces as physical crosslinks which subsequently impede solubility. Recent studies (10, 51) have shown that structural modifications to aromatic polyimides can produce highly soluble

systems in organic solvents. These examples of solubility suggest that at least some aromatic polyimides are not crosslinked, although in some cases semicrystalline morphologies may have been interpreted in this manner.

2.2.3 Solution Imidization

Soluble polyimides can be fully cyclized by the solution imidization technique (52-54). Solution imidization is conducted at temperatures in the range of 150-180°C in NMP which is considerably lower than that required for bulk imidization. Since the poly(amic acid) has more mobility in the solution than in the solid state, imidization can be accomplished at lower temperatures (52, 55-57). An azeotroping agent, such as o-dichlorobenzene or N-cyclohexyl pyrrolidone, can be added to the poly(amic acid) solution to remove the water formed upon cyclodehydration. The imidization is complete after 18 to 24 hours at 150-180°C. The system remains homogeneous for the duration of the imidization as long as the resulting polyimide is soluble in the polar aprotic solvent. Otherwise, of course, the polymer precipitates during the reaction before imidization is complete. The fully cyclized polyimide is normally isolated from the solution by precipitation in a nonsolvent such as methanol or water.

Polyimides prepared by the solution imidization technique do not generally suffer from side reactions such as crosslinking that may occur at the high temperatures required for bulk imidization. Arnold et al (55) have demonstrated that solution imidized polyimides were more soluble than bulk imidized polyimides.

Kim and coworkers (25) utilized solution viscosity measurements, NMR, and nonaqueous potentiometric titration to investigate the kinetics and

mechanism of the formation of fully cyclized polyimides by solution imidization. For the solution imidization, auto acid catalyzed second order kinetics were demonstrated. The reaction showed a dependence on the concentration and acid catalysis of the imidization process was observed. A concerted mechanism was proposed as depicted in Figure 2.4. The rate determining step was the nucleophilic substitution at the carboxyl carbon by the amide nitrogen.

Kim et al (25) provided direct evidence for partial degradation of the poly(amic acid) to the anhydride and/or o-dicarboxylic acid and amine endgroups. Figure 2.5 shows the relation of the % amic acid and the intrinsic viscosity with reaction time. The viscosity continually decreased to a minimum value. As the broken chains recombined, the viscosity began to increase. It was possible to achieve complete recombination and cycloimidization under the appropriate reaction conditions.

2.2.4 Chemical Imidization

Poly(amic acid)s can be chemically converted to the corresponding polyimide at ambient temperature by reaction with a dehydrating agent such as acetic anhydride and a basic catalyst such a pyridine or triethyl amine (22). The proposed mechanism for chemical imidization is shown in Figure 2.6. This method of imidization eliminates the reverse reaction by abstraction of the carboxylate proton by the basic tertiary amine. This converts the carboxylic acid to a stronger nucleophile which attacks the salt of the acetic anhydride. This yields an acetate group which is a better leaving group. Since the acetate

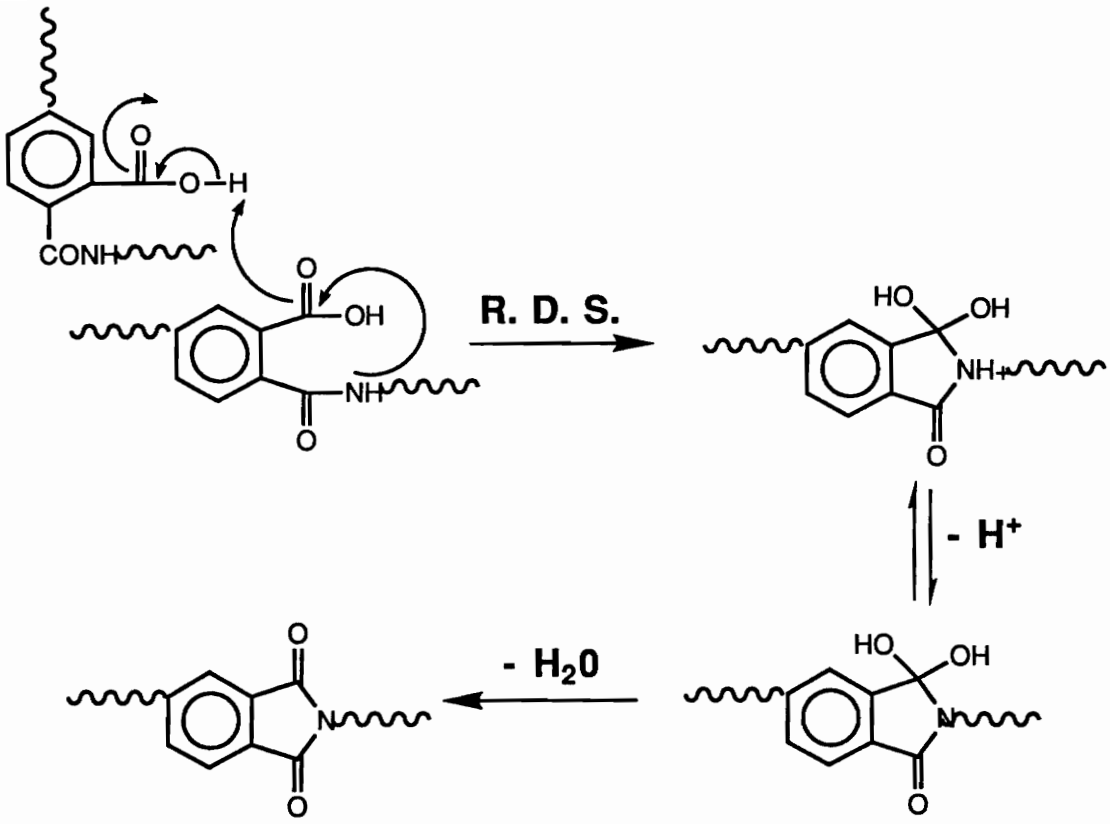

Figure 2.4: Possible Reaction Mechanism for the Solution Imidization Process (25) (RDS = rate determining step)

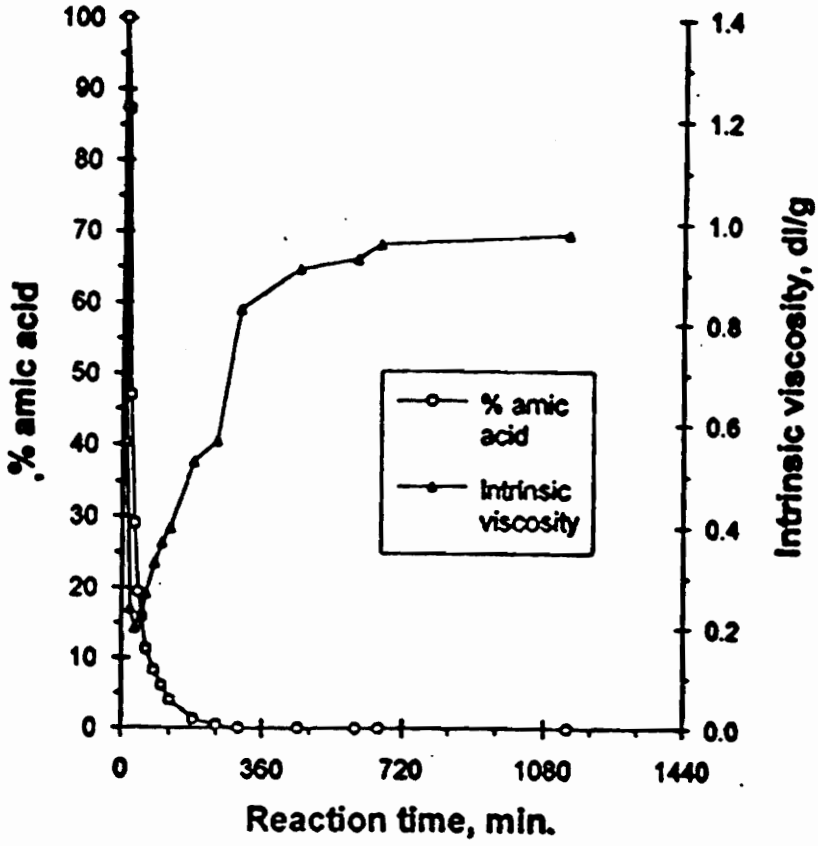

Figure 2.5: The Remaining Amic Acid Content and Intrinsic Viscosity As a Function of Reaction Time At 180°C (25)

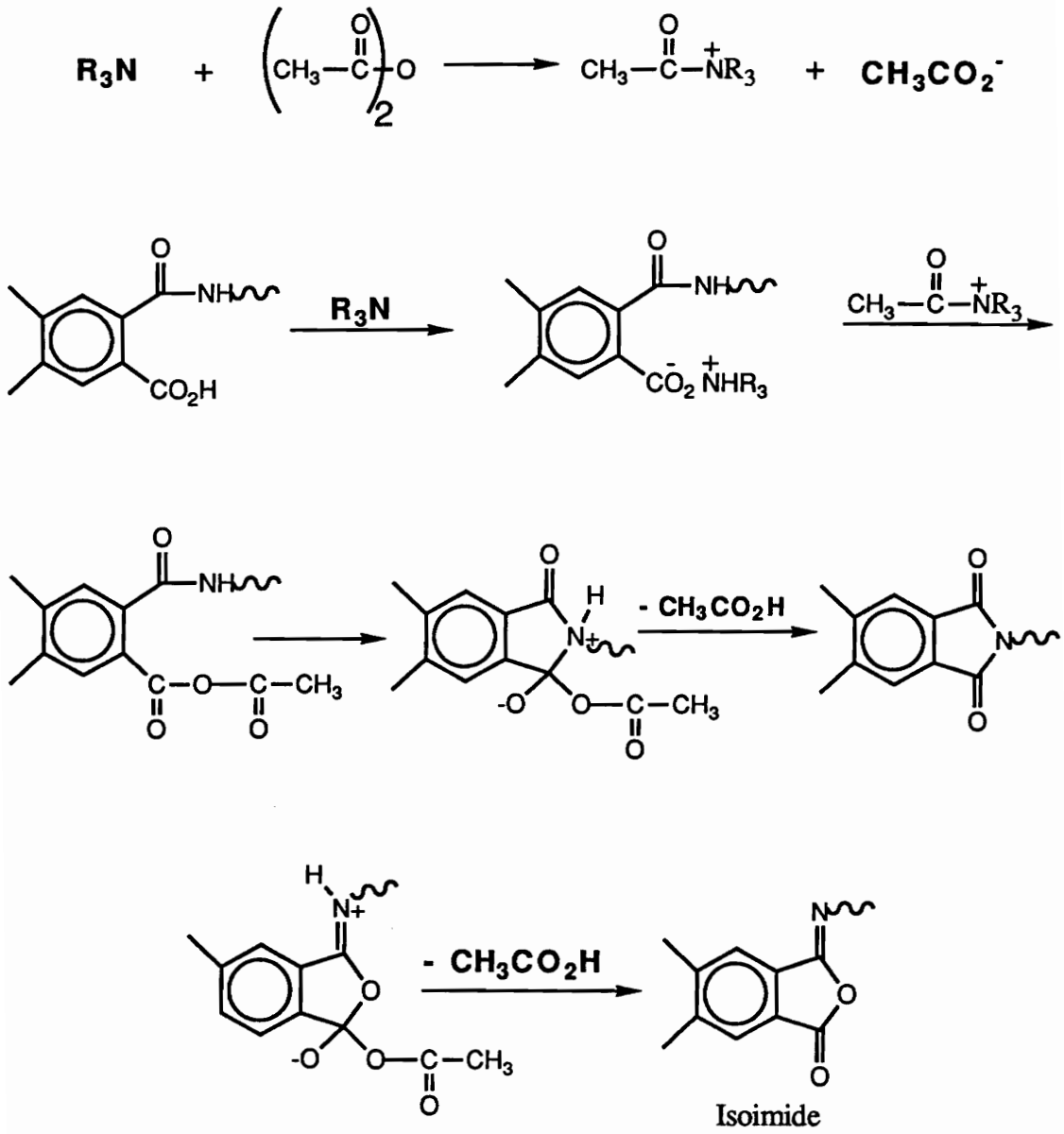

Figure 2.6: A Proposed Mechanism for Chemical Imidization (2)

group is an improved leaving group, the chemical imidization can be conducted at ambient temperature.

The two ring closed products that can form are the imide and the isoimide in which the former is thermodynamically favored and the latter is the kinetic product (2). The isoimide can be converted to imide when heated to elevated temperatures; therefore, chemically imidized polyimides must be briefly heated to near 300°C to convert the isoimide to imide and to ensure complete conversion to the imide form.

2.4 Molecular Weight Control Of Polyimides

Molecular weight (MW) is a very important parameter in determining the possible applications of a polymeric material. The interesting and useful mechanical properties associated with polymeric materials are a consequence of their high MW. Figure 2.7 (58) clearly demonstrates the dependence of the mechanical strength on the MW of the polymer. The strength increases rapidly with increasing MW until the critical molecular weight of entanglement of the polymer is reached. Weber and Gupta (59) conducted a detailed study on a series of commercial polyimide copolymers with different molecular weights. The study showed polymer thermal, mechanical, and solvent resistant properties directly correlated with the MW of the polyimide. As shown in Table 2.3 (59), the 8K polyimide had an elongation at break of 11% while the elongation at break of the 17K polyimide

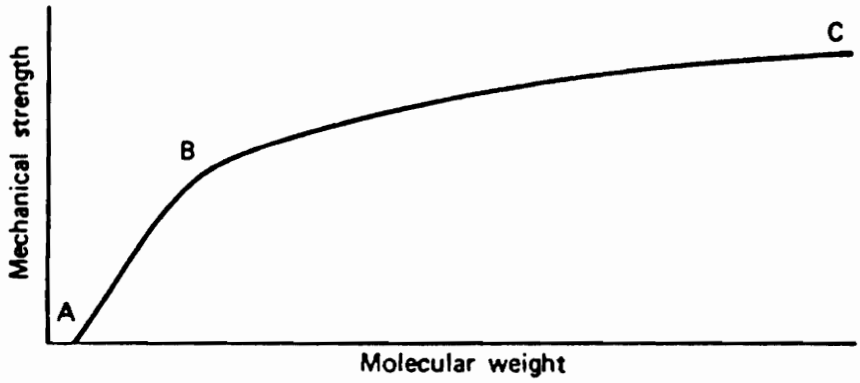

Figure 2.7: Dependence of Mechanical Strength on the Polymer Molecular Weight (58)

Table 2.3: The Molecular Weight of the Poly(amic acid)s and the Tensile Properties of the Corresponding ODA/mPD-BTDA Polyimide Copolymers (59)

SAMPLE	ODA/mPD (mol %)	MW (K) (g/mol)	E (Kpsi)	UTS (Kpsi)	e_B (%)	e_Y (%)
RC-2560	67/37	8	250	16	11	no yield
RC-2527	61/39	17	450	24	18	no yield
RC-2525	56/44	21	500	25	28	12
RC-4734	60/40	28	550	26	41	12

E: Elastic modulus
UTS: Ultimate tensile strength
e_B: Elongation at break
e_Y: Elongation at yield

was 18%. The low MW polyimides did not show yield points in their stress-strain curves whereas the higher MW materials displayed a yield point. Therefore, it was concluded that the high MW polyimides were more ductile. The high MW (21K and 28K) polyimides did not craze after exposure to NMP at 130°C for 8 hours.

Good physical and mechanical properties of polyimides are obtained for molecular weight values in the range of 20,000 to 30,000 g/mol. Once the critical molecular weight of entanglement has been obtained, there is only a moderate improvement in the mechanical properties with increasing molecular weight. Therefore, it is unnecessary to synthesize very high molecular weight polymers- that is far above the critical molecular weight of entanglement. At very high molecular weight, the polymer processability becomes extremely difficult because the melt viscosity is too high resulting in a reduction of melt flow. Rudin (60) discussed other examples describing the necessity of molecular weight control. For plasticized poly(vinyl chloride) sheeting in heat sealing applications, the molecular weight is very critical in determining the utility of the final product. At very high molecular weight, the material does not flow out sufficiently to weld well under the normal sealing conditions. However, if the molecular weight is too low, then the result is excessive thinning of the plastic weakens the strength of the weld area. Therefore, the control of molecular weight is very important for practical applications.

Polyimides with amine and anhydride endgroups can undergo chain extension, branching, or crosslinking during processing at elevated temperatures. Therefore, it is important to control the MW and the polymer chain endgroups to improve physical properties and enhance processability.

Scola (61) studied the influence of stabilization of reactive endgroups of the BDAF-6FDA polyimide. Several endcapping agents were utilized such as aniline, n-hexylamine, and phthalic anhydride. The properties evaluated were inherent viscosity, MW, Tg, thermal stability, and tensile and fracture toughness. The endcapped polyimides had lower inherent viscosities and MWs than the nonendcapped polyimides. This was expected because the nonendcapped polyimides most likely undergo chain extension during thermal imidization; therefore, increasing their MW. Endcapping the systems did not show deleterious effects on the thermal stability and mechanical and physical properties. In specific cases, the melt flow viscosity was reduced by orders of magnitude for the endcapped systems.

The problem of poor processability has recently been a major area of focus. McGrath et al (52, 55-57, 62) have employed MW and endgroup control techniques to overcome the problems associated with polyimides without sacrificing their many desirable characteristics. Molecular weight and/or endgroup functionalization can be achieved through simple stoichiometric control of monomers by following Carother's equation (58, 63, 64). For step growth polymerization of monomers A-A and B-B and B', A-A and B-B are difunctional monomers representing diamines and dianhydrides and B' has the same functional group as the B-B monomer but B' is monofunctional. A-A can only react with B-B or B'. A slight excess of A-A is used so that all the B-B is consumed leaving A endgroups. B' is able to react with A thus endcapping the chain.

.2.5 Properties Of Fluorinated And Semicrystalline Polyimides

2.5.1 Properties of Fluorinated Polyimides

Aromatic polyimides have found widespread use for many aerospace and microelectronic applications due to their excellent mechanical, electrical, and thermal properties. One of the most important commercial polyimides is the ODA-PMDA (Kapton™) polyimide shown in Figure 2.8. Kapton possesses many outstanding properties that include high Tg, high thermal stability, and good mechanical properties. However, Kapton, as well as many aromatic polyimides, suffers from two severe problems which are insolubility and infusibility. These difficulties in processing have limited this materials widespread use. In addition, Kapton has a somewhat high water absorption and high dielectric constant (DE) which minimizes its use in the microelectronics industry (65, 66).

To meet the increasing demands for high performance materials, the effects of structural modifications in the polyimide backbone have been extensively investigated (6, 67-69) to overcome infusibility, insolubility and improve the overall performance of polyimides. In 1967, Rogers (70) prepared polyimides from a fluorine-containing diamine with tetracarboxylic acid dianhydrides in an inert solvent at 175°C. The incorporation of fluorine in the polyimide backbone produced materials with reduced dielectric constant and moisture absorption. Since this discovery, numerous 1,1,1,3,3,3-hexafluorisopropylidene (6F) containing polyimides have been investigated (71). Cassidy and coworkers (72) have reviewed the literature of 6F based polymers.

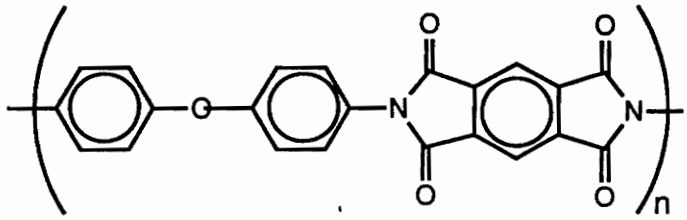

Figure 2.8: Chemical Structure of Kapton (ODA-PMDA)

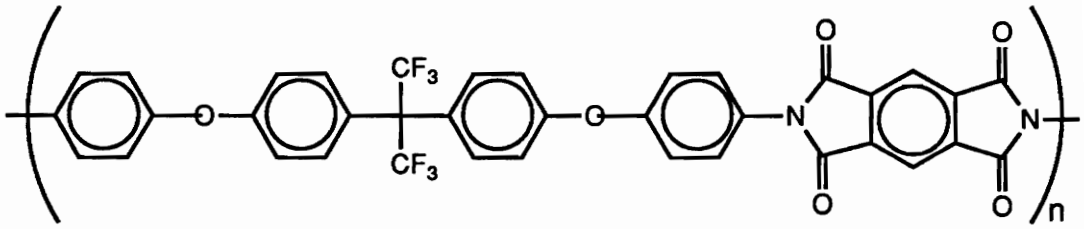

Figure 2.9: Chemical Structure of BDAF-PMDA

The polymer properties imparted by the inclusion of fluorine include decreased dielectric constant (DE) (7, 53, 58, 59), increased solubility (8, 73, 74, 62), improved thermal and thermooxidative stability (75-77, 62), enhanced optical transparency (74, 78, 79), and lower water absorption (74, 80, 81). Polyimides are being exploited for applications in the area of microelectronics which include fabrication aids, passivant overcoats and interlevel insulators, adhesives, and substrate components (82, 83). Consequently, the electrical and insulation properties are important. Most commercial polyimides have DE in the range of 3.2 to 4.0 which varies with moisture content. By the incorporation of fluorinated alkyl groups in the polyimide backbone, St. Clair and coworkers (84) were able to lower the DE to 2.4 to 2.8 and greatly improve the resistance to moisture. Later, Misra et al (85) confirmed these results in their study of the effect of different fluorinated segments on the DE. In addition, Misra showed that at comparable fluorine content, the fluorine bound to the aromatic rings was more effective in lowering the DE than the aliphatic fluorine (6F). Ruiz (80) also showed the advantage of fluorinated polyimide systems, BDAF-PMDA (Figure 2.9), as compared to conventional polyimides such as Kapton. The BDAF derived polyimides exhibited up to a 20% reduction in DE over Kapton. This reduction translates to faster signal speeds throughout the packaging material for advanced microelectronics. The change in DE with humidity for the BDAF-PMDA system was less than for the corresponding nonfluorinated system. St. Clair and coworkers (84) arrived at the same conclusions for water absorption. Table 2.4 summarizes the DE values obtained for BDAF based polyimides (86).

Table 2.4: The Dielectric Properties of Polyimides Prepared From BDAF (86)

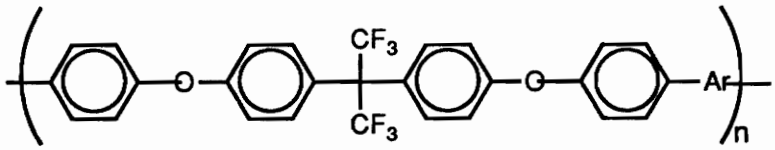

Dianhydride (Ar)	Abbreviation	DE at 10 GHz
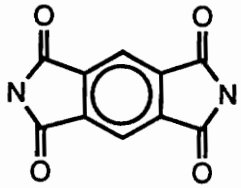	PMDA	2.63
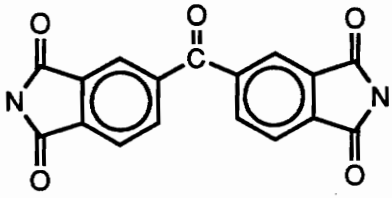	BTDA	2.74
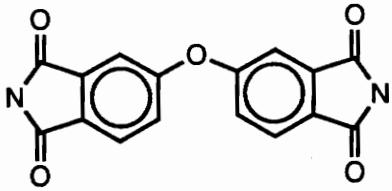	ODPA	2.68
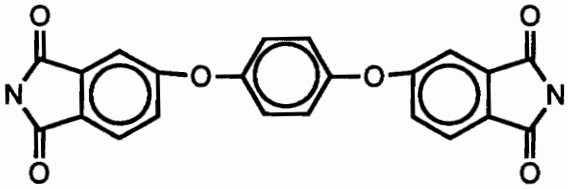	HQDEA	2.56
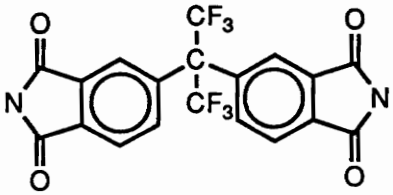	6FDA	2.50

Several factors are believed to contribute to the lowering of DE by fluorine incorporation. The presence of bulky fluorinated alkyl groups reduces interchain electronic interaction and may cause steric changes resulting in less efficient chain packing. This would lead to an increase in the free volume of the polymer; therefore, reducing the DE value. The strong electron withdrawing inductive effect of fluorine may decrease the electronic polarizability resulting in lowering the DE value. Another explanation was cited by Mercer and Goodman (65) who attribute a large part of the reduction in DE and moisture absorption to the total imide content. They suggest that the electronic polarizability of the imide group can induce high dipole moments. They observed a reduction in DE and moisture absorption up to a certain level (about 20%) of fluorine incorporation whereas increasing levels of fluorine did not significantly decrease DE and moisture absorption. Ichino et al (81) prepared polyimides containing fluorinated alkoxy side chains and showed that the DE and water absorption rate decreased with increasing fluorine content.

Thermal and thermooxidative stability of polyimides are important considerations when developing materials for high temperature applications. There is an increasing demand for polymers that are able to withstand elevated temperatures (316-400°C) for use in gas turbine engines, missiles, and in high speed civil transport (87). Fluorine containing poyimides had higher thermal stability than corresponding nonfluorinated systems (75). This result was attributed to the greater strength of the C-F bond compared to the C-H bond. Polyimides derived from BDAF were investigated to determine if the BDAF polyimides could replace commercially available condensation polyimides.

Since the BDAF diamine had a high molecular weight it would provide fewer imide linkages per repeat unit resulting in higher toughness, processability, and long-term hydrolytic stability. Initial studies (76) were conducted to asess the thermooxidative stability, Tg, and processability. A compression molded resin disc was made from BDAF-PMDA which reportedly had a Tg of 390°C as measured by thermomechanical analysis. The disc experienced a 20% weight loss upon isothermal aging at 675°F for 100 hours and 4 atmospheres of compressed air flow. Further investigations (76) showed that the BDAF-PMDA resins were 1) amenable to practical spray coating application techniques, 2) suitable for oxidative barriers and corrosion inhibiting coating at temperatures up to 700°F, and 3) promising as protective coatings for composites. The BDAF-PMDA protective coating adhered well to a variety of substrates and retained its adhesive properties at elevated temperatures over long time periods.

Scola (87) investigated the thermooxidative stability of polyimides derived from meta- and para- phenylene diamine in combination with 6F and 3F containing dianhydrides. At 1 atmosphere of circulating air at 371°C (700°F) for 100 hours, the 3F-pPD and 6F-pPD (Avimid N) polymers (Figure 2.10) displayed similar weight loss of 3%. However, a difference in their thermooxidative stability was evident at the same conditions as above except when 4 atmospheres of circulating air was used. The Avimid N (6F-pPD) exhibited less weight loss than the 3F-pPD. In addition, Scola (87) reported results on the importance of endcapping with relation to the thermal stability. The evidence suggested that the amine endcapped polymer chains

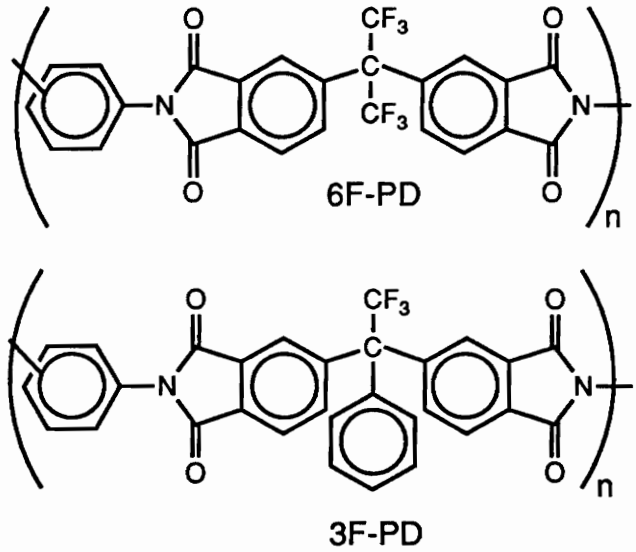

Figure 2.10: Repeat Units For 6F-PD (Avimid-N) and 3F-PD Polyimides (87)

underwent oxidative degradation at a much greater rate than anhydride endcapped polymer chains.

A series of polyimides were prepared from 3,5-diaminobenzotrifluoride (DABTF) with various dianhydrides (88). Their thermal stabilities were evaluated by dynamic thermogravimetric analysis at a heating rate of 2.5°C/min in static air. By comparing the temperatures at 10% weight loss, the order of stability was as follows: BPDA≈PMDA>ODPA≈BTDA>6FDA. See Table 2.5 for the temperature at which weight loss occurred. The low stability of the DABTF-6FDA polyimide was unexpected and the authors stated that this would be more thoroughly investigated. However, another independent thermal stability study (73) yielded the same results in that the 6FDA polyimide had the lowest thermal stability as evaluated in the same manner. Interestingly, after 500 hours at 316°C (600°F) in air, the 6FDA polyimide exhibited the greatest thermooxidative stability which confirmed the long accepted recognition of 6F derived polyimides having outstanding isothermal oxidative stability.

Another major advantage of fluorine incorporation in polymers is the improved solubility. St. Clair and coworkers (73) showed that 6FDA polyimides had greater solubilities than the corresponding polyimides containing BTDA or PMDA. New fluorinated polyimides from 2,2'-bis(trifluoromethyl)-4,4'-diaminobiphenyl (TFDB) have been synthesized (78, 89). The polyimides prepared with more flexible dianhydrides (ODPA, DSDA, and 6FDA) were soluble in m-cresol, NMP, and tetrachloroethane. The TFDB diamine has substituents in the 2 and 2' positions in the aromatic rings which force the rings into a noncoplanar structure. This results in a decrease in crystallinity and

Table 2.5: Thermal Stability (10% Wt. Loss) of Polymers Prepared From DABTF (88)

Dianhydride	Abbreviation	10% Wt Loss (°C)
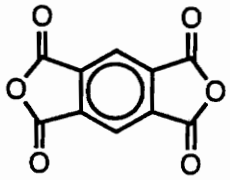	PMDA	570
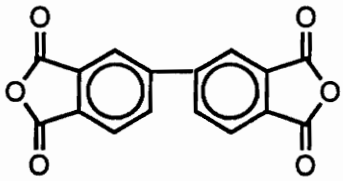	BPDA	572
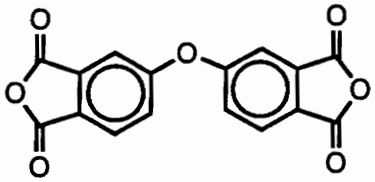	ODPA	558
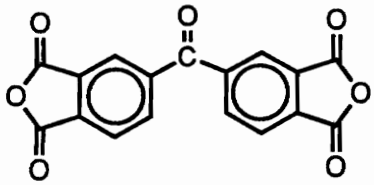	BTDA	551
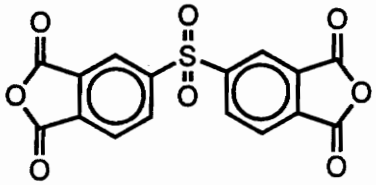	DSDA	525
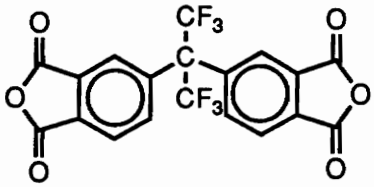	6DFA	511

increase in the solubility. In addition to the improved solubility imparted by TFDB, polyimides from TFDB have low DE (2.8 at 1MHz for TFDB-6FDA), water absorption, and high optical transparency. Aromatic imide model compounds with and without $-CF_2-$ flexible spacers were prepared (10). The compounds with the flexible spacers were readily soluble in organic solvents such as DMF, DMAC, and DMSO. However, the corresponding compounds without the flexible spacers were insoluble.

2.5.2 Properties of Semicrystalline Polyimides

Historically it was generally believed that most aromatic polyimides were amorphous. However, recent work (90, 97-98) has shown that limited crystallinity can occur for some materials especially when exposed to solvents. The fact that solvents induced crystallization of polyimides indicates that the usual lack of crystallinity may not be a result of the long accepted idea that polyimides have an inherent inability to form ordered crystals. According to Waddon and Karasz (91), the failure of polyimides to crystallize is a result of very low crystallization rates at normal crystallization temperatures. Bessonov and coworkers (6) have speculated on the very slow rates of crystallization of aromatic polyimides. To begin to understand the crystalliztion behavior of polyimides, Waddon and Karasz (91) embarked on a study of solution-grown crystals of a sulphonated aromatic polyimide (Figure 2.11) which has a relatively stiff chain. A multilayered, lath-like morphology was observed by transmission electron microscopy (TEM). The authors propose that the generation of this type of morphology was a consequence of the inflexibility of

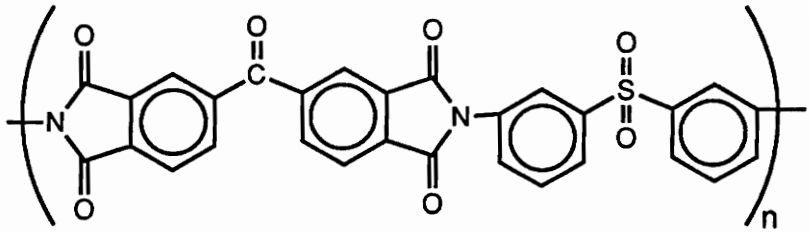

Figure 2.11: BTDA-3,3'-DDS Repeat Unit (91)

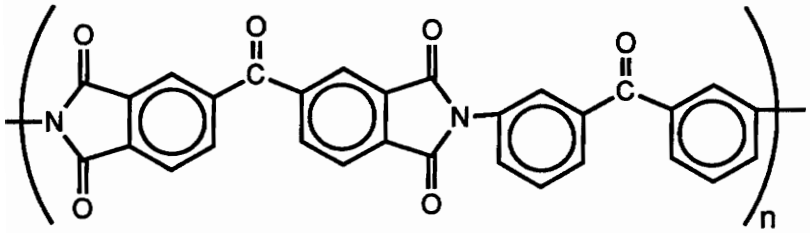

Figure 2.12: The Repeat Unit of LARC-TPI (94)

the polymer chain restricting the ability to readily fold. A thick, amorphous, lamellar surface region develops and the cilia nucleate other crystals instead of folding which produced the multilayers. This behavior has been observed for other rigid polymer systems such as poly(ether ether ketone) (PEEK), poly(phenylene sulphide) (PPS), and certain polyamides (92, 93).

Recent work (90) has shown that solvent-induced crystallization of aromatic polyimides is possible. Wang and coworkers (90) found that NMP solvent induced crystallinity of chemically imidized LARC-TPI polyimide (Figure 2.12) powders from the amorphous state at elevated temperatures. The orginal powders showed a Tm at 288°C on the first heat. No residual crystallinity was observed for the second heating scan indicating that the material was amorphous (Figure 2.13). Before exposing the LARC-TPI powders to NMP, their previous crystallinity was erased by heating the powders to 310°C in argon-filled sealed tubes for 20 minutes. These thermally treated LARC-TPI powders were analyzed by DSC to verify their amorphous nature (Figure 2.13-scan 3). Five LARC-TPI samples were exposed to different quantities of NMP at 200°C for one hour in sealed tubes. The DSC thermograms were different for each of the solvent treated samples which suggested that the NMP content affected the nature of the crystalline phases. To confirm the role of solvent in recrystallization of LARC-TPI, the solvent treated samples were heated to 360°C to erase all traces of crystallinity. The samples were treated with NMP again and the samples recrystallized. Another interesting point is that the LARC-TPI diplays a dual melting behavior in the presence of NMP. The ratio of the enthalpy of the high melting peak to the lower melting peak increased as

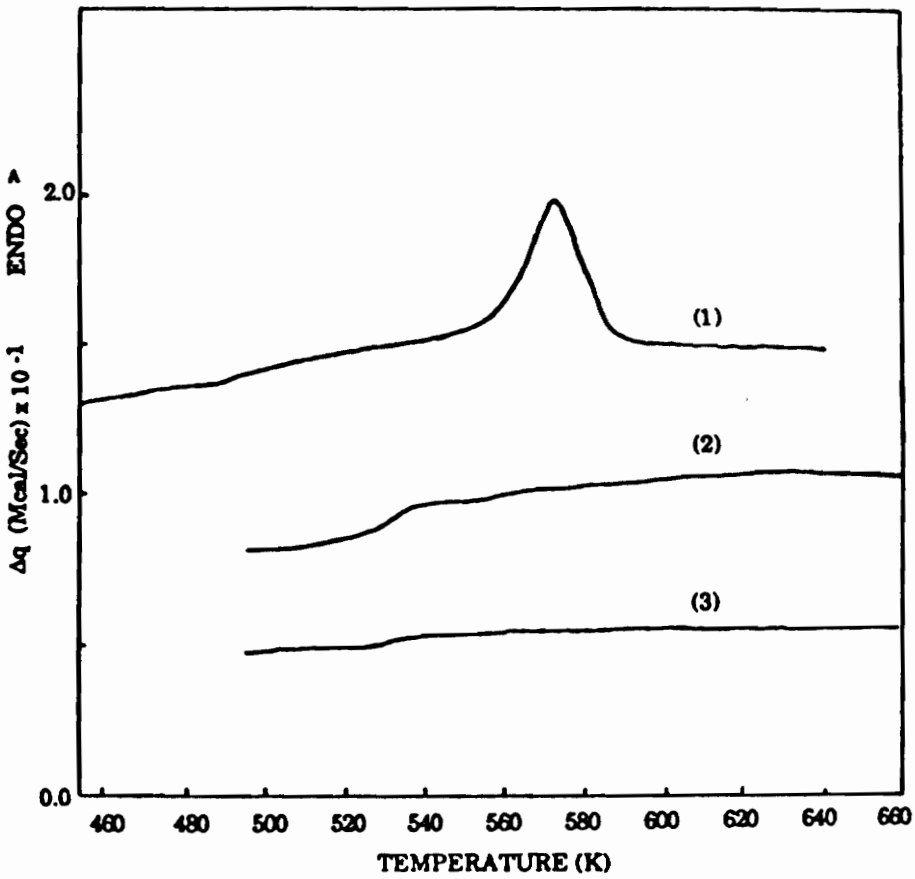

Figure 2.13: DSC Thermograms of the As-Received LARC-TPI: 1) First Heating Scan, 2) Second Heating Scan, 3) After 20 min at 310°C (90)

solvent content increased which is a reflection of the level of lattice defects in the crystal structure. This result is consistent with the work of Brekner and Feger (20, 21) such that the presence of solvent enhances the chain mobility allowing the perfection of the crystal structure.

The chemically imidized LARC-TPI powders displayed a single, broad crystal melting point at about 270°C as determined by DSC (heating rate of 10°C/min) and reordered to higher melting forms depending on thermal treatment (94). The crystallinity diminished at higher thermal treatments (>330°). WAXS analysis verified the crystalline morphology and the level of crystallinity was estimated at approximately 45%. Interestingly, the thermally imidized LARC-TPI polymer was amorphous. In addition, Hou and coworkers (95) showed that the crystalline nature was greatly dependent on the method of preparation of the powders.

The incorporation of aromatic rings provides many advantages such as high thermal stability. However, many aromatic polyimides undergo decomposition before the crystal melting point is reached. Therefore, many aromatic polyimides are extremely difficult to melt process and crystallize. One goal is to lower processing temperatures without compromising the beneficial properties. Synthetic methods to lower the transition temperatures include the incorporation of substituents onto the aromatic rings, introduction of rigid kinks, and addition of flexible units and/or meta linkages into the polymer backbone (96-101). Hou et al (102) used meta linkages in the preparation of NEW TPI (Figure 2.14) which has a Tg of 250°C and a Tm of 380°C as determined by DSC with heating rate of 20°C/min. However, the as-received film was

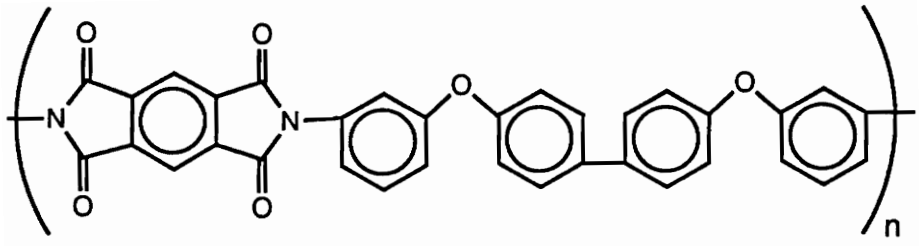

Figure 2.14: The Chemical Structure of NEW TPI (102)

transparent and amorphous as seen by DSC and WAXS. The cold crystallization kinetics of NEW TPI was studied as a function of crystallization temperature (Tc) and time (tc). The $t_{1/2}$, which is the time to reach 50% partial crystallinity, was used as an indicator of the crystallization kinetics. The fastest $t_{1/2}$ was 148 seconds, and by comparison PET and PES have values of a few seconds. Therefore, it was concluded that NEW TPI has relatively slow crystallization kinetics compared with other high performance thermoplastic polymers and these results are in agreement with those reported by Waddon and Karasz (91).

Crystallinity in polymers has been used to improve solvent resistance and increase the modulus. Semicrystalline polyimides prepared by the reaction of PMDA and BTDA with aromatic diamines containing carbonyl and ether linkages exhibited excellent chemical resistance and mechanical properties (97). After 72 hours of immersion, all the semicrystalline polyimides were unaffected by ethylene glycol (deicing fluid), jet fluid, hydraulic fluid, chloroform, and DMAC. In comparison, the amorphous samples quickly failed upon immersion in chloroform and DMAC. All the BTDA derived polyimides were semicrystalline and the results of the WAXS analysis suggested that they crystallized in the same crystal form as indicated by the 3 major reflections of the x-ray diffractograms as shown in Figure 2.15 (97). Flexible linkages depress thermal transitions which was illustrated by the polyimides derived from the 1,3-BABB diamine. When a rigid dianhydride like BTDA was used, the polyimide was semicrystalline. However, the ODPA-1,3-BABB polyimide was amorphous. The authors proposed that the increased flexibility of the ODPA

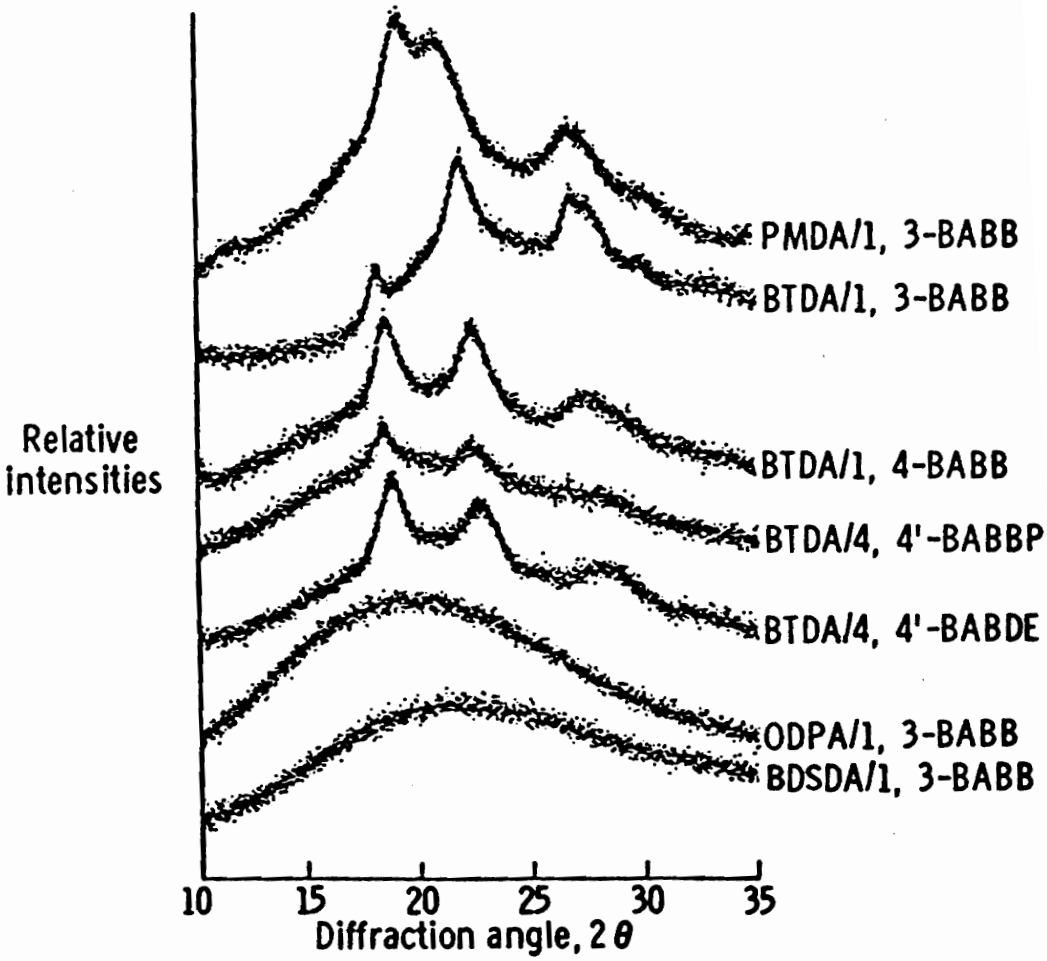

Figure 2.15: X-Ray Diffractograms of Polyimide Films (97)

dianhydride interfered with the packing of the arylene chains during conversion of the poly(amic acid) to polyimide; therefore resulting in a loss of crystallinity.

The crystalline morphology of a ODPA based polyimide containing flexible links was investigated (103-105). The degree of flexibility of the ODPA polyimides was varied by incorporation of different numbers of ethylene glycol units. The polyimide is denoted by ODPA (n=x) (Figure 2.16) where x represents the number of ethylene glycol units. It was discovered that there was a decrease in the time required to reach 5% weight fraction crystallinity with increasing number of ethylene glycol units-with increasing flexibility. The more rigid polymer chains (n=1) exhibit a higher viscosity and therefore slower molecular motion.

In many semicrystalline polymers, there is evidence for the existence of a rigid amorphous fraction (106, 107). This region lies between the crystal and the isotropic amorphous states. This interfacial region has been observed for the ODPA polyimides (108). The fraction is dependent upon the chain flexibility and crystallization conditions (103). As the chain flexibility and crystallization temperature increases, the amount of the rigid amorphous region is reduced.

The Tg is one of the critical parameters in determining the ultimate use temperature of a material. The structure and thermal history dependent enthalpy relaxation at the Tg was studied (104) for this series of amorphous ODPA (n = x) polyimides (Figure 2.16) with different chain flexibilities. The samples were heated above their equilibrium melting temperature, held for 2 minutes, and quenched to produce completely amorphous materials. Table 2.6 summarizes the thermodynamic properties of these ODPA polyimides. An

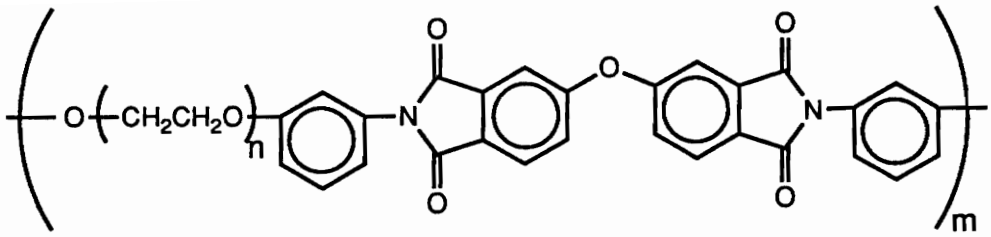

Figure 2.16: The Chemical Structure Representing ODPA (n=x) Polyimides (103)

Table 2.6: The Thermodynamic Properties of ODPA (n=x) Polyimides (104)

ODPA	Tg (K)[a]	ΔCp ($JK^{-1}mol^{-1}$)[a]	T_m^0 (K)[b]	ΔH_f^0 ($kJ\ mol^{-1}$)[b]
n = 1	450	182	613	72.5
n = 2	418	218	577	80.2
n = 3	385	254	541	88.0

[a] Data determined for 100% amorphous polyimides

[b] Data determined by extrapolating to 100% crystallinity of the polyimides

amorphous polymeric material experiences hysteresis in the region of the Tg which is caused by different cooling and heating rates during nonisothermal experiments. The effect of hysteresis was evaluated for the amorphous ODPA polyimides in which the samples were cooled at different heating rates from the supercooled liquid state to the glassy state. A quantitative relationship between the heat of fusion and the logarithm of the cooling rate was observed. The heat of fusion for a given cooling rate increased as the flexibility of the chain increased. In isothermal experiments, annealing of noncrystalline materials below the Tg results in physical aging behavior. This behavior was clearly demonstrated by the ODPA (n = 1) polyimides in which samples were annealed at 400K (50°C below Tg) for various times as illustrated in Figure 2.17. The peak temperature shifts to higher temperature and the enthalpy of the peak increases with longer annealing time. The Tg values of these ODPA polyimides were also influenced by the level of crystallinity. The Tg transitions were shown (105) to broaden toward higher temperatures during isothermal crystallization.

The characterization of semicrystalline polyimides provides invaluable insight into the structure-property relationships, aids in the improvement of processing methods, and the development of polyimide products. To contribute to the knowledge of polyimide crystalline nature, Cheng and coworkers (109) embarked on a study of a semicrystalline polyimide based on BTDA and 2,2-dimethyl-1,3-(4-aminophenoxy)propane (DMDA) (Figure 2.18). DSC analysis (Figure 2.19) showed that this polyimide was capable of recrystallizing upon heating as evidenced by the exothermic crystallization peak at 280°C. The

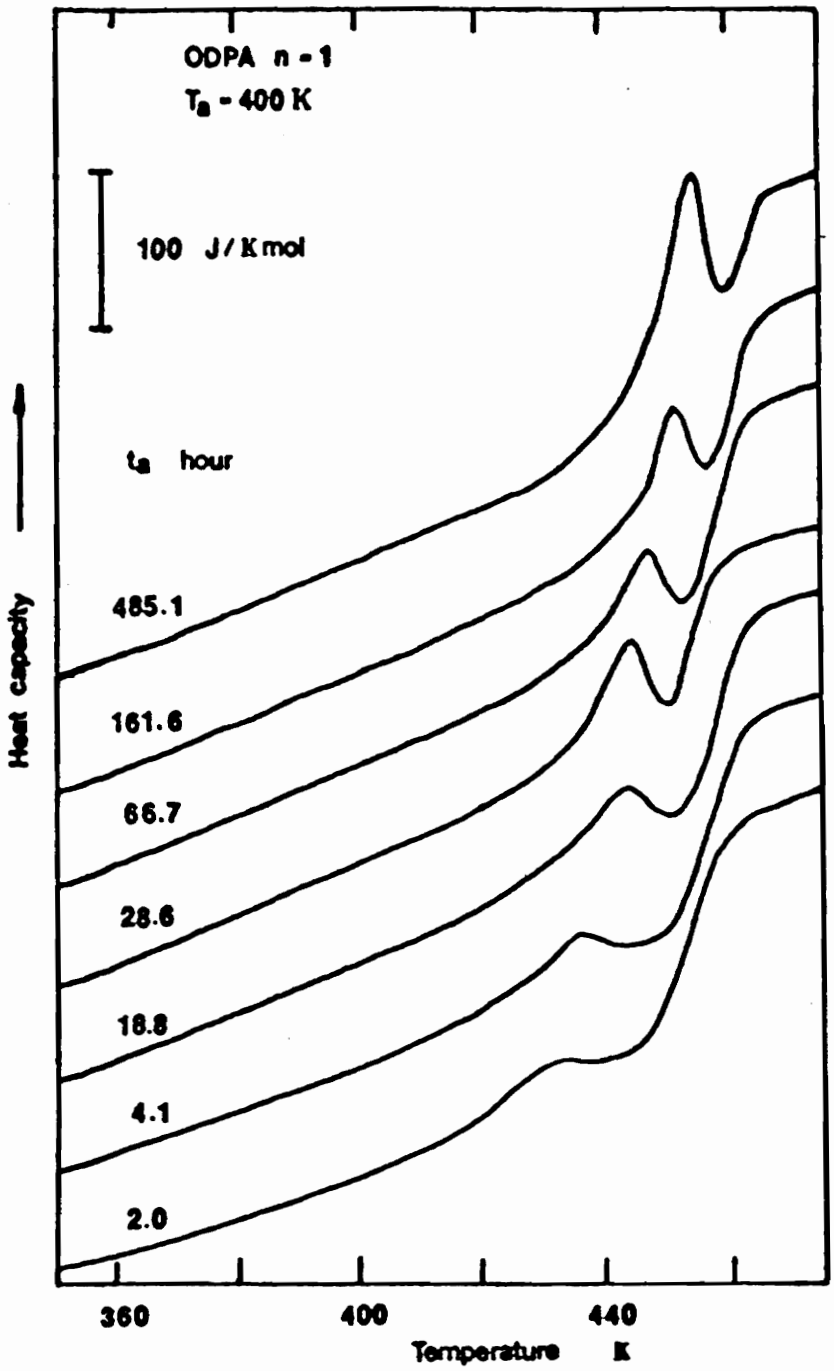

Figure 2.17: DSC Heat Capacity Curves Measured During Heating At 10K/min For ODPA (n=1) Polyimide After The Samples Had Been Annealed At 440K For Various Times (104)

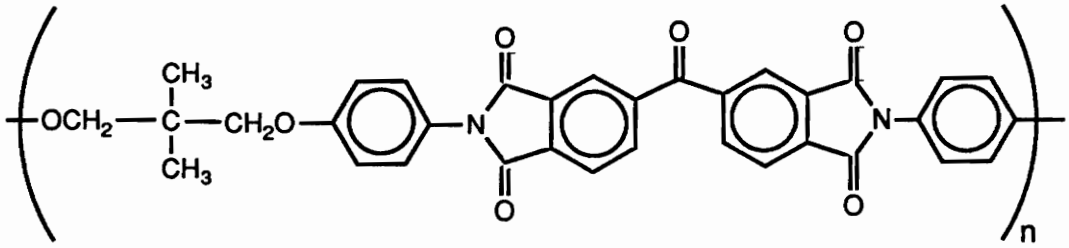

Figure 2.18: Repeat Unit of BTDA-DMDA Semicrystalline Polyimide (109)

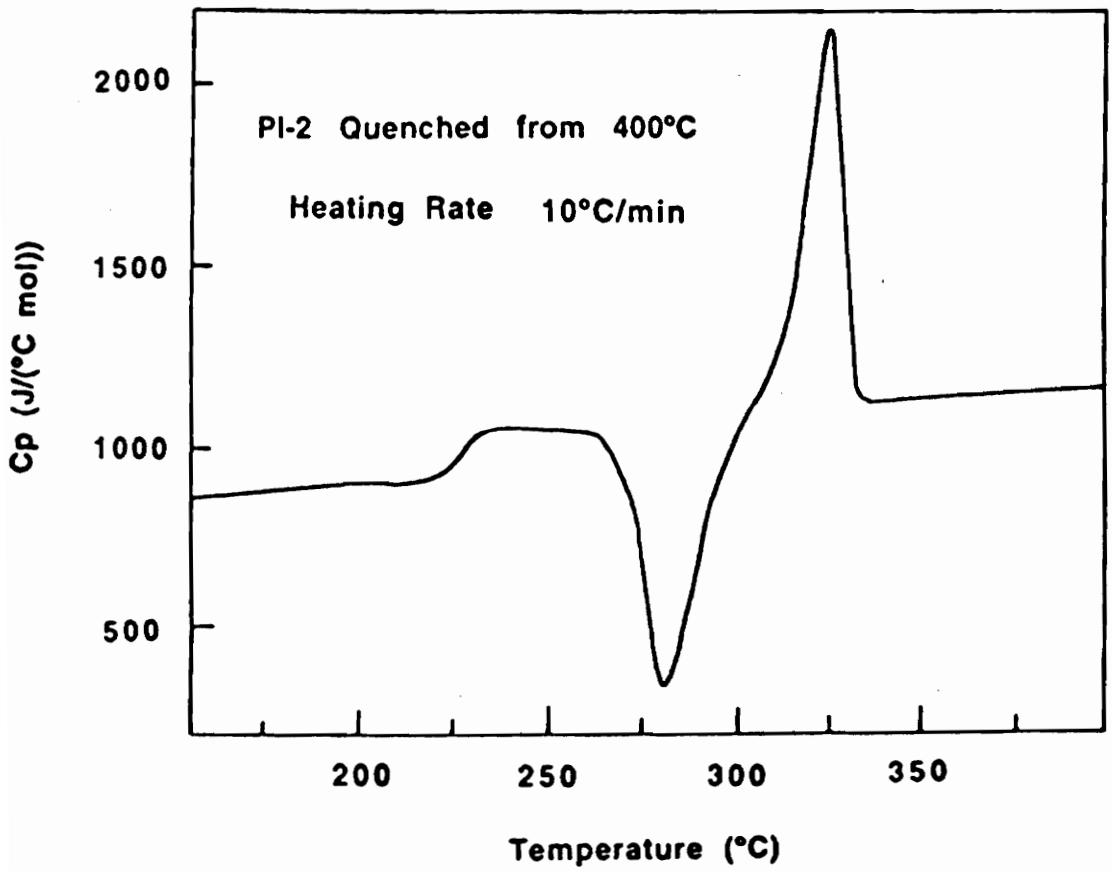

Figure 2.19: DSC Thermogram of BTDA-DMDA Polymer Sample After Quenching From 400°C (heating rate = 10°C/min) (109)

crystallization window, the difference between the Tg and Tm, is 105°C which is one of the lowest documented for commercial thermoplastic, semicrystalline polymers (PEEK has a 180°C crystallization window). This material has a relatively high Tg due to the methyl groups which increase the chain rigidity while maintaining sufficient chain regularity to permit the crystallization. BTDA-DMDA was annealed at high temperature for a long time which led to a second crystallline phase with a higher Tm of 360°C. Varying crystallization time did not significantly change the crystal sizes. In contrast to other polymers which show a decrease in Tg with increasing isothermal crystallization temperatures, the Tg of BTDA-DMDA remained constant after crystallization was completed. Therefore, it was concluded that morphological changes were not evident and the crystals did not become more perfect with increasing temperature and time.

2.6 Composites and Processing

Advanced polymer matrix composites are widely used in the aerospace industry. In addition, composites have found limited applications in the recreational, automotive, and industrial market. The utilization of composites is expected to increase if their cost can be lowered. Composites have potential to replace metals in many of their applications. This is due to the advantages of composites which include versatility and design flexibility, lower density, corrosion resistance, and high specific strength and modulus (110).

A composite is derived from two major components which are the reinforcing fiber and the polymer matrix resin. The matrix resin comprises about 30% to 40% by volume in high performance continuous fiber composites and

serves many functions including acting as the glue which binds together the composite components, protects the fiber, acts as a stress transfer medium, prevents fibers from buckling, and provides interlaminar strength. The polymer matrix resin may be a thermosetting polymer or a thermoplastic polymer. The thermosetting resins are currently the most widely used matrix resins and offer several advantages (110) such as availability, facile processing from oligomers, availability of equipment for processing, existence of a large database for commercially available resins, and low cost of materials. Thermoplastic resins possess many favorable qualities (110, 111) such as indefinite prepreg stability, reprocessing to correct flaws, fast processing cycle, high toughness, good damage tolerance, easy quality control. It is surprising that thermoplastic resins are not as widely used after viewing their attractive features, but thermoplastics suffer several disadvantages that have limited their popularity. The major problems associated with thermoplastic resins are that quality prepreg is difficult to produce, high temperatures and pressures are required, environmental stress cracking may occur, and a limited database is available (110).

Prepregging is the method for combining the matrix resin and the fiber. There are many types of prepregging which include hot melts (112), solutions (113, 114), dry powders (115, 116), and suspensions (117-120). The hot melt prepregging technique has limited use because the high molecular weight thermoplastic materials have high melt viscosities which makes it difficult to wet out all the fibers and results in fiber breakage. In addition, many high performance polymers degrade before the melting point is reached and, therefore cannot be melt processed. Most organic solvents needed to dissolve

high performance polymers are toxic and have high boiling points which make them difficult to remove during consolidation.

There are two primary powder coating techniques which are the "dry" coating (115, 116) and the "wet" coating (117-120). Dry powder coating of carbon fibers overcomes many of the inherent problems associated with melt, solution, and suspension prepregging. The major advantage of dry powder prepregging is the elimination of solvent. Powder coating can be accomplished by use of a fluidized bed with or without the aid of electrostatic deposition (115). The optimum particle size for dry powder prepregging is about 20 μm.

Wet powder prepregging, which is also called suspension prepregging, offers several advantages over the other prepregging techniques. Submicrometer particle sizes can be utilized in suspension prepregging which may be very important in the impregnation of carbon fibers (121). Carbon fibers are approximately 8 micrometers in diameter; therefore, it is reasonable to expect that smaller particles can impregnate the fibers better than larger particles. Solubility problems are eliminated and aqueous suspensions are easy to work with and usually have low viscosities. In addition to these advantages, suspension prepregging allows for the control of the fiber-matrix interphase properties (121).

Water is the most common suspending medium for suspension prepregging. However, the particles aggregate in the presence of water (121) and a dispersing agent is required. It has been shown (117, 121) that the addition of a water soluble polymer such as the ammonium salt of the LARC-TPI poly(amic acid) to the water forms a stable suspension. The addition of the ammonium salt of LARC-TPI poly(amic acid) reduced the aggregation of the

particles producing smaller mean aggregate sizes of the particles as measured by using laser diffraction (117) or light scattering (121) particle size analysis. To form the water soluble poly(amic acid) (PAA), the LARC-TPI PAA was reacted with 12.5% excess of ammonium hydroxide (117) in water. It has been suggested that the PAA absorbs on the surface of the particles resulting in strong electrostatic and steric repulsive forces which reduced the aggregation of the particles, therefore, making it an effective dispersing agent (117, 121). Texier and coworkers (121) observed that during the drying step which is after prepregging but prior to consolidation, the PAA salt formed a dry film coating over the particles and film. Therefore, the PAA salt also serves as a binder.

The one disadvantage of wet and dry powder processing of high performance polymers is the matrix resin must be in the form of small particles. The most common method of preparing particles is by a cyrogenic grinding process which is extremely costly and limits the particle size range. The normal particle size range for grinding is about 100 μm. Smaller sizes are usually obtained by screening (122, 121). Powders of soluble polymers can be prepared by spraying techniques (121). Particles have been prepared by flashing from supercritical solutions (123); however, it is not done on a commercial scale. Recently, PEEK particles have been synthesized in the submicrometer range (124, 121) that can be suspension prepregged. One method to achieve this involves the synthesis of a soluble, amorphous precursor to PEEK called the poly(ketimine). With the careful control of conditions and use of a dilute acid, the poly(ketimine) may be hydrolyzed to semicrystalline PEEK in the form of small particles.

CHAPTER 3: EXPERIMENTAL

3.1 Solvents and Reagents

3.1.1 Solvents

3.1.1.1 1-Methyl -2-Pyrrolidone (NMP: Fisher) was dried over P_2O_5 for 16 hours and then distilled under reduced pressure with a water aspirator. The distilled NMP was stirred over P_2O_5 again for 16 hours and distilled a second time under reduced pressure. The NMP was collected in 500 ml round bottom flasks, sealed with a septum, and stored under a nitrogen atmosphere up to 2 weeks prior to use. (b.p. 205°C)

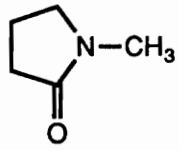

3.1.1.2 Dimethyl Acetamide (DMAC: Fisher) was dried over P_2O_5 for 16 hours and then distilled under reduced pressure with a water aspirator. The distilled DMAC was stirred over P_2O_5 again for 16 hours and distilled a second time under reduced pressure. The DMAC was collected in 500 ml round bottom flasks, sealed with a septum, and stored under a nitrogen atmosphere up to 2 weeks prior to use. (b.p. 165°C/760 mm)

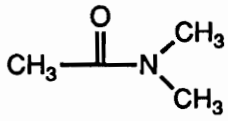

3.1.1.3 o-Dichlorobenzene (ODCB: Fisher) was dried over P_2O_5 for 16 hours and distilled under reduced pressure using a water aspirator. The ODCB

was collected in 500 ml round bottom flasks, sealed with a septum, and stored under a nitrogen atmosphere for up to 2 weeks. (b.p. 180°C)

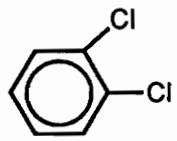

3.1.1.4 Toluene (Fisher) Purification involved a series of washings in which 800 ml of toluene was washed twice with 60 ml of cold sulfuric acid. The residual sulfuric acid was removed by washing twice with 100 ml of water followed by 3 times with 50 ml of saturated sodium bicarbonate until basic. The toluene was stirred over anhydrous magnesium sulfate for 1 to 2 hours and then was decanted off. The toluene was further dried over P_2O_5 overnight and distilled under nitrogen atmosphere from benzophenone and sodium. The purified toluene was stored under a nitrogen atmosphere in round bottom flasks. (b.p. 111°C)

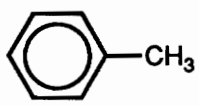

3.1.1.5 Deuterated Dimethyl Sulfoxide (DMSO-d_6; Cambridge Isotopes) was stored over molecular sieves and was used as a NMR solvent. (b.p. 55°C/5mm)

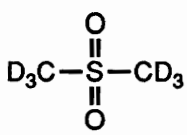

3.1.1.6 Absolute Ethanol (CH_3CH_2OH: Fisher): Ethanol was used as received as a recrystallization solvent. (b.p. 78 - 79°C)

3.1.1.7 Tetrahydrofuran (THF: Fisher): THF was used as received as a solvent for monomer synthesis. (b.p. 67°C)

3.1.1.8 Water (H_2O): Water was purified using a Barnstead NANOPURE II deionizer until the measured resistance was greater than 17 ohms. The purified water was used as the suspension medium in particle size analysis.

3.1.1.9 Glacial Acetic Acid (CH_3COOH: Fisher): Glacial acetic acid was used as received as a recystallization solvent. (b.p. 116 - 118°C)

3.1.2 Monomers and Reagents

3.1.2.1 Pyromellitic dianhydride (PMDA)

Supplier:	Allco
Empirical Formula:	$C_{10}H_2O_6$
Molecular Weight:	218.12
Melting Point:	286°C

Structure:

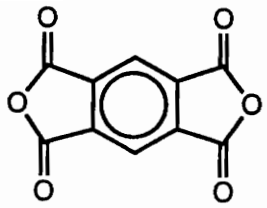

Purification: High purity PMDA was provided by Allco but it was necessary to dry the material at 180°C for 4 to 6 hours under low vacuum prior to use.

3.1.2.2 Hexafluoroisopropylidene-2,2-bisphthalic acid anhydride (6FDA)

Supplier:	Hoechst Celanese Corporation
Empirical Formula:	$C_{19}H_6F_6O_6$
Molecular Weight:	444
Melting Point:	247°C

Structure:

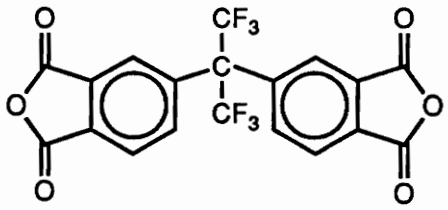

Purification: Polymer grade 6FDA was used after drying in vacuo at 160°C for 12 hours.

3.1.2.3 4,4'-Oxydiphthalic anhydride (ODPA)

Supplier:	Occidental Chemical Corporation
Empirical Formula:	$C_{16}H_6O_7$
Molecular Weight:	310.23

Melting Point: 228°C

Structure:

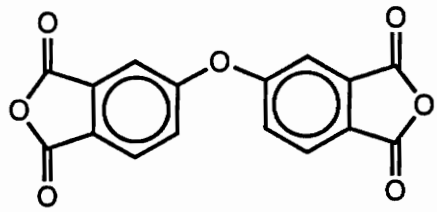

Purification: Polymer grade ODPA was obtained after drying at 160°C in vacuo for 12 hours.

3.1.2.4 3,3',4,4'-benzophenonetetracarboxylic dianhydride (BTDA)

Supplier: Allco

Empirical Formula: $C_{17}H_6O_7$

Molecular Weight: 322.23

Melting Point: 224-226°C

Structure:

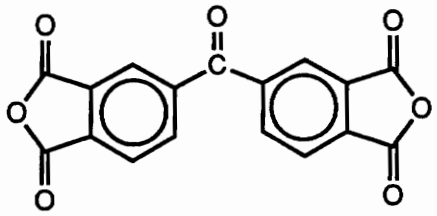

Purification: Polymer grade BTDA was obtained after drying at 160°C in vacuo for 12 hours.

3.1.2.5 3,3',4,4'-biphenylcarboxylic dianhydride (BPDA)

Supplier: Chriskev

Empirical Formula: $C_{16}H_6O_6$

Molecular Weight: 294

Melting Point: 300°C

Structure:

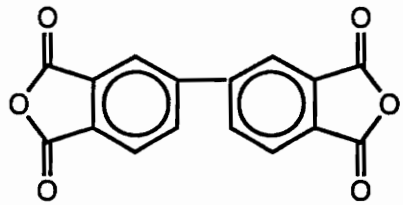

Purification: Monomer grade BPDA was obtained upon drying at 160°C in vacuo for 12 hours.

3.1.2.6 Phthalic anhydride (PA)

Supplier: Aldrich Chemical Company

Empirical Formula: $C_8H_4O_3$

Molecular Weight: 148.12

Melting Point: 134°C

Structure:

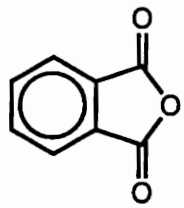

Purification: PA was sublimed under full vacuum with the oil bath temperature at about 110°C.

3.1.2.7 1,1-Bis(4-aminophenyl)-1-phenyl-2,2,2-trifluoroethane (3FDAM)

Supplier:	Dr. H. J Grubbs (Reference 125)
Empirical Formula:	$C_{20}H_{17}N_2F_3$
Molecular Weight:	342.36
Melting Point:	218-220°C

Structure:

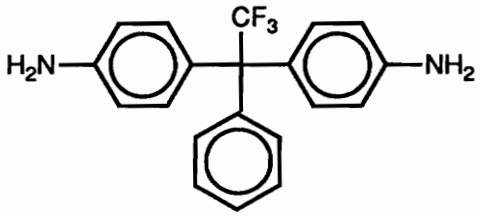

Purification: The 3FDAM was pure as received but required drying at 110°C in vauo to remove moisture prior to use.

3.1.2.8 1,4-Bis(4-aminophenoxy)benzene (TPEQ)

Supplier:	Kennedy and Klim
Empirical Formula:	$C_{18}H_{16}N_2O_2$
Molecular Weight:	292.31
Melting Point:	172.5-173.5°C

Structure:

Purification: TPEQ was recrystallized from toluene and dried in vacuo at 120°C for 24 hours.

3.1.2.9 2,2,2-Trifluoracetophenone

Supplier: Dr. H. J. Grubbs (Reference 125)

Empirical Formula: $C_8H_5F_3O$

Molecular Weight: 172.12

Boiling Point: 165-166°C

Structure:

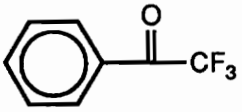

Purification: 2,2,2-Trifluoroacetophenone was distilled under reduced pressure at 100°C.

3.1.2.10 Phenol

Supplier: Aldrich

Empirical Formula: C_6H_6O

Molecular Weight: 94.11

Melting Point: 40-42°C

Structure:

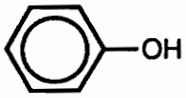

Purification: Phenol was used as received.

3.1.2.11 1-Fluoro-4-nitrobenzene

Supplier: Aldrich

Empirical Formula: $C_6H_4NO_2F$

Molecular Weight: 141.10

Boiling Point: 205°C

Structure:

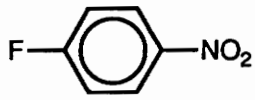

Purification: 4-Fluoronitrobenzene was used as received.

3.1.2.12 Trifluoromethanesulfonic acid (triflic acid)

Supplier: Aldrich

Empirical Formula: CF_3SO_3H

Molecular Weight: 150.07

Boiling Point: 162°C

Structure:

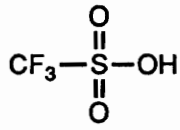

Purification: Triflic acid was obtained in ampules and used as received.

3.1.2.13 Potassium Carbonate

Supplier:	Aldrich
Empirical Formula:	K_2CO_3
Molecular Weight:	138.21
Melting Point:	891°C

Purification: Potassium carbonate was dried in vacuo at 160°C for 24 hours prior to use.

3.1.2.14 2,2-bis[4-(4-aminophenoxy)phenyl]hexafluoropropane (BDAF)

Supplier:	Ethyl Corporation
Empirical Formula:	$C_{27}H_{20}O_2N_2F_6$
Molecular Weight:	518.46
Melting Point:	169°C

Structure:

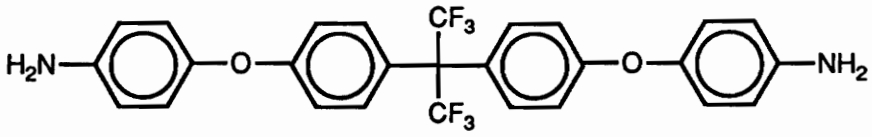

Purification: BDAF was dried in vacuo at 120°C for 12 hours prior to use.

3.1.2.15 <u>LaRC TPI Polyamic Acid:</u> LaRC TPI in the polyamic acid form was obtained from NASA Langley. The amic acid was converted to the ammonium salt by dissolving 26.5 g of the polymer in 800 ml water with 7.2 ml of

ammonium hydroxide. This solution was used as a stabilizer for polyimide particles.

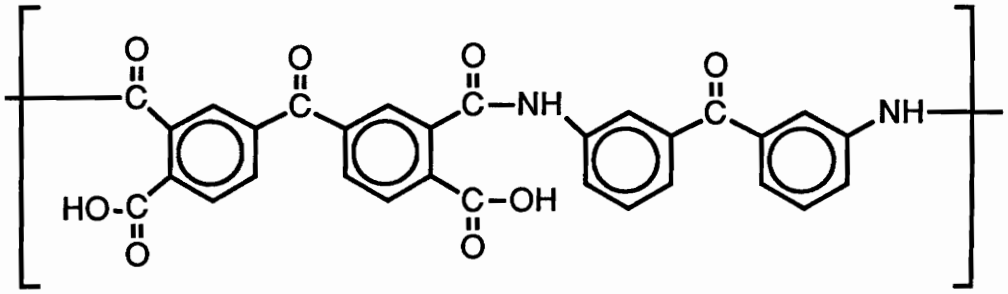

LaRC TPI Polyamic acid

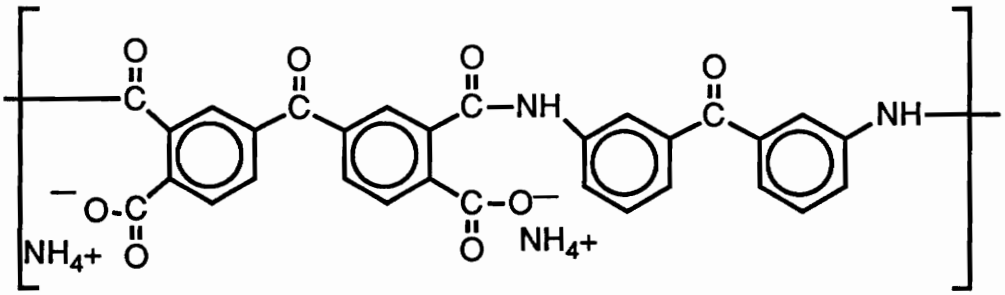

Ammonium Salt of LaRC TPI

3.1.2.16 Triton X-100: Triton X-100, a nonionic surfactant, was purchased from Aldrich and used as a aqueous suspension stabilizer for polyimide particles.

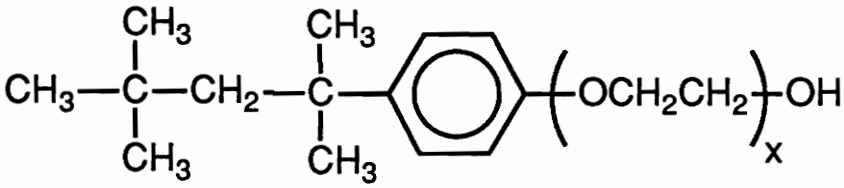

x = 10 (average)

3.2.1 Two Step Procedure to the 1,1-bis[4-(4-nitrophenoxy)phenyl]-1-phenyl-2,2,2-trifluoroethane (3F-Dinitro) Precusor

3.2.1.1 Step 1: Preparation of bis(4-hydroxyphenyl)phenyl-2,2,2-trifluoroethane (3F-bisphenol)

The synthesis of the 3F-dinitro compound is a two step procdure in which the first step is the preparation of bis(4-hydroxyphenyl)phenyl-2,2,2-trifluoroethane (3F-bisphenol). To a 3-necked, 250 ml round bottom flask equipped with an overhead stirrer, nitrogen inlet and drying tube, and a 25 ml liquid addition funnel, 0.10 mole of trifluoroacetophenone and 0.40 mole of phenol were added. The flask was immersed in a temperature controlled silicone oil bath at 50°C to melt the phenol and form a homogeneous and colorless solution. The ampules of trifluoromethanesulfonic acid (triflic acid) were placed in dry ice until very cold. The ampules were broken and the triflic acid was quickly introduced into the liquid addition funnel. The triflic acid in the sealed ampules was colorless but became light yellow upon the exposure to the air during the transfer. Next, 0.10 mole of triflic acid was added dropwise to the mixture via the addition funnel. Within 30 minutes from the addition of the first drop of acid, the reaction mixture formed a dark red-brown solid. The solid product was stirred for 30 minutes in 1 liter of boiling water to remove the residual acid and the excess phenol resulting in a pale pink powder. White product was obtained upon stirring the 3F-bisphenol in methylene chloride (15 ml of methylene chloride per gram of product). The reaction afforded a 80% recrystallized yield with a melting point of 231-232°C as determined by a capillary melting temperature apparatus with a heating rate of 2°C/min.

The optimization of the yield of 3F-bisphenol was investigated in which different acids, combination of acids, and varying the amount of acid were employed in preparation of the 3F-bisphenol. Trifluoromethanesulfonic acid (triflic acid), sulfuric acid, and 3-mercaptopropionic acid (mercapto acid) were selected. The same procedure as discussed previously for the synthesis of the 3F-bisphenol was utilized for each of the different acids and where the amount of acid was varied. The mercapto acid was combined with the triflic acid and separately with the sulfuric acid. In these cases, the 3-mercaptopropionic acid was added to the solution of trifluoracetophenone and phenol followed by the dropwise addition of the triflic acid or the sulfuric acid.

3.2.1.2 Step 2: Formation of (1,1-bis[4-(4-nitrophenoxy)phenyl]-1-phenyl-2,2,2-trifluoroethane) (3F-Dinitro) Precursor Via a Nucleophilic Aromatic Substitution Reaction With the 3F-Bisphenol

The second step was the formation of the 3F-dinitro compound via a nucleophilic aromatic substitution reaction involving the 3F-bisphenol and 4-fluoronitrobenzene. To a 250 ml, 4-necked, round bottom flask, equipped with a Dean Stark trap, mechanical stirrer, and nitrogen inlet and drying tube, 30 g (0.087 mole) of the 3F-bisphenol and 24.08 g (0.1742 mole, 50% excess) of potassium carbonate, and 19.4 ml (0.182 mole, 10% excess) of toluene were added. The reagents were dissolved in NMP to produce a 20% by weight solution. While under a nitrogen purge, the reaction vessel was placed in a temperature controlled silicone oil bath at 140°C for four hours in which the toluene azeotroped with the water and the weak base, K_2CO_3, formed the phenolate anion, affording a faint rose-colored solution. Dropwise, 19.4 ml (0.182 mole, 10% excess) of 4-fluoronitrobenzene was added yielding a yellow,

opaque solution. The temperature was increased to 160°C and the progess of the reaction was followed by TLC.

The solvent system used for the TLC study was 60% hexane and 40% ethyl acetate. The disappearance of the 3F-bisphenol compound was clearly observed over time. As indicated by TLC, the reaction was complete in three hours and the mixture was cooled to room temperature. The 3F-dinitro compound was isolated from the solution by precipitation of the solution into a blender of 500 ml of water producing fine yellow particles. The product was filtered, recrystallized from acetic acid, and dried in vacuo at room temperature for 24 hours and 12 hours at 110°C to afford 97% of pure 3F-dinitro derivative with a melting point of 196.5-197.2°C as determined by a capillary melting temperature apparatus with a heating rate of 2°C/min.

3.2.2 One Step Procedure to (1,1-bis[4-(4-nitrophenoxy)phenyl]-1-phenyl-2,2,2-trifluoroethane) (3F-Dinitro) Precursor

3.2.2.1 Hydroxyalkylation Reaction With Nitrophenyl phenyl ether

The 3F-dinitro precursor to the fluorinated diamine was synthesized by a novel one step procedure involving a hydroxyalkylation reaction of trifluoroacetophenone with nitrophenyl phenyl ether. To a 3-necked, 250 ml round bottom flask equipped with a magnetic stirrer, nitrogen inlet and drying tube, condenser, and a 25 ml liquid addition funnel, trifluoroacetophenone (0.100 mol), 4-nitrophenyl phenyl ether (0.205 mol) , and 1,2-dichloroethane (20% (w/v) solid concentration) were added resulting in a homogeneous, yellow solution. Triflic acid (0.105 mol) was transferred from cooled ampules to the liquid addition funnel and added dropwise to the solution over a period of 15 minutes producing a dark red solution. The mixture was allowed to stir at

ambient temperature for 24 hours after which the solvent was removed by rotary evaporation. The resulting orange solid was stirred in 100 ml of hot (~50°C) water for 1-2 hours to remove residual acid and acid by-products. The product was filtered and washed with 100 ml of fresh water producing a light orange powder which was recrystallized twice from acetic acid, and dried in vacuo at 110°C for 24 hours affording a tan-colored powder (85%): mp 196-197°C.

3.2.3 Preparation of 1,1-bis[4-(4-aminophenoxy)phenyl]-1-phenyl-2,2,2-trifluoroethane (3FEDAM) Via Hydrogenation of the 3F-Dinitro Precursor

The novel fluorine-containing diamine (1,1-bis[4-(4-aminophenoxy) phenyl]-1-phenyl-2,2,2-trifluoroethane (3FEDAM)) was synthesized by the hydrogenation of the 3F-dinitro compound. A pressure reactor was charged with 0.100 mol of the 3F-dinitro compound, 0.00100 mol of the palladium catalyst (10% Pd/C) with respect to the 3F-dinitro compound, and 200 ml each of tetrahydrofuran and ethyl acetate. The reactor was purged 3 times with hydrogen and then maintained at 50 psi of hydrogen. The temperature was controlled at 50°C (±2°C) and the reaction mixture was stirred vigorously for 6-8 hours. Samples were removed periodically to follow the conversion of the nitro to the amine. Filtration over Celite followed by rotorary evaporation (temperature of water bath was ~40°C) of the solvent afforded an amber colored, highly viscous liquid. After 3 to 5 days, the diamine crystallized.

The best method of purification was recrystallization of the viscous, liquid diamine from absolute ethanol. Hot absolute ethanol was slowly added to the viscous liquid. Upon the first aliquot of absolute ethanol, a white powdery

material precipitated but dissolved with the addition of more ethanol. Ethanol (~15 ml of ethanol per gram of diamine) was added until a homogeneous, amber-colored solution formed. Decolorizing charcoal was added to the ethanol solution followed by boiling for 10 to 15 minutes. The hot solution was filtered over Celite yielding a light yellow filtrate. Upon cooling to room temperature, a fine powder began to precipitate. The flask was placed in the refrigerator overnight to promote maximum precipitation. The light tan-colored product was collected by filtration and washed with 200 ml of cold ethanol. The product was placed in a vacuum oven at room temperature for 24 hours to remove most of the solvent. Over a 4 to 6 hour period, the temperature was increased to 110°C and held for 12 hours affording an off-white powder (95%): mp 169°-170°C.

3.3 Polymer Synthesis

3.3.1 Molecular Weight and Endgroup Control for Step Growth Polymerizations

Molecular weight control and endgroup functionalization is very important in preparing well defined polymer systems. The principles of molecular weight (MW) and endgroup control for step growth polymerizations were first derived by Carothers (126). Through stoichiometric control of the monomers, the control of MW and endgroups can be achieved. This section describes the derivations for the equations used in the preparation of polyimides with well defined molecular architectures such as controlled molecular weight and endgroups.

To prepare a generic step growth polymer from a difunctional monomer, A-A, with "A" functional groups and difunctional monomer, B-B, with "B"

functional groups, let N_A represent the number of A-A monomer molecules and N_B represent the number of B-B monomer molecules so that

(3-1) $$N = (N_A + N_B)/2$$

where N is the total number of initial monomer molecules.

The molecular weight can be controlled by off-setting the stoichiometry so that one of the monomers (B-B) is added in excess and the endgroups will have the functionality (B) of the excess monomer. This allows one to define r as the stoichiometric imbalance ratio as in Equation 3-2 and is defined to be less

(3-2) $$r = N_A/N_B$$

than unity. Now one can define the fractional extent of reaction, p, as the fraction of A groups that have reacted and rp is the fraction of B groups that have reacted. Let (1-p) and (1-rp) stand for the amount of unreacted A and B, respectively; therefore

(3-3) $$\text{total unreacted A} = N_A\,(1-p)$$

(3-4) $$\text{total unreacted B} = N_B\,(1-rp)$$

where the sum of the total unreacted monomers is the total number of chain

(3-5) $$\text{total \# of chain ends} = N_A\,(1-p) + N_B\,(1-rp)$$

ends. Since each polymer chain has 2 chain ends, the total number of polymer molecules is one half the total number of chain ends as shown in Equation 3-6.

(3-6) total # of polymer molecules = $[N_A (1-p) + N_B (1-rp)]/2$

The number average degree of polymerization, Xn, represents the average number of structural units per molecule. For A-A and B-B type polymerizations,

(3-7) $Xn = 2Dp$

and

(3-8) Dp = (number average MW)/(repeat unit MW)

where Dp is the average number of repeat units per polymer molecule.
Xn is also defined as

(3-9) Xn = total # initial molecules/total # polymer molecules

by substitution

(3-10) $Xn = [(NA + NB)/2]/[N_A (1-p) + N_B (1-rp)]/2$

and rearranging provides

(3-11) $Xn = (1 + r)/(1 + r - 2rp)$

To achieve high molecular weight polymers, the polymerization must reach high conversions such that p approaches 1; therefore Equation 3-11 can be simplified to

(3-12) $$Xn = (1 + r)/(1 - r)$$

solving for r provides

(3-13) $$r = (Xn - 1)/(Xn + 1)$$

The MW can be controlled by the addition of a monofunctional reagent which serves as the endcapping agent. The incorporation of a monofunctional endcapper must not disturb the stoichiometric imbalance ratio, r, to obtain the same molecular weight as without the endcapping agent. Therefore, the r must be modified to treat the addition of the monofunctional monomer as shown in Equation 3-14

(3-14) $$r = N_A/(N_B + 2N_B')$$

where N_B' is the number of monofunctional monomer molecules. N_B' is multiplied by 2 because two molecules of the monofunctional endcapper are required for every polymer chain. The modified stoichiometric imbalance ratio

(3-15) $$N_B + 2N_B' = N_A/r$$

can be rearranged to give the amount of endcapper necessary to obtain the target number average molecular weight of the polymer. In order to obtain polymers that are only endcapped with the monofunctional endcapper, the moles of B functional groups must equal the moles of A functional groups. This is expressed in the following equation

(3-16) $N_B + N_B' = N_A$

By solving equations 3-15 and 3-16 simultaneously, N_B and N_B' can be calculated and an example of these monomer calculations is provided below.

The example describes the procedure utilized to prepare a polyimide (BDAF-PMDA-PA) with a number average molecular weight of 30,000 g/mol in which the following variables will be employed.

MWBDAF = A = molecular weight of BDAF

MWPMDA = B = molecular weight of PMDA

MWPA = B' = molecular weight of phthalic anhydride

Mn = target number average molecular weight

Step 1: Determine molecular weight of repeat unit (MWru)

MWru = MWBDAF + MWPMDA - 2MWwater

MWru = 518.46 + 218.12 - 2(18) = 700.58

There are 2 molecules of water evolved upon the formation of the polyimide; therefore, 36 is subtracted when determining the MWru.

Step 2: Determine Xn (equations 3-7 and 3-8)

Xn = 2 Mn/MWru

Xn = 2 (30,000)/700.58 = 85.643324

Step 3: Calculate r (equation 3-13)

$r = (Xn - 1)/(Xn + 1)$

$r = (85.643324 - 1)/(85.64332 + 1) = 0.9769169$

Step 4: Determine the moles of monomers by solving equations 3-15 and 3-16 and setting NA equal to 0.1

$N_B + 2N_{B'} = N_A/r = 0.1/0.9769169 = 0.1023629$

$N_B + N_{B'} = N_A = 0.1$

Subtraction of equation 3-16 from equation 3-15 gives

$N_{B'} = 0.0023629$

Step 5: Calculate NB, the number of moles of PMDA by substituting $N_{B'}$ into equation 3-16

$N_B + 0.0023629 = 0.1$

$N_B = 0.0976371$

Step 6: Calculate the mass of monomers

BDAF: $N_A = 0.1$	mass = 0.1mole x 518.46g/mole = 51.8460g
PMDA: $N_B = 0.097671$	mass = 0.097671mole x 218.12g/mole = 21.3040g
PA: $2N_{B'} = 0.0047258$	mass = 0.0047258mole x 148.12g/mole = 0.7000g

3.3.2 Formation of Poly(amic acid)

High molecular weight polyimides were prepared by the conventional two step method in which the poly(amic acid) precursor was prepared from an aromatic dianhydride and an aromatic diamine in a polar aprotic solvent. The

molecular weight was controlled by off-setting the stoichiometry using the Carother's equations and adding the monofunctional endcapping agent, phthalic anhydride. Two methods of cyclodehydration of the poly(amic acid) were employed depending on the solubility of the resulting polyimide. For those polyimides that were insoluble in DMAC or NMP, the thermal/bulk imidization route was used and the solution imidization route (53) was used for the polyimides that were soluble in NMP or DMAC.

The synthesis of the BDAF-PMDA-PA polyimide of a number average molecular weight of 30,000 g/mol will serve as an example for a typical preparation of a homopolymer. The poly(amic acid) was prepared in a four-neck round bottom flask equipped with an overhead stirrer, nitrogen inlet and drying tube, and a thermocouple. The flask was flame dried under a nitrogen purge prior to addition of the reagents. Via a glass powder funnel, the solid diamine, BDAF (51.8460 g: 100.0 mmole), was introduced to the flask. To afford nonreactive endgroups and controlled molecular weight, phthalic anhydride (0.7000 g: 4.726 mmole) was added to the prepared diamine solution. Lastly, the dianhydride, PMDA (21.3040 g: 97.671 mmole), was added as a solid in small increments while the flask was under nitrogen purge. Each reagent was allowed to completely dissolve before the addition of the next monomer and each was quantitatively rinsed in to the flask with the solvent to provide a 15-20 % (w/w) solid concentration. The temperature was held at room temperature for at least 24 hours while under a nitrogen atmosphere to reach high molecular weight and to allow for equilibration to a most probable molecular weight distribution.

The order of monomer addition for the copolyimides was basically the same as for the homopolymers except for minor changes. The less reactive comonomer was added first to ensure randomization. For the BDAF-PMDA/6FDA-PA copolyimides, the 6FDA was added first followed by PMDA. In the case of the BDAF/3F diamine-PMDA-PA copolyimides, the PMDA was added to a solution of 3F diamine followed by the addition of PA. The BDAF comonomer was added last.

3.3.3 Cyclodehydration

3.3.3.1 Bulk Imidization

Insoluble polyimides were imidized by the conventional thermal cyclodehydration method. The poly(amic acid) solutions were cast onto pyrex glass plates. If the final film thickness was unimportant, then the poly(amic acid) solution was diluted to 5-10% solids and poured onto the plate. When a certain film thickness was required, the 15-20% solids poly(amic acid) solution was poured onto the glass plate and then spread with a doctor blade to the appropriate thickness. The majority of the solvent was removed by placing the films in a dry box under dry air purge. Usually 24 hours was sufficient to produce nontacky films which were placed in a vacuum oven. The films were heated incremently at 100°C, 200°C, and 300°C for one hour at each temperature. The films were allowed to cool in the oven to below 200°C before removal from the oven.

3.3.3.2 Solution Imidization

For soluble polyimides, cyclodehydration of the poly(amic acid) was performed by solution imidization techniques. An inverse Dean Stark trap and a condenser was added to the apparatus. Ortho-dichlorobenzene was used as an azeotroping agent for the water that was produced upon cyclization in which an 80/20 (v/v) solution of NMP/DCB was used. The imidization was carried out at 165°C for 24 hours to insure complete cyclization during which the reaction solution remained homogeneous. The solution was then cooled to room temperature, precipitated in methanol or water, filtered, and dried in a vacuum oven for 18 hours at 200°C and for 1 hour at 300°C.

3.4 Preparation of Polyimide Powders

The polyimide particles were prepared by the solution imidization technique in which the procedure was basically the same as previously described. In all cases, expect in the study of the influence of the imidization temperature on particle size, DMAC was the solvent. For the cyclodehydration of the amic acid to the imide, the solution was diluted to a specific concentration with DMAC and 20% dichlorobenzene with respect to the DMAC was added to the PAA solution. The flask was immersed in a silicone oil bath controlled to the desired temperature. Within 1 hour, the solution became turbid indicating the polymer was precipitating from solution as the amic acid was converted to the imide. The temperature was maintained at the controlled temperature for a total of two hours and allowed to cool to room temperature. The partially imidized particles were isolated by adding the DMAC slurry to 250 ml of water and stirred

in a blender for 10 to 15 minutes. The particles were filtered and treated again with 250 ml fresh water. In some cases, the powders were dried and the influence of drying on the particles size will be discussed in the Results section.

3.5 Characterization

3.5.1 High Performance Liquid Chromatography (HPLC). Reversed phase HPLC analyses were performed on a Vista 5500. The mobile phase was 75% acetonitrile/25% methanol with a flow rate of 1 ml/minute. The monomers were dissolved in 100% acetonitrile before analysis.

3.5.2 Nuclear Magnetic Resonance Spectroscopy (NMR). Proton NMR studies were in deuterated dimethyl sulfoxide performed on a Varian Unity NMR spectrometer operating at 400 MHz with chemical shifts reported in ppm vs TMS.

3.5.3 Fourier Transform Infrared (FTIR) Spectroscopy. FTIR spectra were obtained with a Nicolet MX-1 FTIR spectrometer which provided qualitative information describing the conversion of the poly(amic acid) to the polyimide. FTIR analysis was also utilized to follow the reduction of the 3F-dinitro compound to the 3FEDAM diamine.

3.5.4 Potentiometric Titration. Potentiometric titration was utilized to assess the purity of the fluorinated diamine, 3FEDAM. An MCI Automatic Titrator Model #GT-05 was used in conjunction with a standard Glass-Body Combination Electrode with Ag/AgCl reference. The HBr titrant was dispensed

by means of an automatic microburet with a volume resolution of 2 ml. The diamine was dissolved in chloroform and acetic acid.

3.5.5 Intrinsic and Inherent Viscosities. The viscosities were measured on the soluble polyimides or the poly(amic acid)s of semicrystalline polyimides. As will be noted in the Results, some of the poly(amic acid)s were isolated in water, filtered, and dried in vacuo at room temperature for 2 to 3 days and 50°C for 1 day. The poly(amic acid)s that were not isolated by precipitation were measured directly in the original NMP solution. The polymers were run in NMP or chloroform at 25°C in a Cannon-Ubbelohde dilution viscometer with various capillary sizes. The intrinsic viscosity values were obtained by using four different polymer concentrations and the results were linearly extrapolated to the zero concentration. Inherent viscosities were determined from one concentration value of 0.5 g/dl.

3.5.6 Gel Permeation Chromatography (GPC). GPC was performed on A Waters 150-CALC/GPC chromatograph equipped with a refractive index detector and a Viscotek Model 100 differential viscometer. The mobile phase was chloroform with a flow rate of 1ml/min at 30°C. The columns were Permagel with pore sizes of 500, 10^3, 10^4, 10^5 Å. The injection volume was 200 µL with a sample concentration of 3 mg/ml.

3.5.7 Thermal Analysis. Thermal analysis was performed on a Perkin-Elmer Series 7 thermal analyzer. Differential scanning calorimetry (DSC) was used to determine the glass transition temperatures (Tg) and melting points

(Tm). Scans were performed at a heating rate of 10°C/minute in a nitrogen atmosphere. Usually, the sample was heated at 10°C/min to a temperature above the melting point and then quenched cooled in the DSC which cools at a rate of 200°C/min. The second heat was also analyzed at 10°C/min. The Tg values were determined from the second heat scan in which values were obtained from the inflection point. In most cases, the polyimides exhibited an endothermic transition on the first heat in which the peak value of the transition was evaluated. The sample size for films was in the range of 10 to 15 mg and less than 10 mg for powder samples.

Thermooxidative stabilities were determined on a Perkin-Elmer TGA7 thermogravimetric analyzer at a heating rate of 10°C/minute in an air atmosphere. The dynamic TGAs were used to evaluate the thermooxidative stabilities by measuring the temperature at which 5% weight loss occurred. Isothermal TGAs were performed at 371°C in an air atmosphere. Sample sizes were in the range of 3 to 5 mg.

Long term thermooxidative stability studies were conducted in a computer controlled Blue M forced air oven. The films (5-10 mils thick) were heated to 150°C and weighed on an analytical balance to measure the initial dry weight. The samples were maintained at the test temperature (600°F or 700°F) for the extended period of time with an air atmosphere flowing over the samples at 25 cubic feet per hour. The samples were periodically removed from the oven and weighed to measure weight loss as a function of time at the elevated temperature.

3.5.8 Wide Angle X-ray Scattering. Wide angle X-ray scattering (WAXS) measurements were made in transmission with a Siemens X-ray diffractometer using CuK_{α} radiation ($\lambda = 1.54$ Å). Samples were scanned through 2θ values of 3° to 60° at 0.05° increments with a dwell time of 10 seconds.

3.5.9 Solubility Tests. The solubility of polyimides was investigated by examining 1% by weight solutions in small capped glass vials. The solutions were stirred vigorously with a magnetic stir bar at room temperature. The solubility was qualitatively evaluated after 18 hours.

3.5.10 Particle Size Analysis (PSA). The sample preparation for particle size analysis (PSA) has been shown by Professor R. M. Davis et al (121) to greatly effect the results; therefore, much care and consistency is required to produce accurate data. The first step of the procedure was to weigh 0.1 g of the particles in to a small vial. Via pipet, 2-3 drops (~ 5 weight percent) of Triton-X 100 was added. The vial was filled with deionized water and sonicated 3 minutes at 75 Watts. For very concentrated solutions (for dried particles), half of the solution was placed in a second vial and diluted with water. The solution was sonicated again for 3 minutes at 75 Watts. Finally, the solution was placed in a quartz cell and the size of the particles was evaluated in a centrifugal particle size analyzer Shimadzu Model SA-CP3. This instrument measures the turbidity of the sedimenting suspension and utilizes Stokes Law to correlate the sedimentation rate to particle size. The solvent density, solvent viscosity, and the density of the particle are required in the calculations (127).

Samples of polyimide powders were prepared to determine the percent of imidization. The DMAC slurry was placed in a separatory funnel and the slurry was added dropwise to 250 ml of water in a blender. Upon the completion of addition, the particles were stirred for 10 to 15 minutes and filtered. The treatment in the water was repeated. The powders were placed in a plastic bottle with 250 ml of water and sonicated 5 minutes at 75 Watts for a total of 4 times allowing the sample to cool between sonications. The powders were filtered and washed with 250 ml of water and placed in a vacuum oven at room temperature for 3 days. Over the course of 4 hours, the temperature was increased to 75-80°C and held for 2 hours. The samples were allowed to cool to room temperature while in vacuo.

3.5.11 Polymer Density. The size analysis of the particles requires the density of the polymer. The density of individual particles cannot be measured; therefore, the density of the corresponding film was utilized in the measurements. The bulk density of the BDAF-PMDA-PA film and Kapton film were determined using the ASTM C373-88 method.

3.5.12 Environmental Scanning Electron Microscopy (ESEM). An Electro Scan-E-3 Environmental SEM operating at 5 torr water vapor and 20 kV. A dilute suspension of the particles was applied to a copper strip and the samples were lightly gold sputtered to improve resolution. This method was used to verify the results of the PSA.

3.5.13 Sintering of Polyimide Powders. The ability to sinter polyimide powders was investigated. The samples were prepared in the form of a disk in which 0.3 g of the dried polyimide powder was placed in a 2.85 cm die and cold pressed in a Carver Laboratory press at 15,000 psi for 4-5 minutes. The disks had sufficient integrity to be handled and were in the range of 0.5 mm thick. The disks were placed on Pyrex glass plates and put in the Blue M convection oven in a nitrogen atmosphere for the desired time and temperature.

3.5.14 Mechanical Testing. A die was used to cut dogbone samples from the sintered disks that were prepared as previously discussed in Section 3.5.13. The dogbone samples were tested on a Polymer Laboratories miniature tensile frame (Minimat) with a strain rate of 5 mm/min. The values of the mechanical properties were averaged over a minimum of 4 samples.

CHAPTER 4: RESULTS AND DISCUSSION

4.1 Synthesis of the Fluorine Containing Monomers

Polyimides containing the trifluoroethylidene (3F) or the hexafluoroisopropylidene (6F) linkages are very interesting and were studied in depth in this thesis research. The 3F monomers were based on the percursor, trifluoroacetophenone. The 3F diamine, 1,1-bis(4-aminophenyl)-1-phenyl-2,2,2-trifluoroethane (3FDAM) was first used by Alston and Gratz (128).

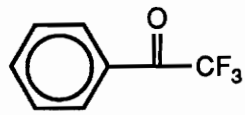

2,2,2-Trifluoroacetophenone

They demonstrated that the 3FDAM based materials had exceptional thermal and mechanical properties but, in general their "cured" polyimides were insoluble. By contrast, fully cyclized 3FDAM containing polyimides prepared by the solution imidization technique with molecular weight and end group control were amorphous, soluble in polar aprotic solvents, demonstrated outstanding

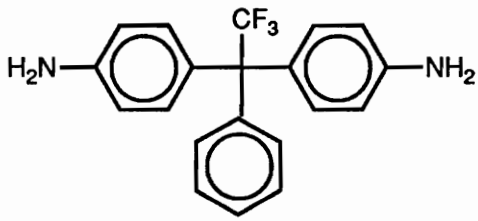

1,1-bis(4-aminophenyl)-1-phenyl-2,2,2-trifluoroethane (3FDAM)

thermal and mechanical properties, and displayed high glass transition temperatures (Tg) (62,129). The high Tg (some in the range of 430°C) may be ascribed to the bulky structure of the 3F group which retards segmental mobility and hence results in a more rigid system.

It is of interest to investigate new organic materials that might set new standards for high temperature/performance applications. A novel diamine has been synthesized that has a bulky phenyl ring substituent (the "3F" link) which is attributed to the very high Tg and the ether links which provides sufficient chain mobility and proper symmetry to allow development of crystallinity. The novel diamine is 1,1-bis[4-(4-aminophenoxy)phenyl]-1-phenyl-2,2,2-trifluoroethane (3FEDAM) and this section of the thesis will report the synthesis of 3FEDAM and the characterization of homopolyimides and statistical copolymers prepared from this new monomer.

4.1.1 Two Step Procedure to the 1,1-bis[4-(4-nitrophenoxy)phenyl]-2,2,2-trifluoroethane (3F-Dinitro) Precursor

The novel 3FEDAM diamine was prepared via two reaction pathways (Figure 4.1) in which one pathway involved a three step procedure and the second pathway consisted of two steps. The three steps in the first procedure were an hydroxyalkylation reaction of trifluoroacetophenone with phenol to form the 3F-bisphenol followed by a nucleophilic aromatic substitution reaction of the 3F-bisphenol with 4-fluoronitrobenzene affording the 3F-dinitro compound, and the last step was the reduction of the 3F-dinitro compound to the diamine, 3FEDAM.

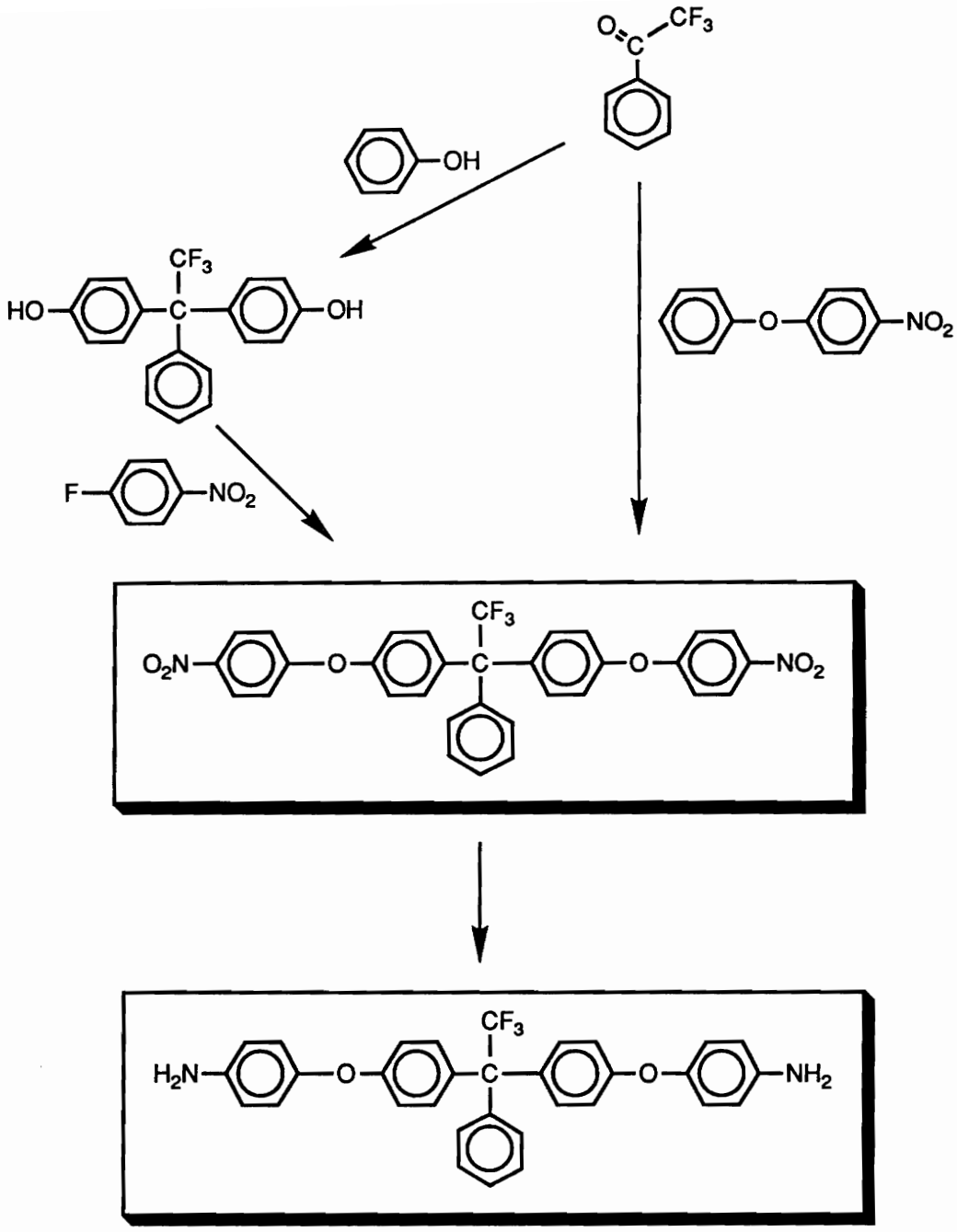

Figure 4.1: General Reaction Pathways to 1,1-bis[4-(4-aminophenoxy)phenyl]-1-phenyl-2,2,2-trifluoroethane (3FEDAM)

4.1.1.1 Step 1: Preparation of 1,1-bis[4-(4-hydroxyphenyl)phenyl]-2,2,2-trifluoroethane (3F-Bisphenol)

The hydroxyalkylation reaction is the condensation of aromatic rings with aldehydes and ketones (130, 131). This reaction can be utilized to synthesize alcohols; however, the alcohol initially produced will condense with a second aromatic ring to give diarylation and the later is common with phenols. The trifluoroacetophenone is a ketone which undergoes diarylation with phenol to give the 3F-bisphenol. The proposed mechanism for the hydroxyalkylation is shown in Figure 4.2. An acid is required to promote the hydroxyalkylation in which a mineral acid is usually sufficient. However, sulfuric acid was not sufficiently acidic to promote the condensation of trifluoroacetophenone with phenol. Trifluoromethanesulfonic acid (triflic acid) was used to prepare the 3F-bisphenol.

The yield of the 3F-bisphenol was dependent upon the type and concentration of the acid. These parameters were varied to determine the optimum conditions to produce the highest yield. Sulfuric acid, triflic acid, and 3-mercaptopropionic acid, which is a well known catalyst for the commercial synthesis of bisphenol-A, were selected for the study. Under identical reaction conditions, each of the three acids were added to the reaction mixture in a 1:1 molar ratio with respect to trifluoroacetophenone. No 3F-bisphenol was obtained under these reaction conditions when sulfuric acid or mercapto acid was used alone. However, 3F-bisphenol was obtained in about 70% yield when triflic acid was used. Triflic acid was added in a 5% excess and the yield was increased to 85%. However, the addition of 10% excess of triflic acid did not improve the yield above 85%. These results are summarized in Table 4.1.

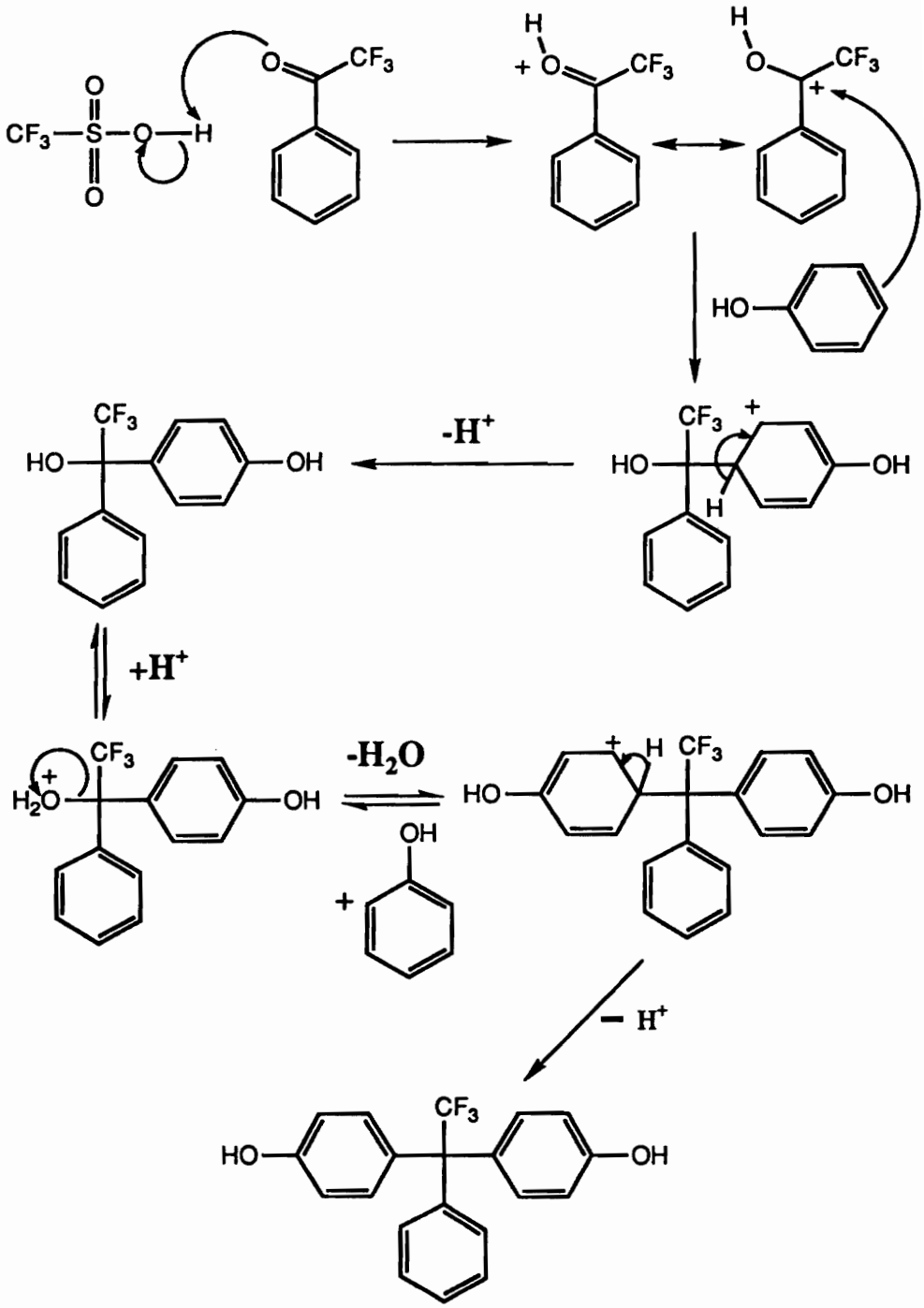

Figure 4.2: Proposed Mechanism for the Hydroxyalkylation Reaction of Trilfluoroacetophenone With Phenol

Table 4.1: The Influence of the Type of Acid and the Concentration of Acid on the Percent Yield of 3F-Bisphenol at Ambient Temperature For 12 Hours

ACID	MOLE % OF ACID	% YIELD OF BISPHENOL
Sulfuric	100	0
Mercapto	100	0
Triflic	40	50
Triflic	100	70
Triflic	105	85
Triflic	110	85

A 1:1 molar ratio of the triflic acid with respect to the ketone was necessary to produce reasonable yields of the 3F-bisphenol. The addition of 5% excess of the triflic acid significantly increased the percent yield of product. A possible explanation for this result may be due to the moisture sensitivity of the triflic acid. Triflic acid was quickly hydrolyzed upon the transfer of the triflic acid in the ampules to the liquid addition funnel as evidenced by the change of the color of the triflic acid from colorless to yellow. Therefore, a slight excess replaced the triflic acid lost from hydrolysis and boosted the product yield. However, the addition of a larger excess of triflic acid did not show an improvement of the yield. This suggested that less than 5% of the triflic acid was hydrolyzed and a larger excess of the acid was not required.

Triflic acid is a relatively expensive acid and the scale-up of this reaction would be potentially very costly. Therefore, an investigation was pursued to reduce the amount of triflic acid required for the synthesis of the 3F-bisphenol. In the literature (132), it was cited that mercapto acids can improve the yield in hydroxyalkylation reactions. Therefore, triflic acid and sulfuric acid were combined with 3-mercaptopropionic acid in different ratios to determine the effect of acid combinations on the percent yield of the 3F-bisphenol. The combinations of the sulfuric and mercapto acids did not produce product. However, 80% yield of 3F-bisphenol was obtained in the presence of 75% triflic acid and 25% mercapto acid. The proposed mechanism (Figure 4.3) suggests that in the presence of mercapto acid a better leaving group could be formed, therefore, enhancing the reaction.

Proton (^{1}H) NMR, FTIR, mass spectroscopy, and elemental analysis were used to confirm the structure of the 3F-bisphenol. As shown in Figure 4.4, the

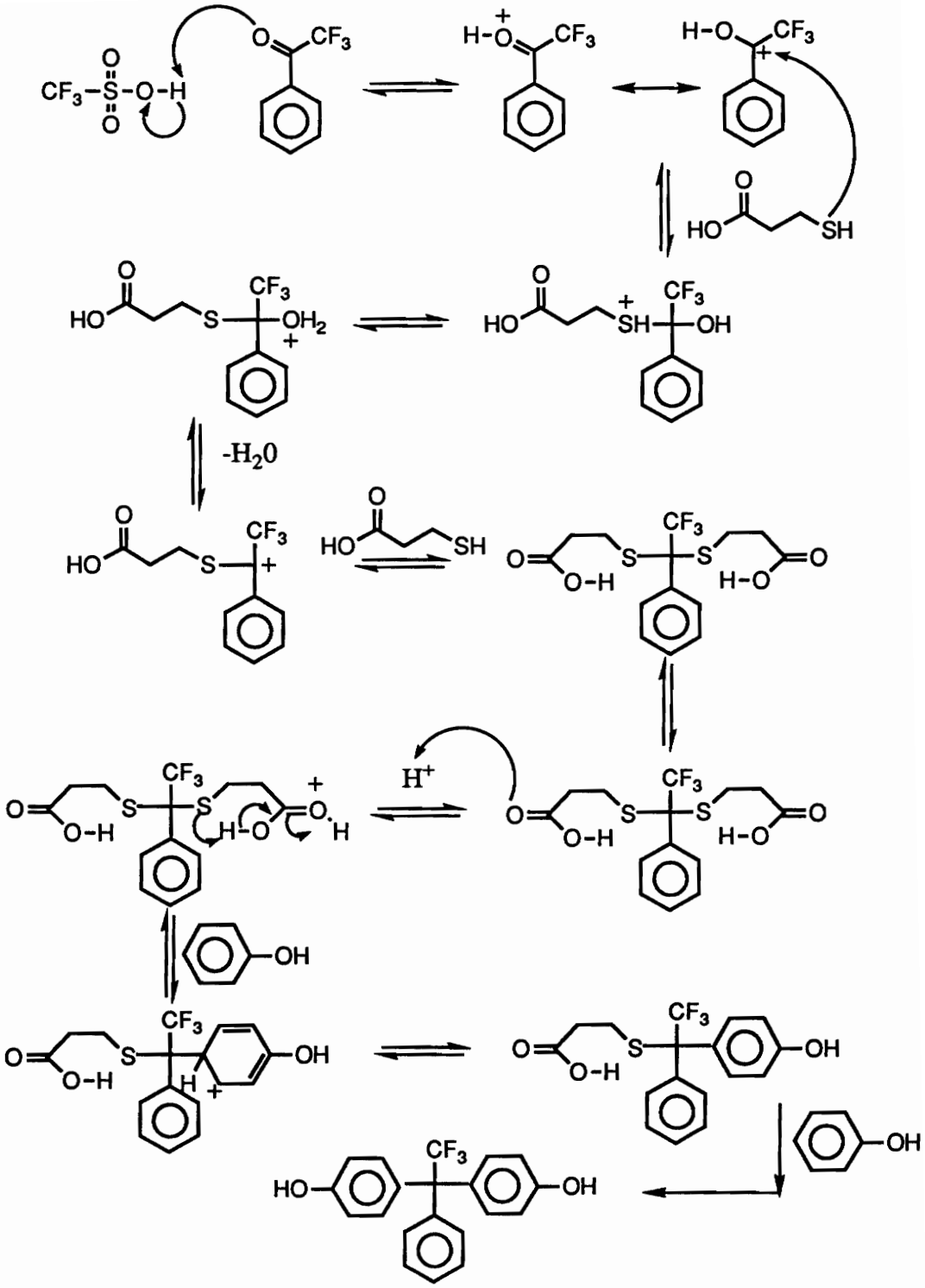

Figure 4.3: A Proposed Mechanism for the Hydroxyalkylation Reaction of Trifluoroacetophenone in the Presence of Triflic and Mercapto Acids

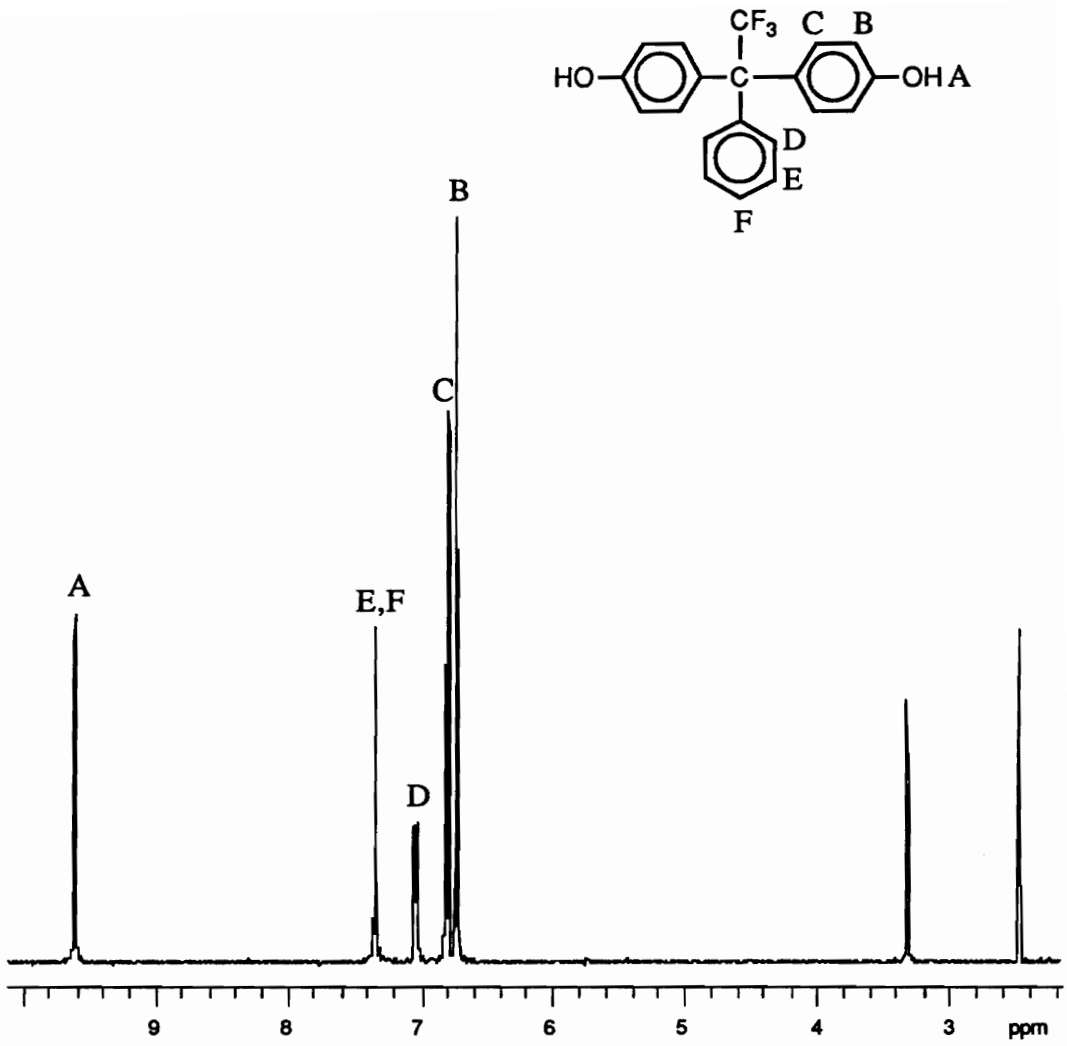

Figure 4.4: The 400 MHz Proton NMR Spectrum of 3F-Bisphenol (1,1-bis(4-hydroxyphenyl)-1-phenyl-2,2,2-trifluoroethane)

peaks in ^1H NMR of 3F-bisphenol were assigned and the integration of the peaks correlate well with the theoretical values. The FTIR analysis (Figure 4.5) shows the strong, broad peak at 3250 cm-1 which is characteristic of the hydroxyl group on the 3F-bisphenol. The molecular weight of 3F-bisphenol is 344 g/mol and the parent ion peak in the mass spectrogram (Figure 4.6) appeared at 344. A major peak occurred at 275 which correlates to the 3F-bisphenol minus the trifluoromethyl group (CF_3). This species may be formed because the loss of the CF_3 group would produce a trityl ion which is stabilized by three aromatic rings. Lastly, the elemental analysis (Table 4.2) shows a good correlation between the theoretical and the experimental values.

4.1.1.2 Step 2: Formation of the 3F-Dinitro Precursor Via a Nucleophilic Aromatic Substitution Reaction

The second step in this procedure is the formation of the 3F-dinitro compound via a nucleophilic aromatic substitution reaction of the 3F-bisphenol with 4-fluoronitrobenzene as shown in Figure 4.7. This is a quantitative reaction but after purification the best yield obtained was 95%. It was necessary to purify the 3F-dinitro compound prior to the hydrogenation. Otherwise, it was extremely difficult to purify the diamine. The 3F-dinitro compound was characterized by ^1H NMR (Figure 4.8). The chemical shift for the aromatic protons ortho to the electron withdrawing nitro functionality appear downfield at 8.2 ppm and the peak integration values matched the theoretical predictions. Bands representative of the nitro functionality were identified in the FTIR spectrum (Figure 4.9) which were the asymmetrical stretch at 1580 cm^{-1} and the symmetrical stretch at 1340 cm^{-1} (133). The band at 880 cm^{-1} representative of

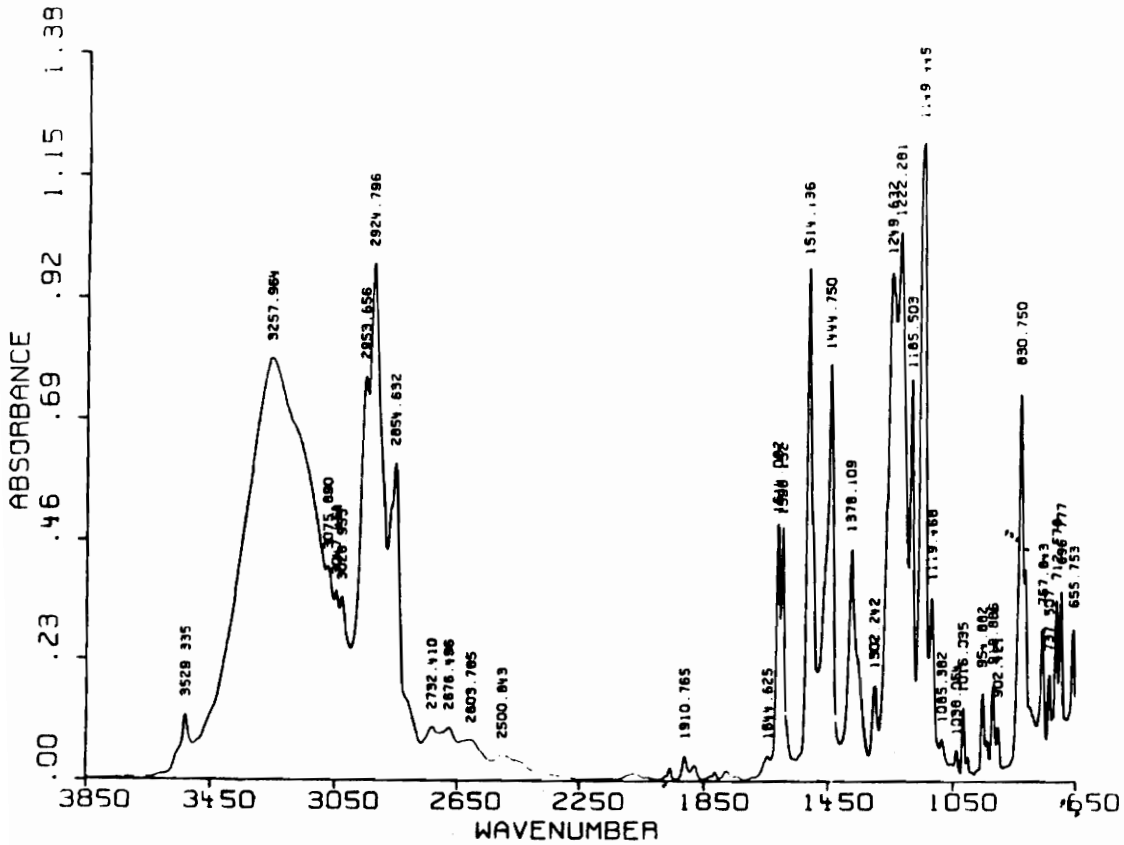

Figure 4.5: The FTIR of 3F-Bisphenol (A: O-H stretch at 3250 cm^{-1})

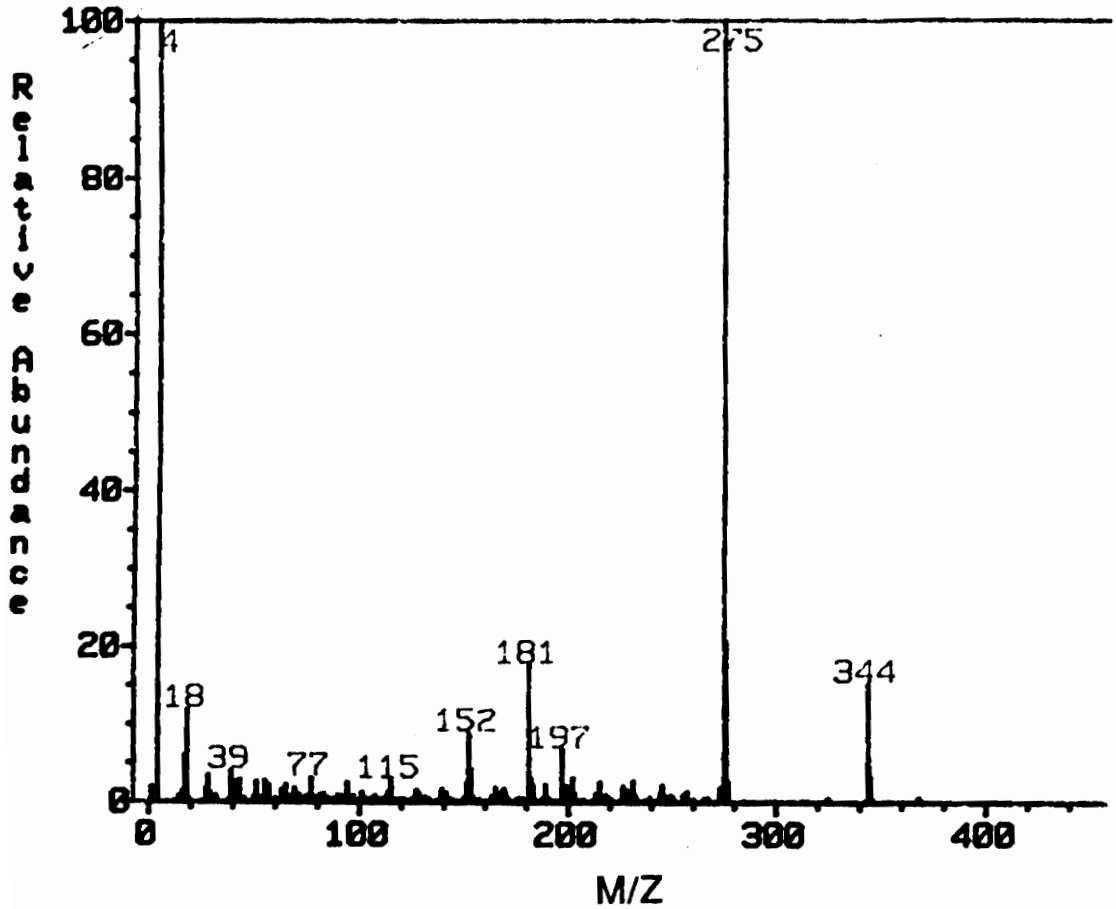

Figure 4.6: Mass Spectrum of 3F-Bisphenol

Table 4.2: Elemental Analysis of the 3F Monomers

MONOMER	CARBON		HYDROGEN		NITROGEN	
	Theor.	Exper.	Theor.	Exper.	Theor.	Exper.
3F-Bisphenol	0.698	0.696	0.044	0.043	---	---
3F-Dinitro	0.655	0.654	0.036	0.036	0.048	0.047
3FEDAM	0.730	0.728	0.048	0.047	0.053	0.053

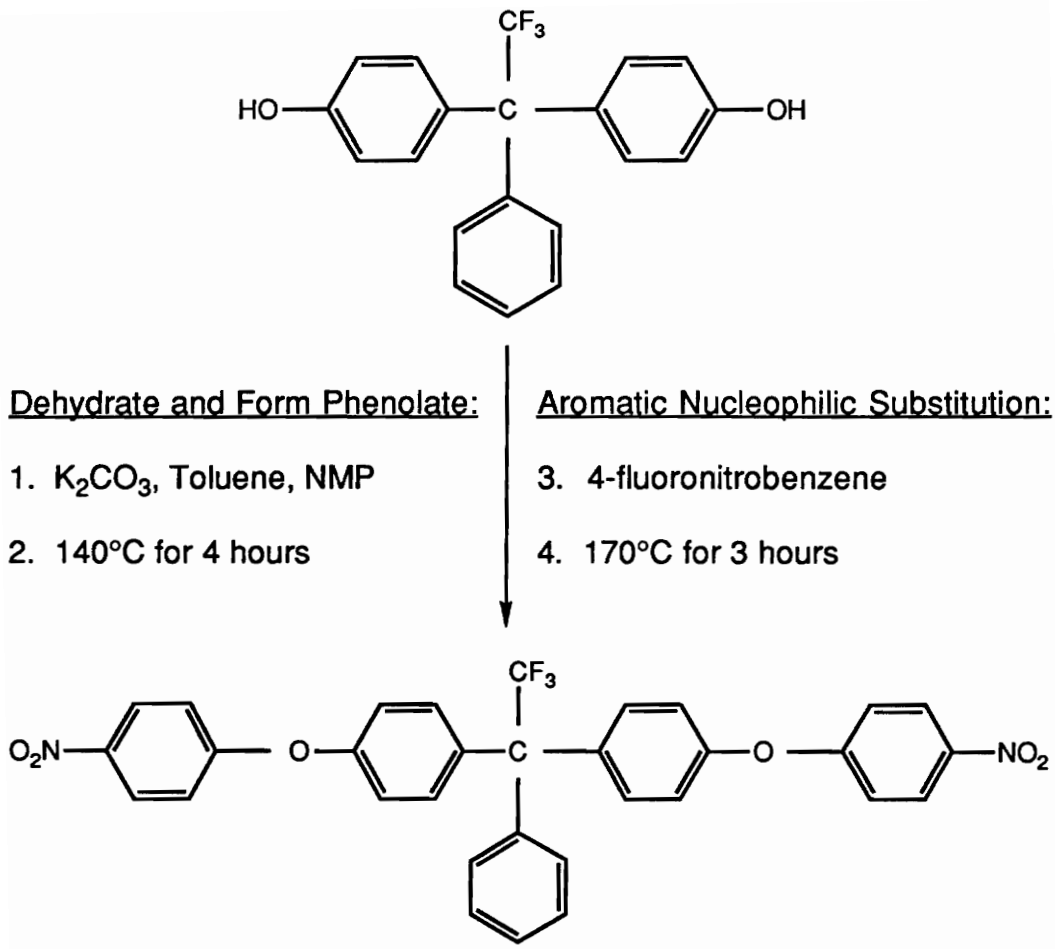

Figure 4.7: Synthesis of 1,1-bis[4-(4-nitrophenoxy)phenyl]-2,2,2-trifluoroethane (3F-Dinitro) Via Nucleophilic Aromatic Substitution Reaction

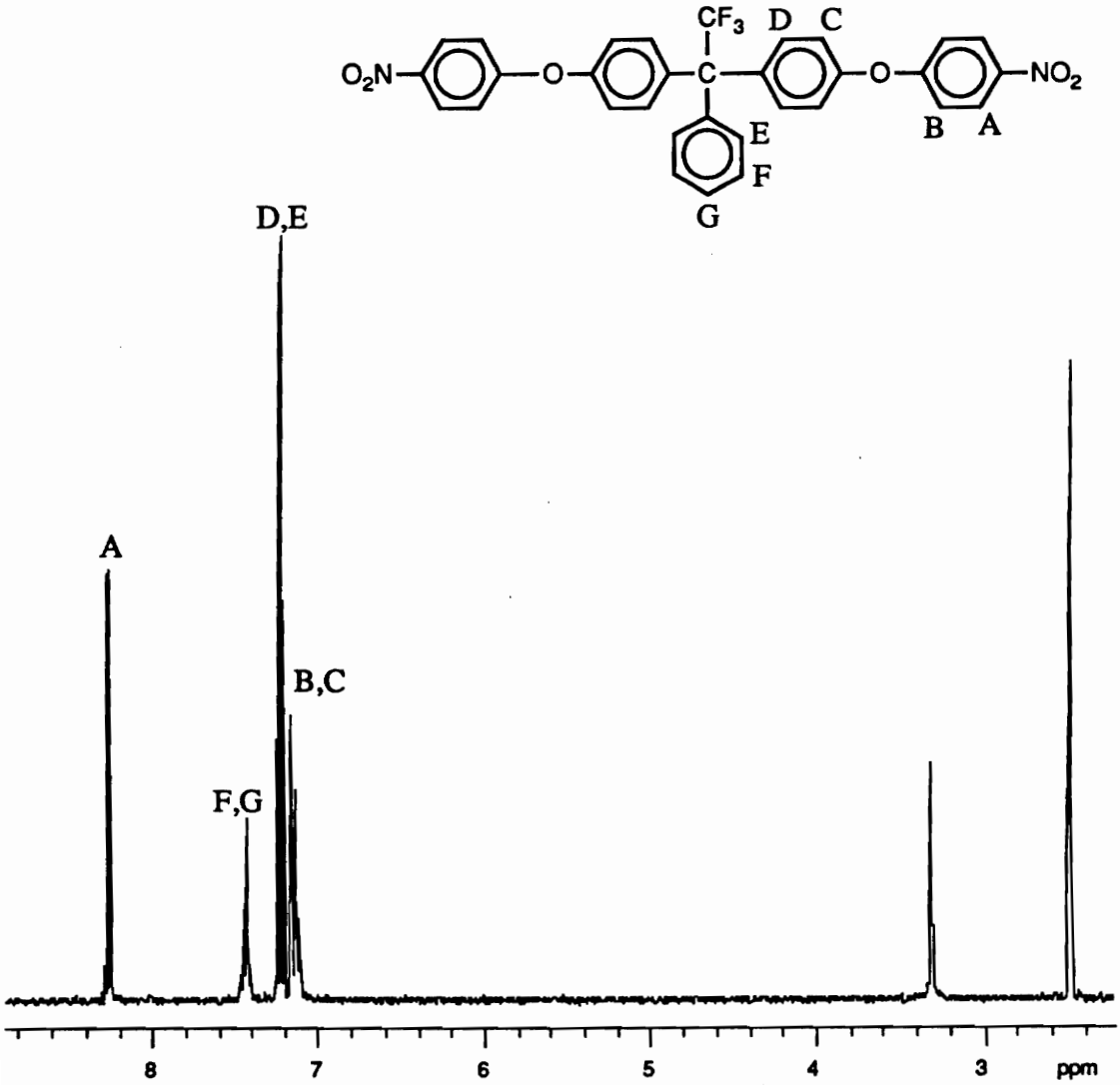

Figure 4.8: The 400 MHz Proton NMR Spectrum of 1,1-bis[4-(4-nitrophenoxy)phenyl]-2,2,2-trifluoroethane (3F-Dinitro)

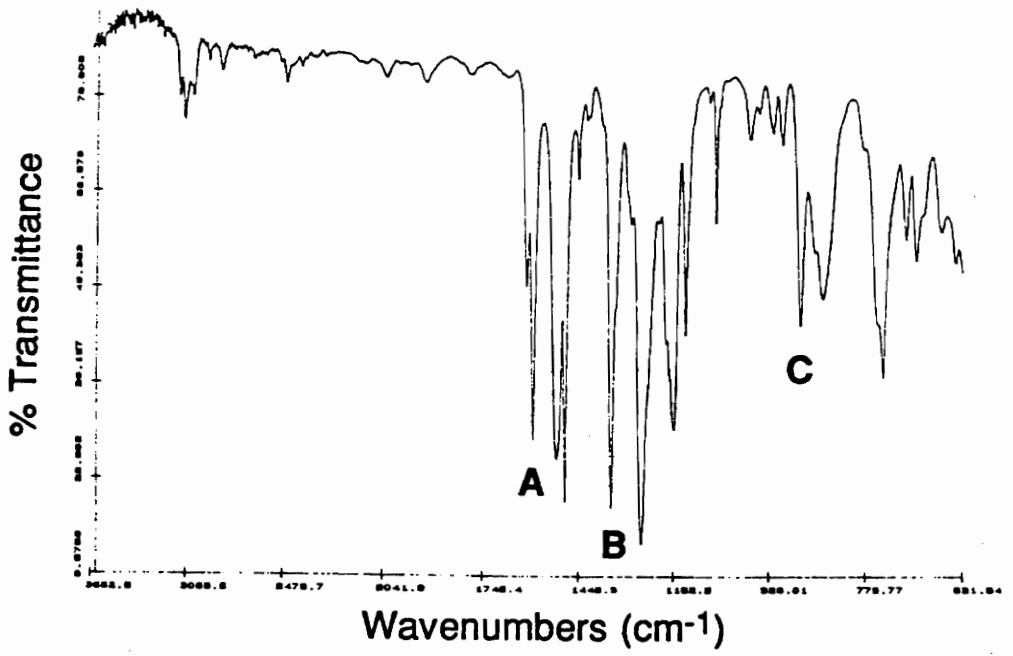

Figure 4.9: The FTIR of 3F-Dinitro (A: asymmetrical stretch at 1584 cm^{-1}; B: symmetrical stretch at 1347 cm^{-1}; C: C-N stretch at 880 cm^{-1})

the C-N stretch was also apparent in the FTIR spectrum. The elemental analysis results are summarized in Table 4.2.

4.1.2 One Step Procedure to the 1,1-bis[4-(4-nitrophenoxy) phenyl]-1-phenyl-2,2,2-trifluoroethane (3F-Dinitro) Precursor

4.1.2.1 Hydroxyalkylation Reaction of Trifluoroacetophenone With 4-Nitrophenyl Phenyl Ether

The 3F-dinitro precursor can also be prepared via a one step method as shown in Figure 4.1. The first step is a hydroxyalkylation reaction of the trifluoro-acetophenone with 4-nitrophenyl phenyl ether to provide the 3F-dinitro compound as shown in Figure 4.10. This hydroxyalkylation reaction must be treated in the same manner as previously discussed for the hydroxyalkylation reaction of trifluoroacetophenone with phenol. The maximum yield of the 3F-dinitro compound was approximately 85% when 5% excess triflic acid was used. The ^{1}H NMR, FTIR, melting point, and elemental analysis of the 3F-dinitro compound synthesized via the hydroxyalkylation were identical to the 3F-dinitro compound prepared by the nucleophilic aromatic substitution reaction.

4.1.3 Preparation of 1,1-bis[4-(4-aminophenoxy)phenyl]-1-phenyl-2,2,2-trifluoroethane (3FEDAM) Via Hydrogenation of the 3F-Dinitro Precursor

The final step of both procedures to prepare the 3FEDAM diamine was catalytic hydrogenation (134) of the 3F-dinitro compound (Figure 4.11). Methanol (135) and ethanol (136) are common solvents for hydrogenations. However, the 3F-dinitro compound is insoluble in alcohols. Lau and Vo (137)

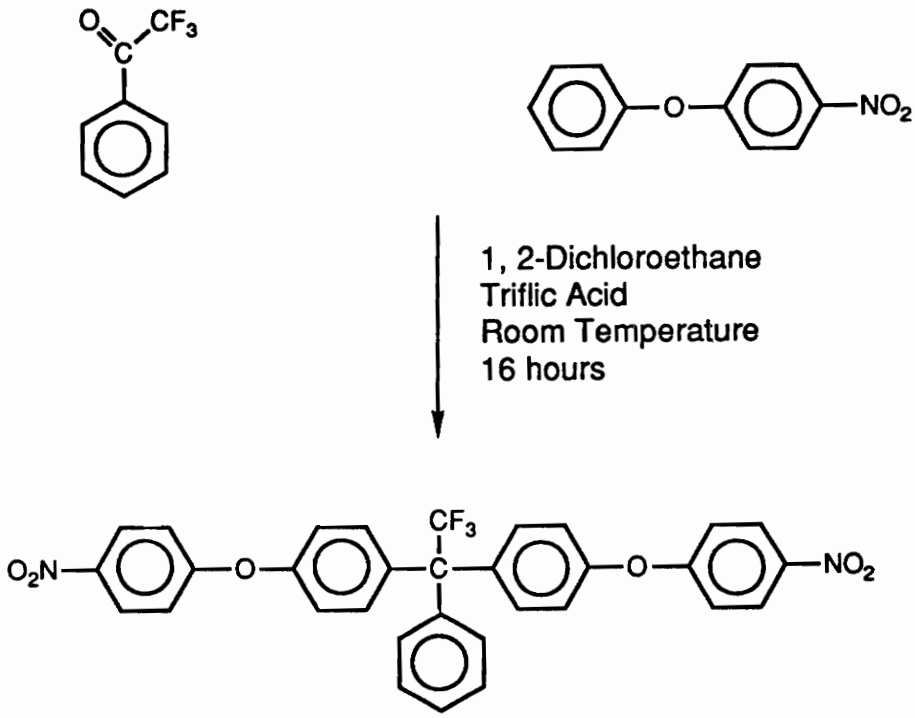

Figure 4.10: The Synthesis of 3F-Dinitro Via Hydroxyalkylation of Trifluoroacetophenone With 4-Nitrophenyl Phenyl Ether

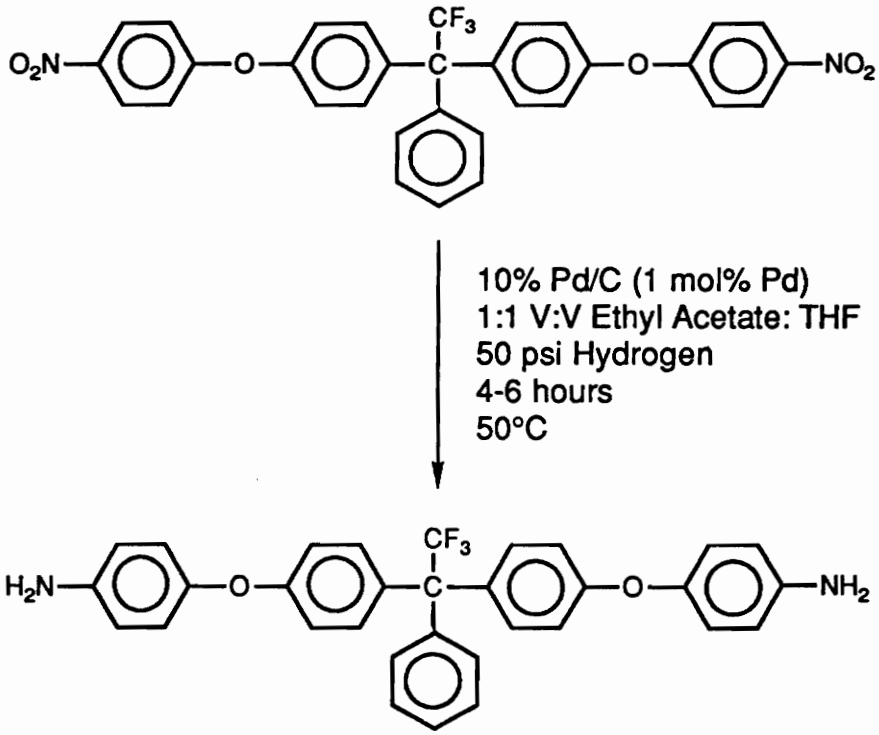

Figure 4.11: The Synthesis of 3FEDAM Via Catalytic Hydrogenation of 3F-Dinitro

prepared aromatic diamines via hydrogenation of bis-nitro compounds in which a 1:1 v/v mixture of THF and ethyl acetate was used. The 3F-bisphenol was soluble in a 1:1 v/v mixture of THF and ethyl acetate was a good solvent for the hydrogenation. In addition, this solvent system was easily removed from the final product which enhanced the ease of purification.

The course of the reaction was monitored by hydrogen consumption and by high resolution proton NMR. When the consumption of hydrogen ceased, the reaction was considered to be complete. ^{1}H NMR was an excellent tool to follow the hydrogenation as shown in Figure 4.12. The peak for the protons that are ortho to the nitro functionality appear at 8.2 ppm and the peak at 6.6 ppm denotes the aromatic protons ortho to the amine functionality. As the hydrogenation proceeds, the peak at 8.2 ppm disappears and the peak at 6.6 ppm grows in intensity. By taking the ratio of the integration of the peaks at 8.2 ppm and 6.6 ppm, the degree of hydrogenation can be estimated. As shown in Figure 4.12, approximately 30% of the nitro groups have been converted to amine groups. The reduction of the 3F-dinitro precursor was quantitatively complete when the chemical shift at 8.2 ppm was absent in the NMR spectrum of 3FEDAM (Figure 4.13). The chemical shift at 5.0 ppm which is characteristic of the primary aromatic amine protons was also used to identify the diamine. Infrared spectroscopy was employed to demonstrate conversion of the dinitro compound to the diamine compound. Absorptions at 3464 and 3377 cm^{-1} representative of the aromatic primary amine are exhibited in Figure 4.14 and bands for nitro groups are absent. HPLC analysis was utilized to ascertain the level of purity of 3FEDAM. This showed a single peak indicating that the 3FEDAM was monomer grade purity. Fluorine-19 NMR (Figure 4.15) was

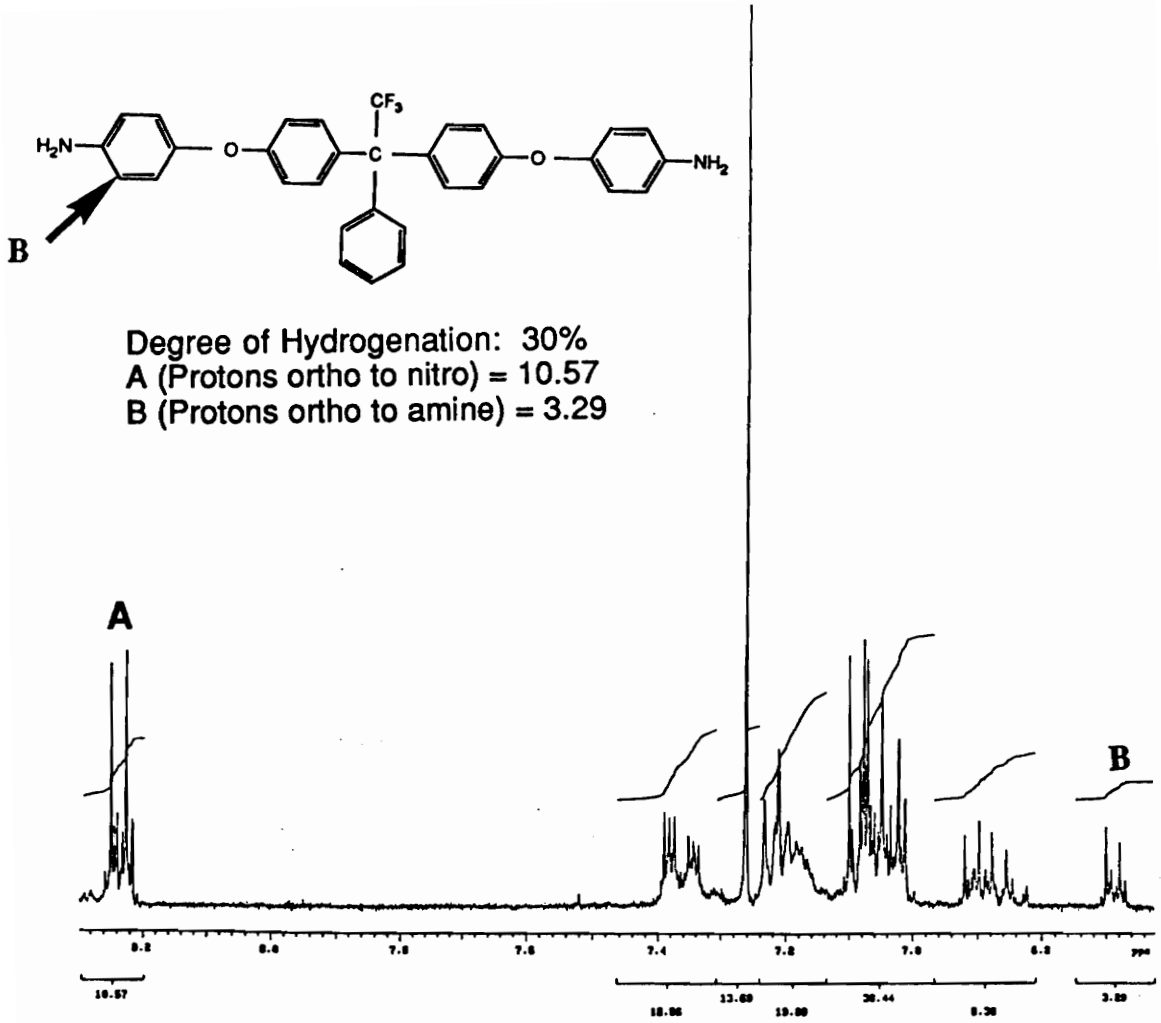

Figure 4.12: The 400 MHz Proton NMR Spectrum of the Partial Hydrogenation of 3F-Dinitro to the 3FEDAM Compound

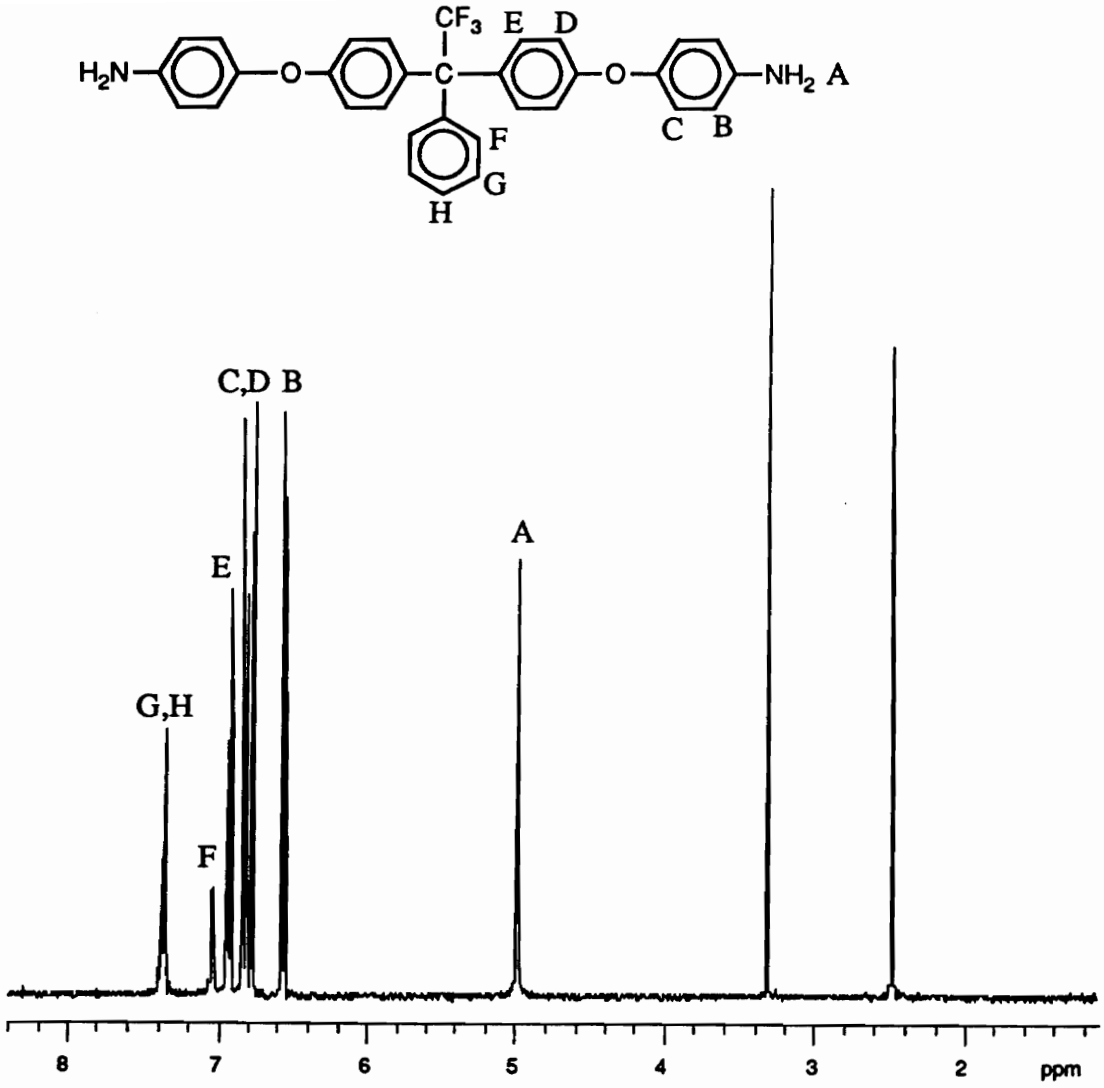

Figure 4.13: The 400 MHz Proton NMR Spectrum of 1,1-bis[4-(4-aminophenoxy)phenyl]-1-phenyl-2,2,2-trifluoroethane (3FEDAM): The Quantitative Hydrogenation of 3F-Dinitro Compound

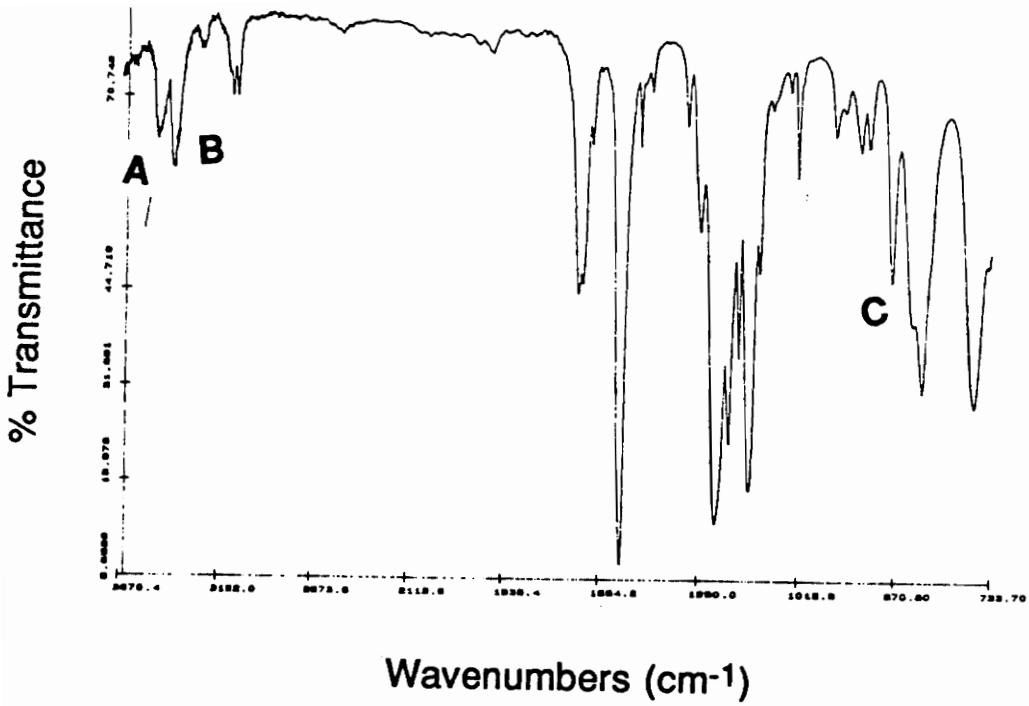

Figure 4.14: The FTIR Spectrum of 1,1-bis[4-(4-aminophenoxy)phenyl]-1-phenyl-2,2,2-trifluoroethane (3FEDAM) (A: asymmetrical stretch at 3464 cm^{-1}; B: symmetrical stretch at 3377 cm^{-1}; C: C-N stretch at 871 cm^{-1})

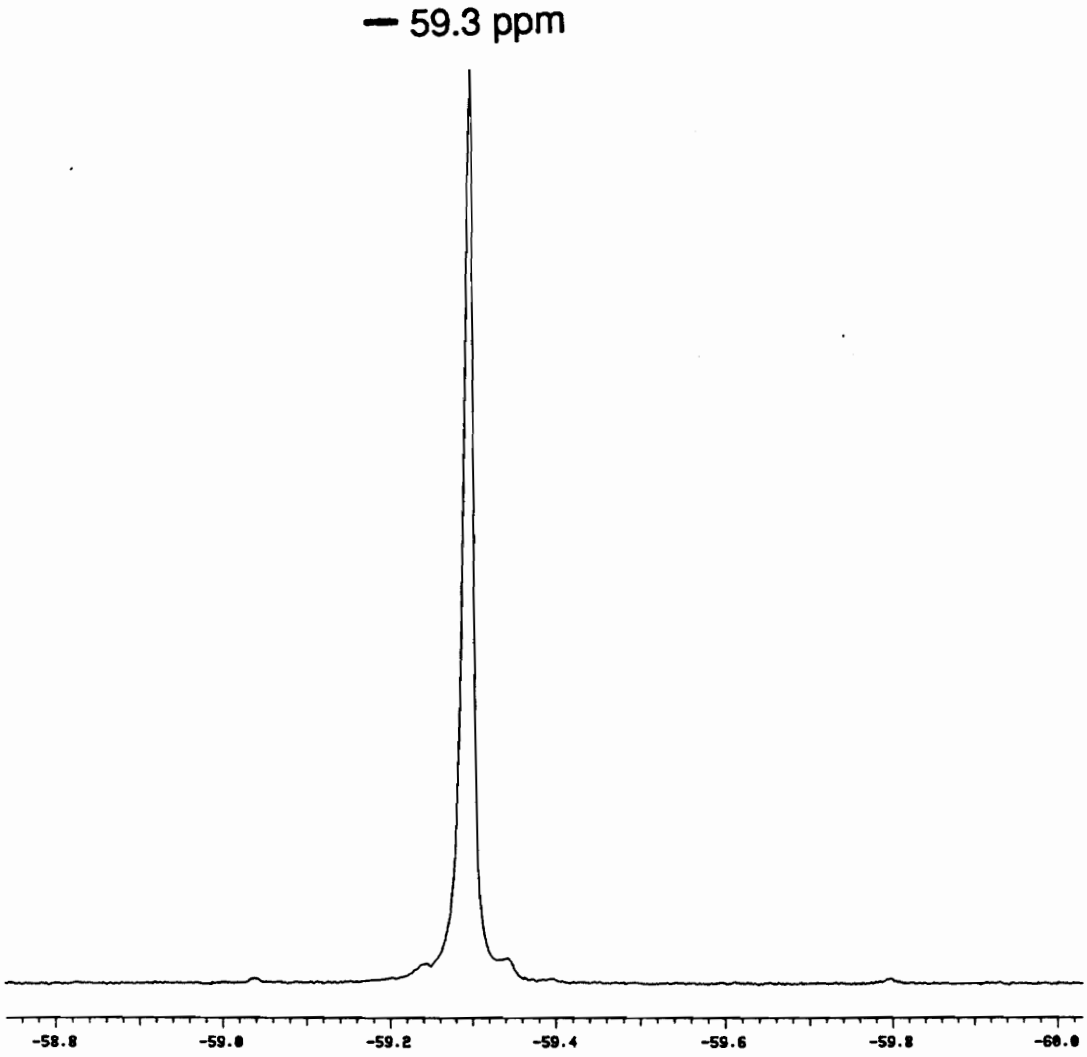

Figure 4.15: The ^{19}Fluorine NMR Spectrum of 1,1-bis[4-(4-aminophenoxy)phenyl]-1-phenyl-2,2,2-trifluoroethane (3FEDAM)

employed to prove that only one product was formed. Since the fluorine NMR displayed a single peak, it was concluded that only one fluorinated species was present.

Potentiometric titration was also used to identify the novel diamine and the level of purity. Potentiometric titration has been used to determine the degree of imidization of polyimides (26) and to characterize the formation of poly(amide-imides) (138). In this case, potentiometric titration provided the molecular weight of the diamine which was 525.3 g/mol. The theoretical molecular weight for 3FEDAM is 526.5 g/mol which is within instrumental error of the experimental result.

The characteristic monomer properties are summarized in Table 4.3.

4.2 Polyimide Characterization

4.2.1 Synthesis of Polyimides

The polyimides were prepared by the reaction of diamines with dianhydrides to form the poly(amic acid) followed by cyclodehydration as illustrated in Figure 4.16. A solution imidization procedure was used to quantitatively convert the poly(amic acid) intermediates to the corresponding polyimides. The solution imidization of the amic acid was done in a NMP/DCB cosolvent system of NMP with DCB and was conducted at milder temperatures than the classical bulk imidization. The bulk imidization requires temperatures of approximately 300°C. However, the solution imidization technique was performed at 165°C for 24 hours. Addition of the cosolvent into the poly(amic acid) solution acts as an azeotroping agent. A 8:2 mixture of NMP/DCB efficiently removed the water formed upon conversion of the amic acid to the

Table 4.3: Summary of the 3F Monomer Properties

Monomer	Color	Melting Point	% Yield	Recryst. Solv.
3F-Bisphenol	White	231.0-232.0	85	CH_2Cl_2‡
3F-Dinitro	Tan	196.5-197.2	95*, 85**	Acetic Acid
3F-EDAM	Off-white	169.0-170.0	95	100% Ethanol

‡Monomer was washed in methylene chloride
*Via the aromatic nucleophilic substitution reaction
**Via the hydroxyalkylation reaction

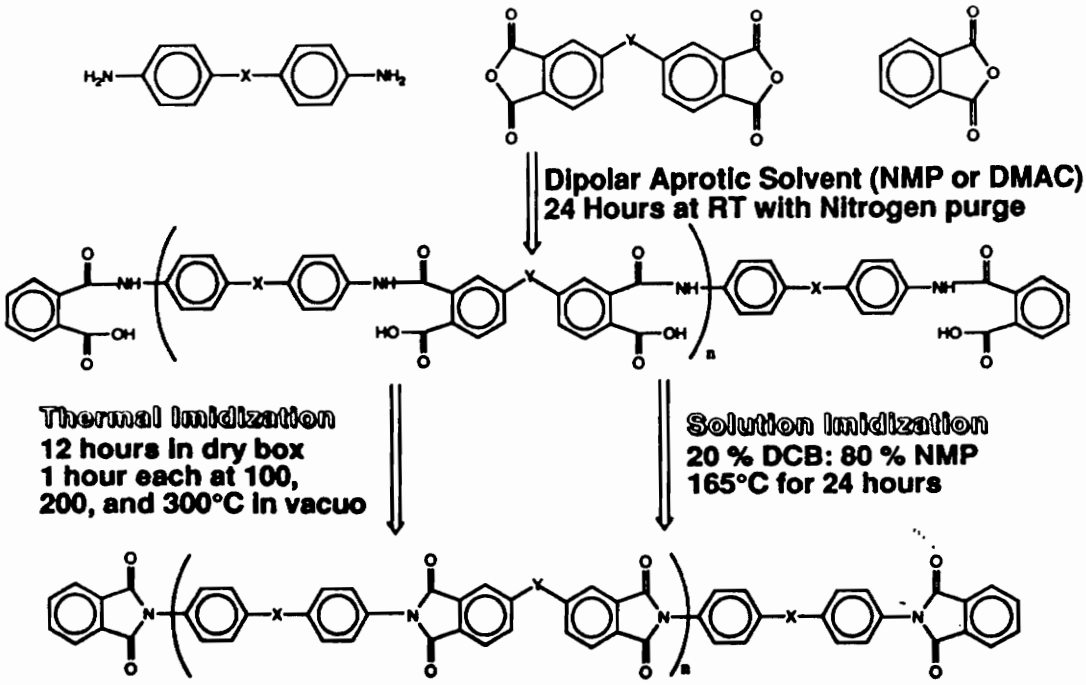

Figure 4.16: Synthesis of Fully Cyclized Polyimides

imide. Conversion of the poly(amic acid) to the fully cyclized polyimide may be monitored by FTIR (53, 55, 139). The FTIR spectrum of a fully cyclized t-butyl phthalimide endcapped 3FDAM-PMDA polyimide is shown in Figure 4.17. Complete cyclodehydration was confirmed by the appearance of characteristic imide related infrared absorption bands in the range of 1770-1780 cm^{-1} (symmetrical imide I), 1710-1735 cm^{-1} (asymmetrical imide I), and the disappearance of the amic acid band at 1535 cm^{-1}. In adddition, absorption bands at 3460 and 3370 cm^{-1} which are representative of primary aromatic amines are not observed in this spectrum. Therefore, the amine endgroups are assumed to be quantitatively capped with t-butyl phthalic anhydride.

4.2.2 Molecular Weight and Endgroup Control

Molecular weight and endgroup control can be assessed by several techniques which include NMR, GPC, and dilute solution viscosity. Many of the amorphous polyimides were soluble in several solvents which allowed analysis by solution techniques. However, the semicrystalline polyimides were highly solvent resistant and could not be analyzed in this manner. The solution viscosity of the corresponding poly(amic acid)s were measured to estimate the molecular weight of the semicrystalline polyimides.

To demonstrate the effectiveness of endgroup and molecular weight control, the number average molecular weight of a series of 3FDAM-PMDA polyimides endcapped with t-butyl phthalic anhydride was measured by ^1H NMR. A characteristic ^1H NMR spectrum of the 20,000 molecular weight material is provided in Figure 4.18. The t-butyl phthalimide is clearly identified by the resonance observed at about 1.4 ppm. The t-butyl peak can be ratioed to

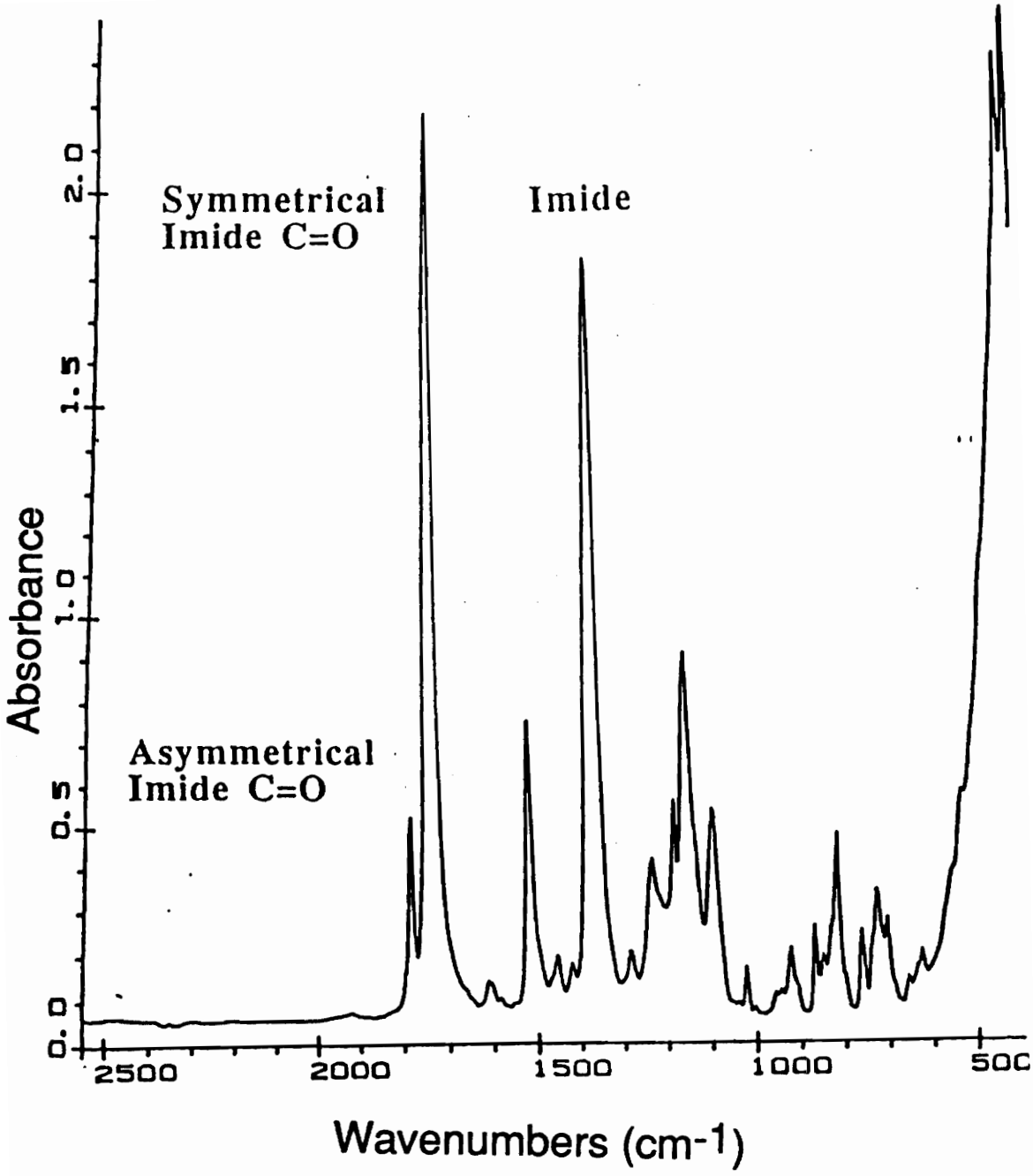

Figure 4.17: FTIR Spectrum of the Fully Cyclized t-Butyl Phthalamide Endcapped 3FDAM-PMDA Polyimide

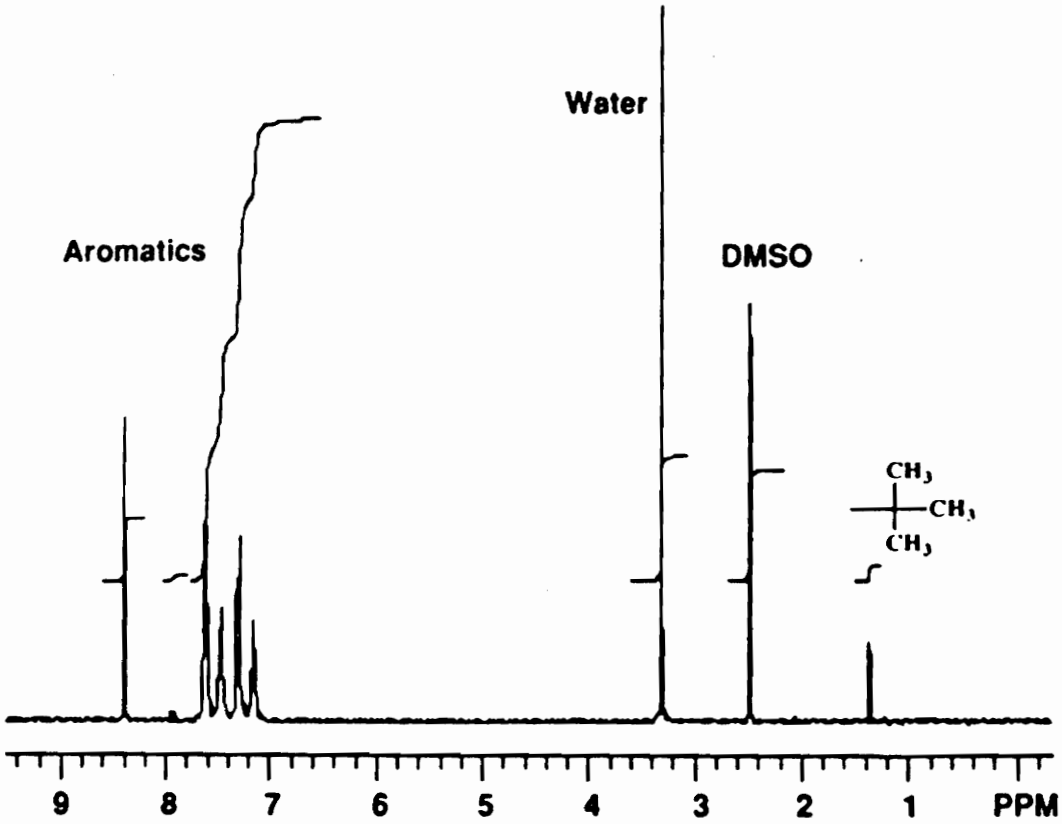

Figure 4.18: The 400 MHz Proton NMR Spectrum of the 20,000 g/mol 3FDAM-PMDA Polyimide Endcapped With t-Butyl Phthalimide

the aromatic protons to allow an estimate number average molecular weight. The number average molecular weight determined by ^1H NMR are in good agreement with the theoretical calculations (Table 4.4). The intrinsic viscosities were also measured and seem reasonable given the calculated molecular weights. The NMR spectrum of the polyimide also provides evidence that the chain ends are endcapped with t-butyl phthalic anhydride. In the ^1H NMR (Figure 4.19) of the 3FDAM diamine monomer, the chemical shift for the aromatic primary amine protons are observed at 5.2 ppm. Upon inspection of the ^1H NMR of the polyimide, the chemical shift for the amine protons are absent; therefore, the amine ends of the chain have been quantitatively capped with t-butyl phthalic anhydride.

Absolute molecular weights can be determined using GPC with universal calibration. These measurements were conducted by Dr. M. Konas. Several soluble polyimides were prepared with a target number average molecular weight (Mn) of 30,000 g/mol. The GPC and intrinsic viscosity results are summarized in Table 4.5. The absolute molecular weight of the BDAF-BPDA and the 3FEDAM-BPDA polyimides were 30,000 g/mol which is in excellent agreement with the theoretical calculations. The intrinsic viscosity values determined by the Viscotek detector correlate well with the intrinsic viscosity values that were determined independently using Cannon-Ubbelohde viscometers. The influence of solvent on the intrinsic viscosity values is shown in Table 4.6. NMP is highly polar and is a better solvent for polyimides than the less polar chloroform. Therefore, the hydrodynamic volume of the polyimides in NMP should be greater than in chloroform. Consequently, the intrinsic viscosity values in NMP should be higher than those measured in chloroform. However,

Table 4.4: Molecular Weight Evaluation of 3FDAM-PMDA-tBuPa Polyimides Via NMR and Solution Viscosity

Mn theor (g/mol)	Mn NMR (g/mol)	[η] (dL/g)
10,000	10,200	0.32
20,000	18,500	0.47
30,000	33,600	0.65

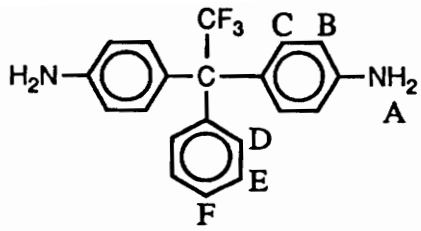

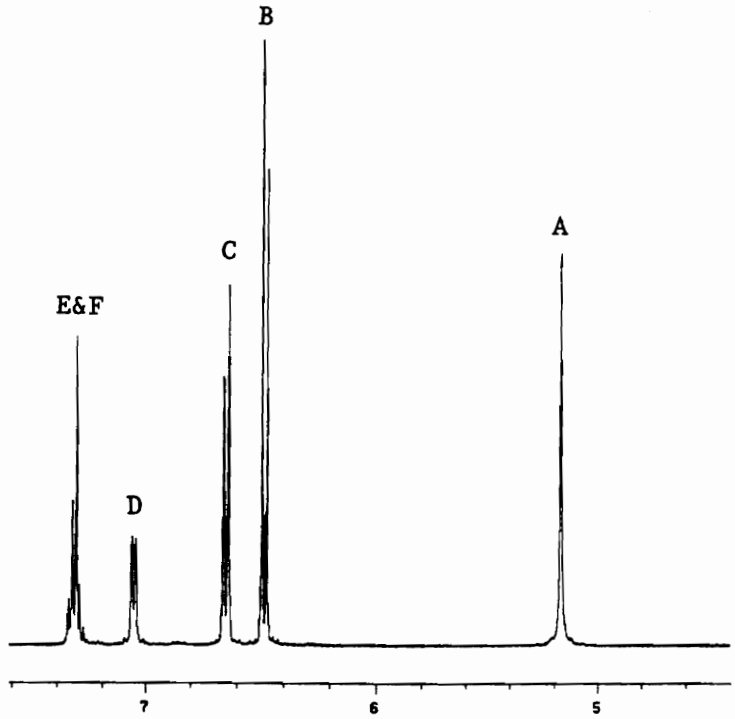

Figure 4.19: The 400 MHz Proton NMR Spectrum of 3FDAM

Table 4.5: Determination of Absolute Molecular Weights Via GPC With Universal Calibration of Soluble Polyimides

Polyimide	Mn theor (g/mol)	Mn GPC (g/mol)	[η]* GPC (dL/g)	[η]** (dL/g)
3FEDAM-BPDA-PA	30,000	30,900	0.70	0.67
3FDAM-BPDA-tBuPA	30,000	46,000	0.29	0.37
BDAF-PMDA-PA	30,000	30,100	0.66	0.69

*Chloroform at 30°C

**Chloroform at 25°C

Table 4.6: Intrinsic Viscosity Values of Several Soluble Fluorinated Polyimides In NMP and Chloroform

Polyimide	Mn theor (g/mol)	[η]* (dL/g)	[η]** (dL/g)
BDAF-ODPA-PA	30,000	0.66	---
3FDAM-BPDA-PA	30,000	0.44	0.67
3FDAM-6FDA-PA	30,000	0.36	---
3FEDAM-6FDA-PA	30,000	0.47	0.82

*NMP at 25°C

**$CHCl_3$ at 25°C

the viscosities measured in NMP were lower than in chloroform. A reasonable explanation for these results may be the NMP contained water because the NMP was used as received. The presence of water may deleteriously effect the solubility of the polyimide; therefore, reducing the hydrodynamic volume and lowering the viscosity.

The molecular weight of semicrystalline polyimides was estimated by measuring the solution viscosity of the poly(amic acid)s. In most cases, the poly(amic acid)s were isolated by precipitation into cold water. The water and residual solvent must be completely removed to provide accurate values of the viscosity. The polymers were extensively dried in vacuo at room temperature for several days and up to 50°C for 1 to 2 days. Several molecular weights of TPEQ-ODPA polyimide systems were prepared by utilizing the

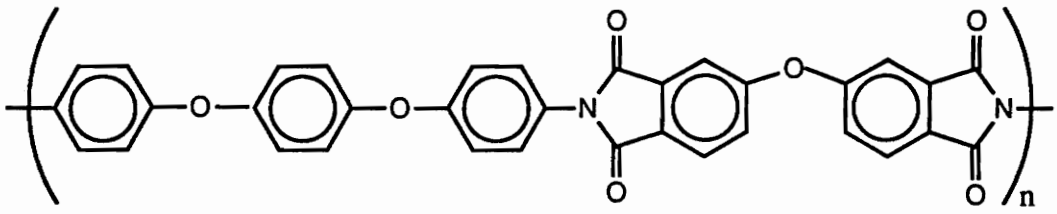

Repeat Unit Representing the TPEQ-ODPA Polyimide

Carother's equation to calculate the amount of phthalic anhydride needed. The intrinsic viscosity values of the poly(amic acid)s were determined and are shown in Table 4.7. These values can be used to qualitatively evaluate the molecular weight. As the target Mn increased, the intrinsic viscosity increased as expected.

Table 4.7: Intrinsic Viscosity Values of TPEQ-ODPA-PA Poly(amic acid)s

Mn theor (g/mol)	$[\eta]_{NMP}^{25°C}$ (dL/g)
7,500	0.25
10,000	0.29
15,000	0.32
20,000	0.34
30,000	0.42

4.2.3 3FEDAM Based Polyimides

4.2.3.1 Homopolyimides Derived From 3FEDAM

Films of 3FEDAM based polyimides were prepared by bulk imidization of the poly(amic acid). An uncontrolled molecular weight 3FEDAM-PMDA polyimide was synthesized by adding the stoichiometric amount of each monomer. As calculated from the Carother's equation, an appropriate amount of the monofunctional endcapping reagent, phthalic anhydride, was added to synthesize a 3FEDAM-PMDA polyimide with an Mn of 30,000 g/mol. The resulting thermally imidized polyimide films were transparent and yellow to amber in color. The thermal properties of these films were analyzed by differential scanning calorimetry (DSC) and thermogravimetric analysis (TGA) (Table 4.8). The high molecular weight (MW) polyimide displayed a Tg of316°C and did not exhibit an endothermic transition on the first heat in the DCS thermogram. WAXS analysis (Figure 4.20) showed a broad amorphous halo indicating that the material was noncrystalline. However, it was possible to induce crystallinity by annealing. After holding at 400°C in the DSC for 30 minutes, a broad endotherm with a peak value of 482°C and a heat of fusion of 20 J/g was observed.

The controlled MW 3FEDAM-PMDA-PA polyimide displayed a large endotherm with a peak value of 476°C on the first heat (Figure 4.21) which is very different from the result of the high MW polyimide. A reasonable explanation for these results may be unveiled by considering the melt viscosity of the two materials during bulk imidization. The melt viscosity is lower for the controlled MW polyimide and correspondingly the chains have more mobility, thereby providing a higher propensity to attain the correct orientations to

Table 4.8: Thermal Analysis Results of 3FEDAM-PMDA Homopolyimides

Polymer	Tg (°C)*	Tm (°C)*	5% Wt Loss (°C)**
HIGH MW	316	482 (A)	552
30K MW	308	476	528

*in nitrogen at 10°C/min
**in air at 10°C/min

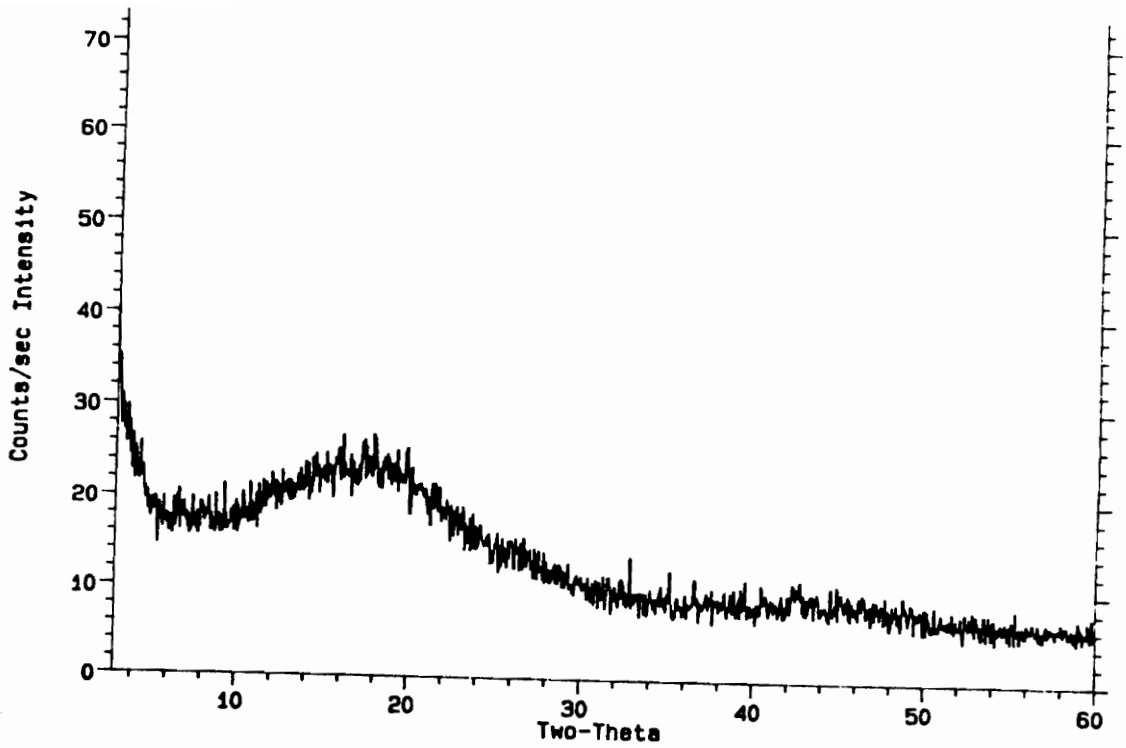

FIGURE 4.20: WAXS Analysis of 3FEDAM-PMDA Polyimide

(uncontrolled molecular weight)

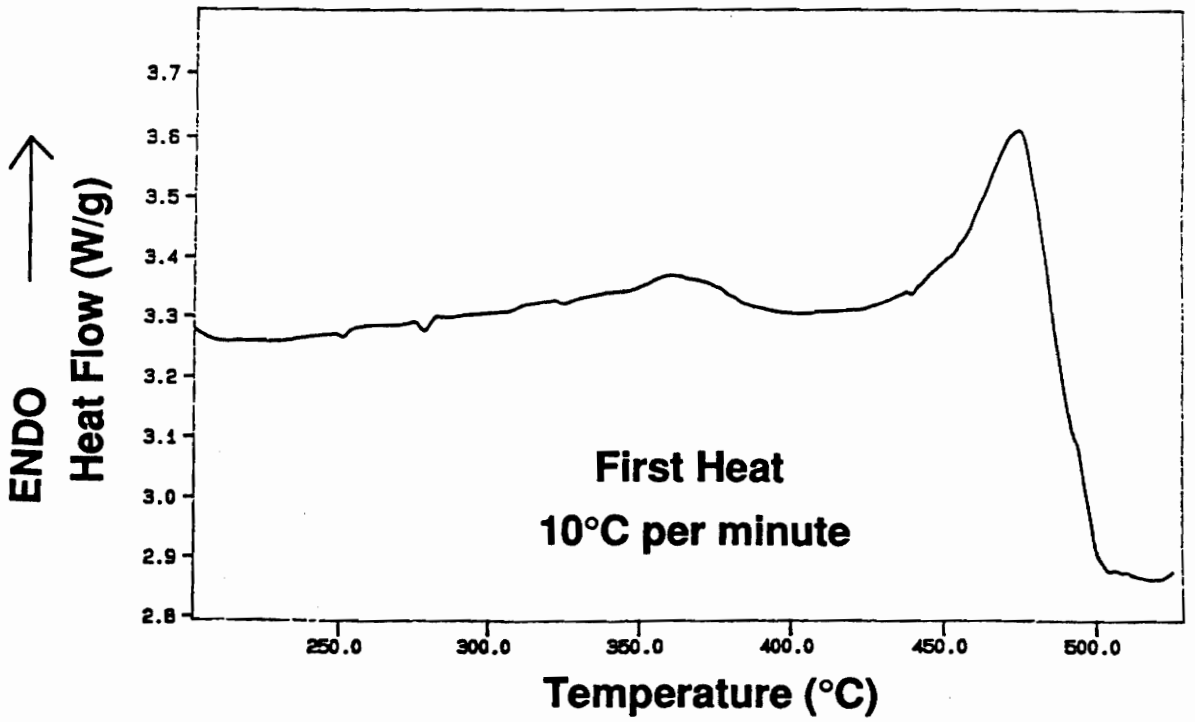

Figure 4.21: Thermal Analysis of 3FEDAM-PMDA-PA (30K)

First Heat

crystallize. Unfortunately, the 3FEDAM-PMDA-PA (30K) polyimide begins to degrade upon melting. Therefore, the heat of fusion of the melting transition was not evaluated. In the second heat of the thermogram (Figure 4.22), the endothermic transition was not observed. This suggests that the crystallinity may have been solvent induced. As discussed in the literature review, Waddon and Karasz (91) prepared a semicrystalline polyimide from solution and Wang and coworkers (90) discovered that NMP induced crystallization of a chemically imidized aromatic polyimide.

As in the case of the high MW 3FEDAM-PMDA polyimide, crystallinity could be induced thermally. The initial crystallinity of the polyimide sample was erased by heating to 500 °C and holding for 1 minute. After annealing at 400°C for 60 minutes, a broad endothermic peak was observed at 448°C which is 28°C lower than the untreated polyimide. It appears that these materials have the potential to crystallize; however, it is most likely that the rate of crystallization is very slow, similar to other stiff chain systems. Waddon and Karasz (91) stated that aromatic, stiff-chain macromolecules have very low crystallization rates which they attributed to chain rigidity. Huo and coworkers (102) discovered that the aromatic polyimide, NEW TPI, had relatively slow crystallization kinetics compared to other high performance thermoplastic polymers.

The effect of annealing the 3FEDAM-MDA-PA (30K) polyimide is clearly evident in the WAXS analysis (Figure 4.23). Since the values for the heat of fusion for the untreated and the annealed polyimides could not be compared, WAXS was instrumental in determining effects of the thermal treatment. The 3FEDAM-PMDA-PA (30K) polyimide was held at 400°C for 30 minutes. The annealed 3FEDAM-PMDA-PA polyimide showed less amorphous character

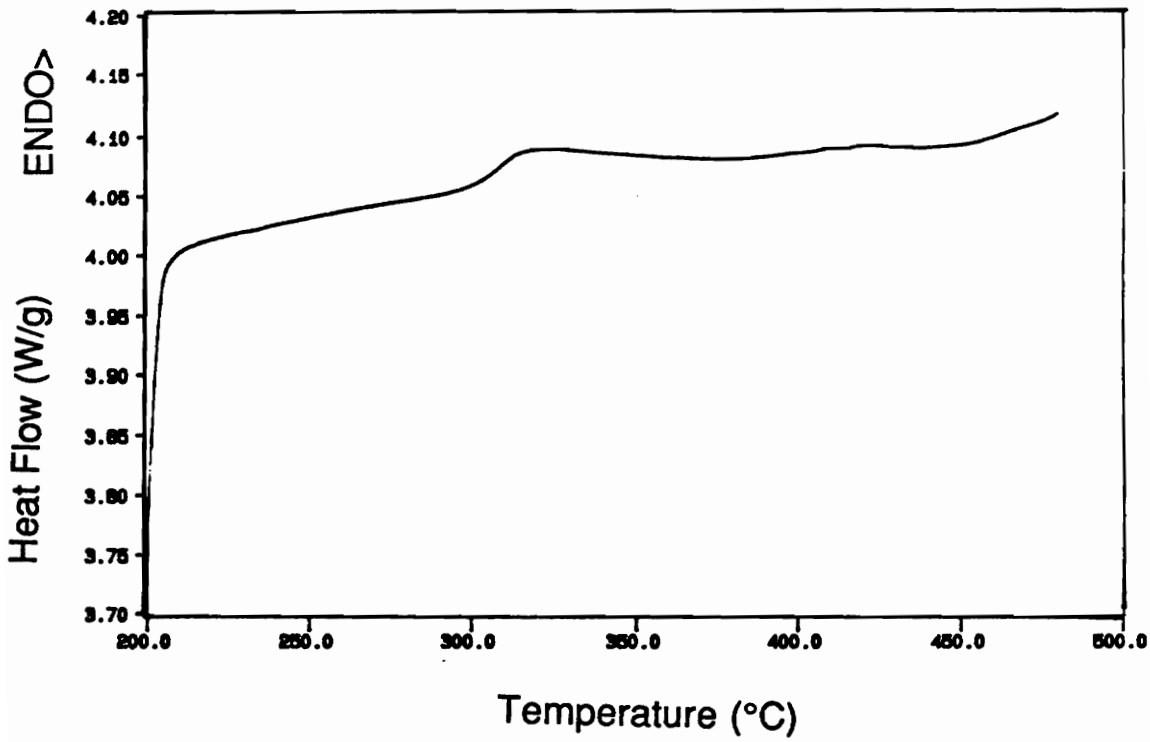

Figure 4.22: DSC Thermogram of 3FEDAM-PMDA-PA (30K)

Second Heat

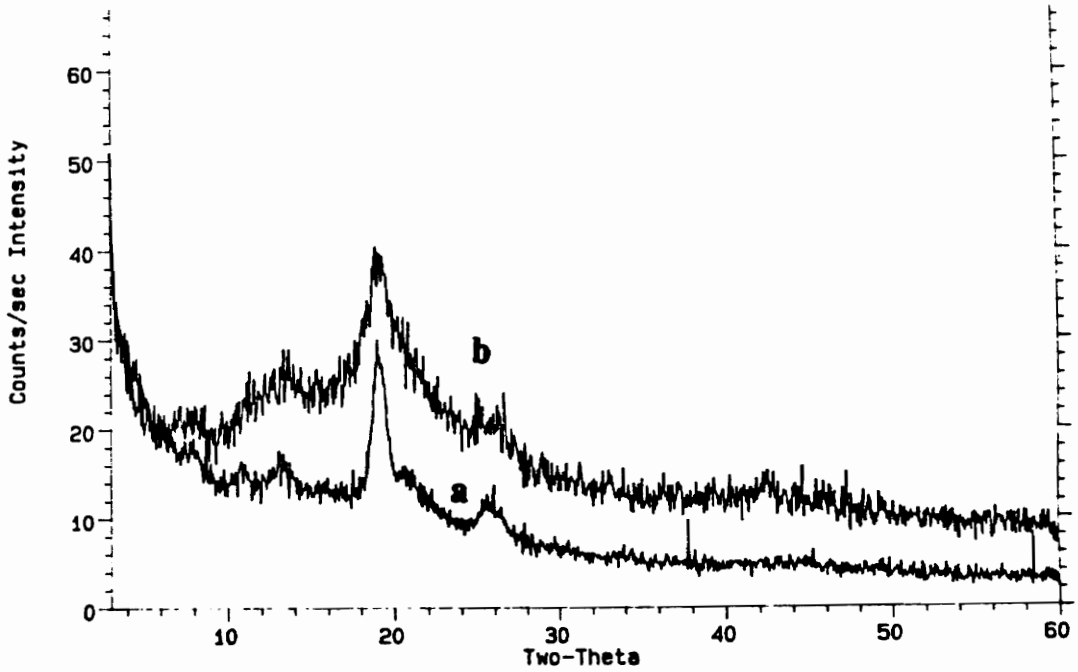

Figure 4.23: WAXS Analysis of 3FEDAM-PMDA-PA (30K)

(a: annealed at 400°C for 30 minutes; b: untreated sample)

and sharper peaks than the untreated polyimide. These results suggest that the crystallinity was enhanced for the thermally treated material.

The Tg of the 3FEDAM-PMDA-PA (30K) polyimide was clearly visible in the second heat (Figure 4.22) and had a value of 308°C. The controlled molecular weight polyimide had a lower Tg than the high molecular weight polyimide. This was an expected result because the lower molecular weight polymer has more chain mobility due to less entanglements.

4.2.3.2 Copolyimides Derived From 3FEDAM

The 3FEDAM-PMDA-PA homopolymer degraded upon melting; therefore, the material could not be melt processed. Consequently, several copolymers were prepared with the goal of depressing the Tm and producing a melt stable material. The 6FDA dianhydride was selected as the comonomer. As expected, the Tg and Tm (Table 4.9) decreased with increasing mole percent of 6FDA incorporated in the 3FEDAM-PMDA system. In each case, the melting endotherm was only observed on the first heat of the DSC thermogram. The limit to the amount of 6FDA incorporated without destroying the crystallinity was approximately 20%. The 3FEDAM-20% 6FDA/PMDA-PA polyimide had a Tg of 277°C and a Tm of 440°C which appeared to show satisfactory short term thermal stability above the Tm (Figure 4.24). An endotherm was not present for the copolymer with 30% incorporation of 6FDA. The influence of the comonomer concentration was evident in the WAXS analysis. As illustrated by the WAXS in Figure 4.25, the 20% 6FDA copolymer was semicrystalline. However, a broad amorphous halo of the original 30% 6FDA copolymer indicated the absence of crystallinity.

Table 4.9: Results of the Thermal Analysis of 3FEDAM-6FDA/PMDA-PA Copolyimides

Wt % 6FDA	Tg (°C)*	Tm (°C)*	5% Wt Loss (°C)**
0	308	476 (1)	528
10	293	461 (1)	560
20	286	440 (1)	559
30	284	NONE	550
100	257	NONE	557

*Nitrogen atmosphere at a heating rate of 10°C/min
**Air atmosphere at a heating rate of 10°C/min
1: First Heat

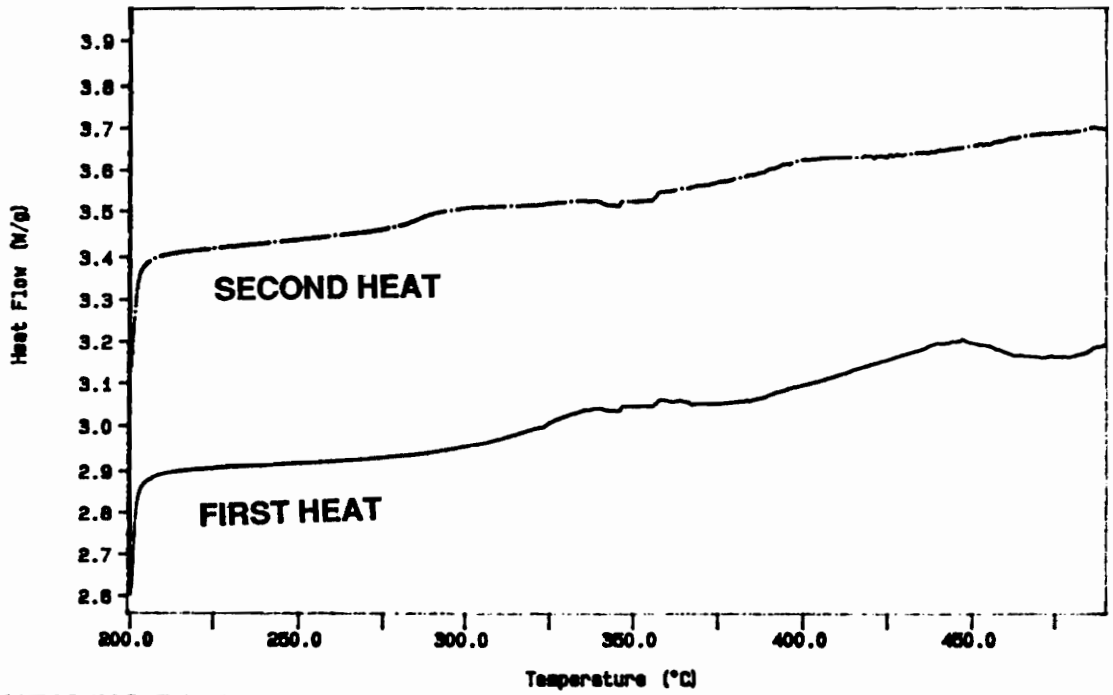

HEATING RATE: 10°C/MIN

Figure 4.24: DSC Analysis of 3FEDAM-20% 6FDA/80% PMDA-PA (30K)

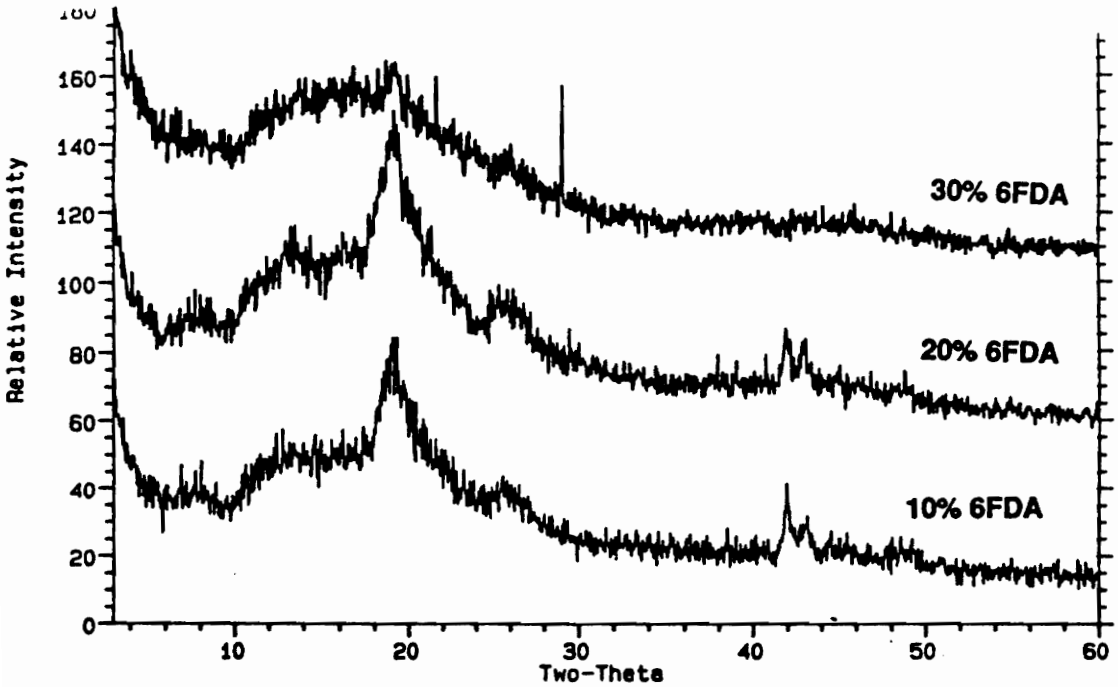

Figure 4.25: WAXS Analysis of 3FEDAM-6FDA/PMDA-PA Copolyimides: The Influence of Comonomer Concentration on Crystalline Order

The 3FEDAM-10% 6FDA/90% PMDA-PA and the 3FEDAM-20% 6FDA/90% PMDA-PA copolymers were annealed to determine if the crystallinity could be enhanced. In the first experiment, the initial crystallinity was not erased. The polyimides were annealed for 30 minutes at 368°C, a temperature between Tg and Tm. In each case, the resulting Tm's were increased by several degrees. In the second experiment, the original crystallinity was erased before thermal treatment. These amorphous polyimide samples were held at 368°C for 30 minutes. The Tm values were more than 10°C lower than the untreated materials. These results are summarized in Table 4.10.

4.2.3.3 Thermooxidative Stability of 3FEDAM Polyimides

The polyimide degradation temperatures (Tables 4.8 and 4.9) showed that these fluorinated polymers were thermally stable to 475°C in air. The homopolymers and copolymers exhibited 5% weight loss values at temperatures greater than 500°C. Figure 4.26 shows the dynamic TGA of 3FEDAM-PMDA-PA (30K) in which 5% weight loss occurred at 528°C. Isothermal TGA studies have been initiated. An isothermal TGA (Figure 4.27) of the 30K 3FEDAM-PMDA-PA polyimide showed less than 1% weight loss after 24 hours at 371°C (700°F) in air.

4.2.3.4 Solvent Resistance of 3FEDAM Polyimides

These fluorinated, semicrystalline polyimides were highly solvent resistant as shown in Table 4.11. As expected, the semicrystalline polyimides are not soluble in polar aprotic solvents such as NMP while the amorphous polyimides had enhanced solubility in the selected solvents. It required

Table 4.10: Thermal Treatment Study of 3FEDAM-6FDA/PMDA-PA (30K) Copolymers

Copolymer	Tm Initial* (°C)	Tm Anneal• (°C)	Tm Anneal‡ (°C)
3FEDAM-10%6FDA/90%PMDA-PA	461	464	454
3FEDAM-20%6FDA/80%PMDA-PA	440	446	427

*Measured on first heat of untreated material
•Annealed at 368°C for 30 minutes
‡490°C for 1 min and annealed at 368°C for 30 minutes

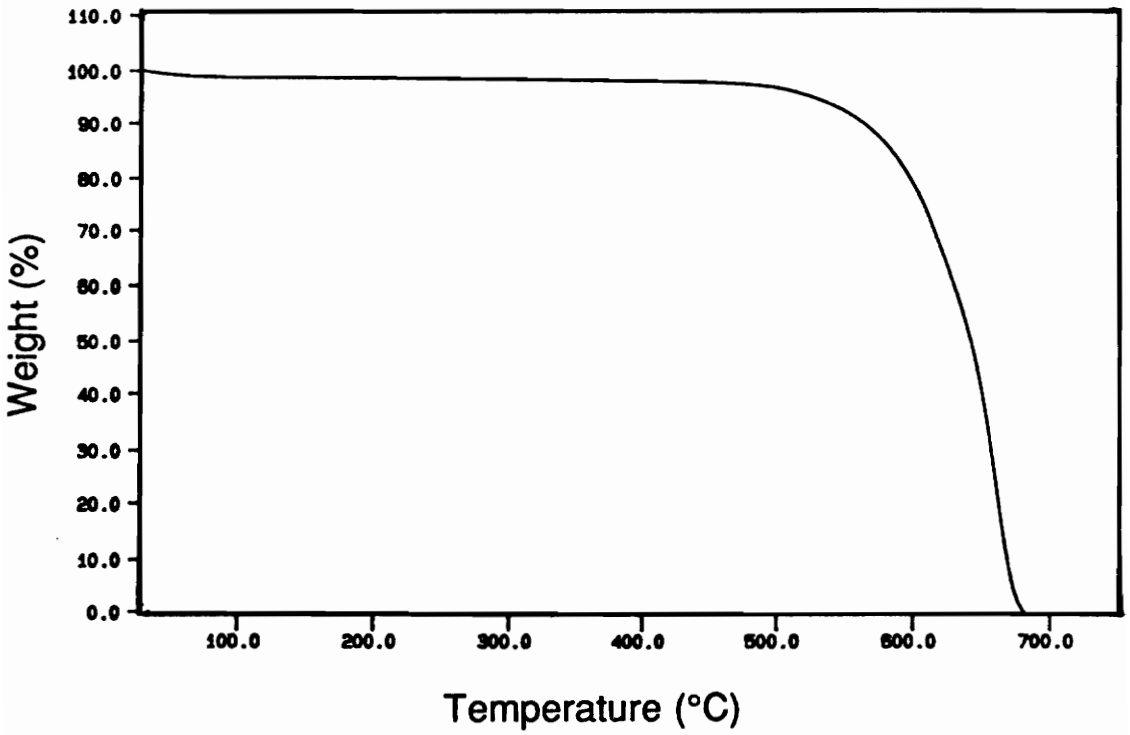

Figure 4.26: Dynamic TGA of 3FEDAM-PMDA-PA (30K)

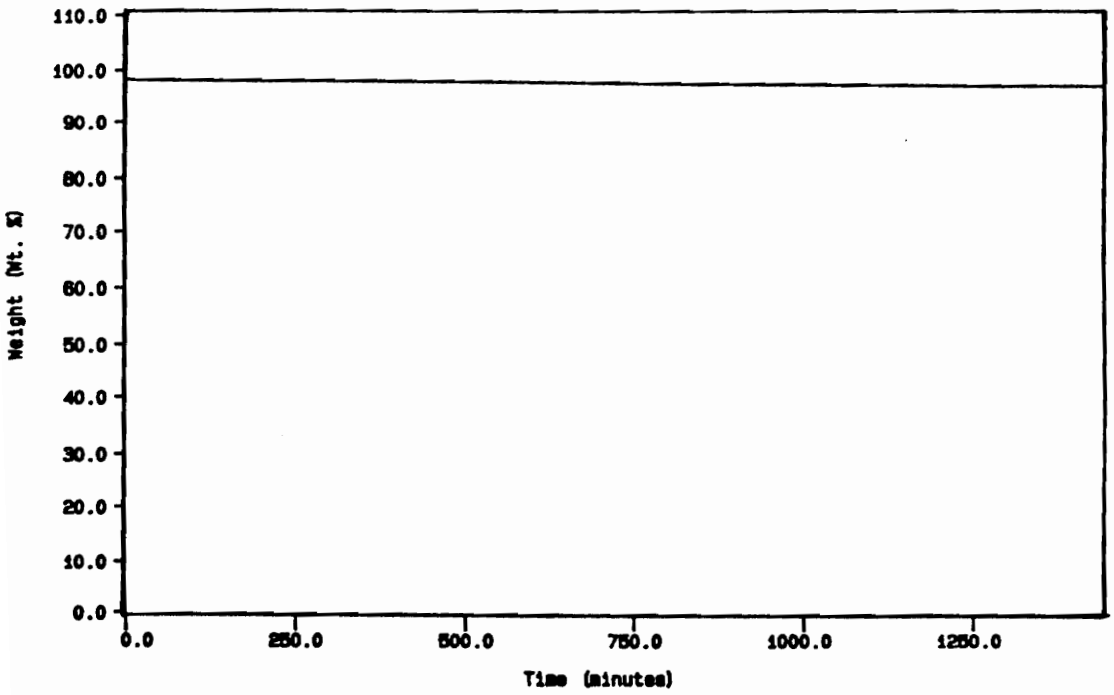

Figure 4.27: Short Term (24 hours) Isothermal TGA at 371°C of 3FEDAM-PMDA-PA (30K) Polyimide

Table 4.11: Solubility Study of 3FEDAM Based Polyimides

Polymer	NMP	DMSO	$CHCl_3$	THF
3FEDAM-PMDA	I	I	I	I
3FEDAM-PMDA-PA	I	I	I	I
3FEDAM-BPDA-PA	S	I	S	I
3FEDAM-10%6FDA/PMDA-PA	I	I	I	I
3FEDAM-20%6FDA/PMDA-PA	I	I	I	I
3FEDAM-30%6FDA/PMDA-PA	I	I	I	I
3FEDAM-6FDA-PA	S	I	S	S

*1% Solids, Room Temperature, Stirring, 24 Hours

I = Insoluble and S = Soluble

approximately 50 mole percent incorporation of the comonomer, 6FDA, to impart solubility to the copolymers.

4.2.4 BDAF Based Polyimides

4.2.4.1 Homopolyimides Derived From BDAF

The BDAF monomer was first prepared in 1975 by TRW on a NASA Lewis research contract (76). Polyimides derived from BDAF were investigated to assess their potential to replace then available condensation polyimides. Initial studies suggested that the BDAF-PMDA system had promise as a protective coating for composites and was suitable for use as an oxidative barrier and/or corrosion inhibiting coating at temperatures up to 700°F. In these studies, the properties of the polyimides were reported but no explanation for the outstanding performance of the BDAF-PMDA polyimide was offered. This research has uncovered a semicrystalline phase in the BDAF-PMDA polyimide which we suggest is contributing to the solvent resistance and thermal stability. Our studies showed that the BDAF-PMDA polyimide has a very high melting point (Tm) near 470°C.

The conventional bulk thermal imidization route was utilized for the insoluble polyimides, such as the BDAF-PMDA polyimides. A final cure temperature of 300°C was necessary for removal of residual solvent and to insure complete cyclization. The films were transparent, amber to yellow in color, and relatively tough.

The thermal transition temperatures of the BDAF containing polyimides were accurately measured by DSC. The BDAF-PMDA-PA (30K) polyimide exhibited a melting endotherm on the first heat at a peak value of 472°C (Figure

4.28). The controlled molecular weight BDAF-PMDA-PA (30K) polyimide had a larger endothermic peak suggesting a greater degree of crystallization than that of the uncontrolled, presumably higher molecular weight BDAF-PMDA polyimide (Figure 4.29). The glass transition temperature of the BDAF-PMDA-PA (30K) polyimide was 306°C which was determined from the second heat (10°C/min) after a rapid cool from above the Tm. At a heating rate of 10°C/min, TMA results showed a Tg of 305°C (Figure 4.30).

4.2.4.2 Copolyimides Derived From BDAF

The BDAF-PMDA polyimide cannot be melt processed due to the very high Tm and subsequent degradation upon melting. Successful attempts to improve the tractibility of polyimides have included incorporation of flexible bridging units (76, 140, 141), bulky side groups (142), or the asymmetric meta catenation (99, 143) into the rigid backbone. The "6F" dianhydride with a hexafluoro-isopropylidene unit and the "3F" diamine with a trifluorophenylethylidene linkage are flexible comonomers; therefore, incorporation of these comonomers should depress the Tm as anticipated for random or statistical copolymers where the second component (eg. "6F" dianhydride) does not crystallize. Through incorporation of flexible comonomers, the Tm may be depressed to a temperature where melt fabrication might be feasible. 6FDA and 3F diamine were investigated as comonomers in the BDAF-PMDA polyimides since neither system is crystallizable. DSC and TGA results of the BDAF-6FDA/PMDA-PA copolymers are shown in Table 4.12. Incorporating 20 mole % of the 6FDA comonomer lowers the Tm by 30°C to 440°C and has a lower Tg at 276°C. A melting

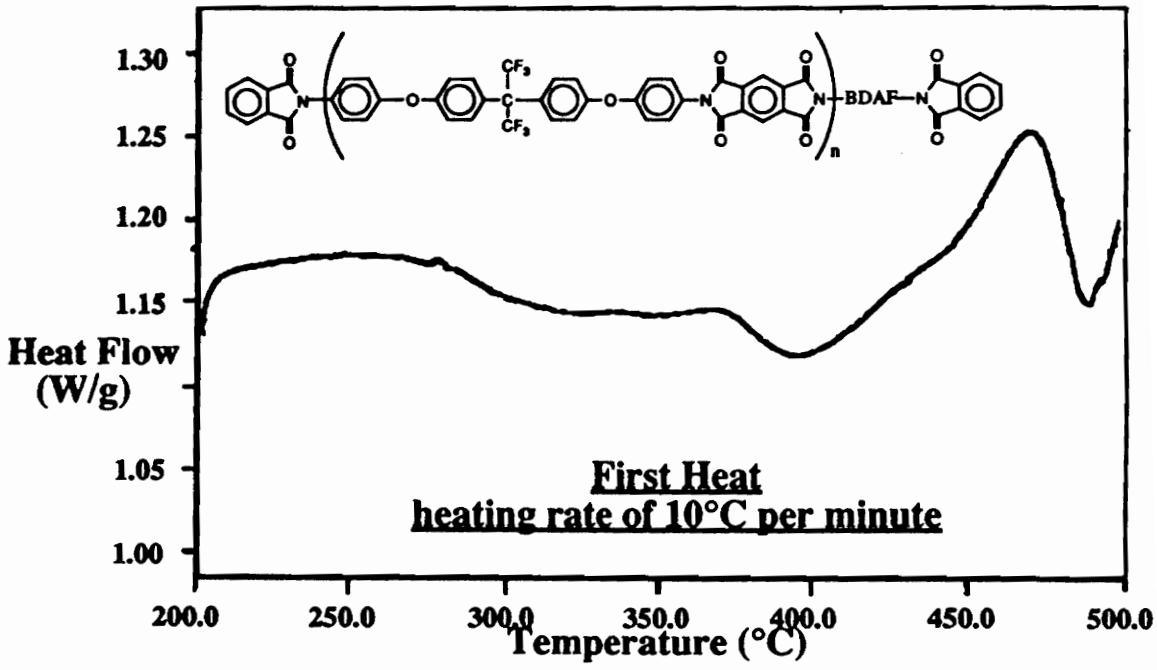

Figure 4.28: First Heat DSC Thermogram of the BDAF-PMDA-PA (30K) Polyimide Film

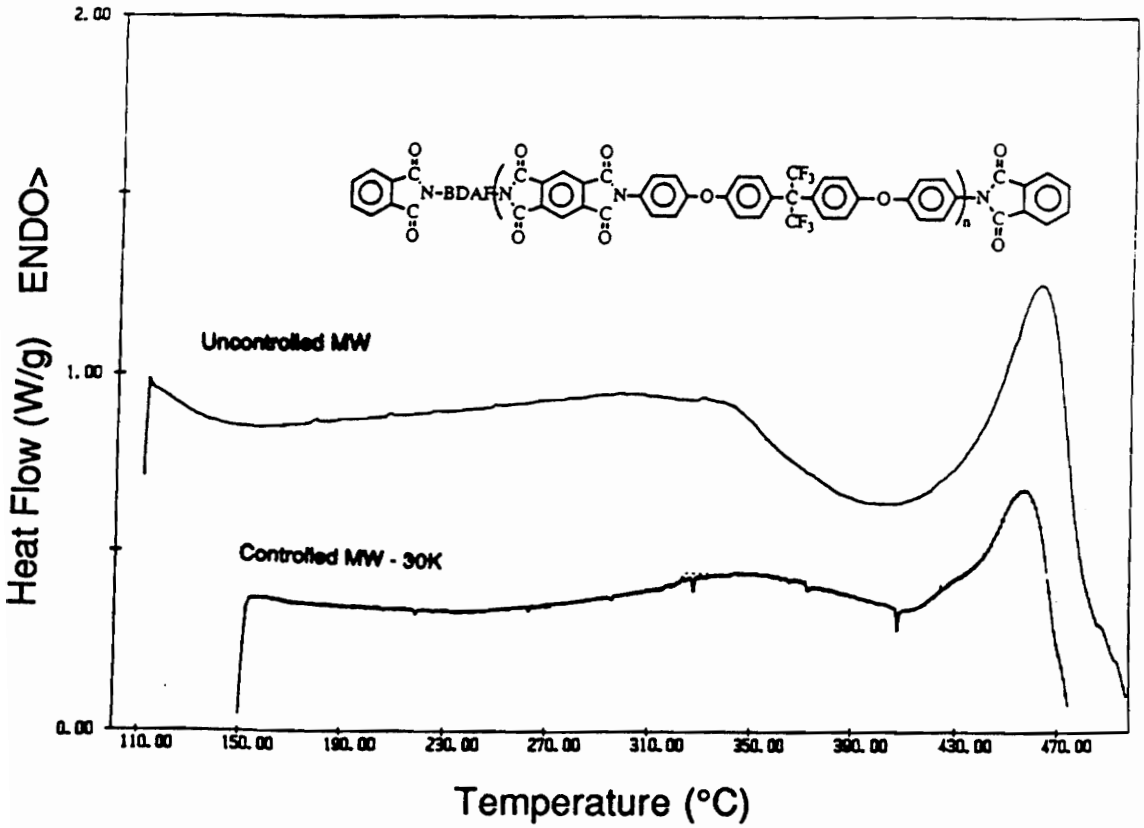

Figure 4.29: First Heat DSC Thermogram of Different Molecular Weight BDAF-PMDA Polyimides

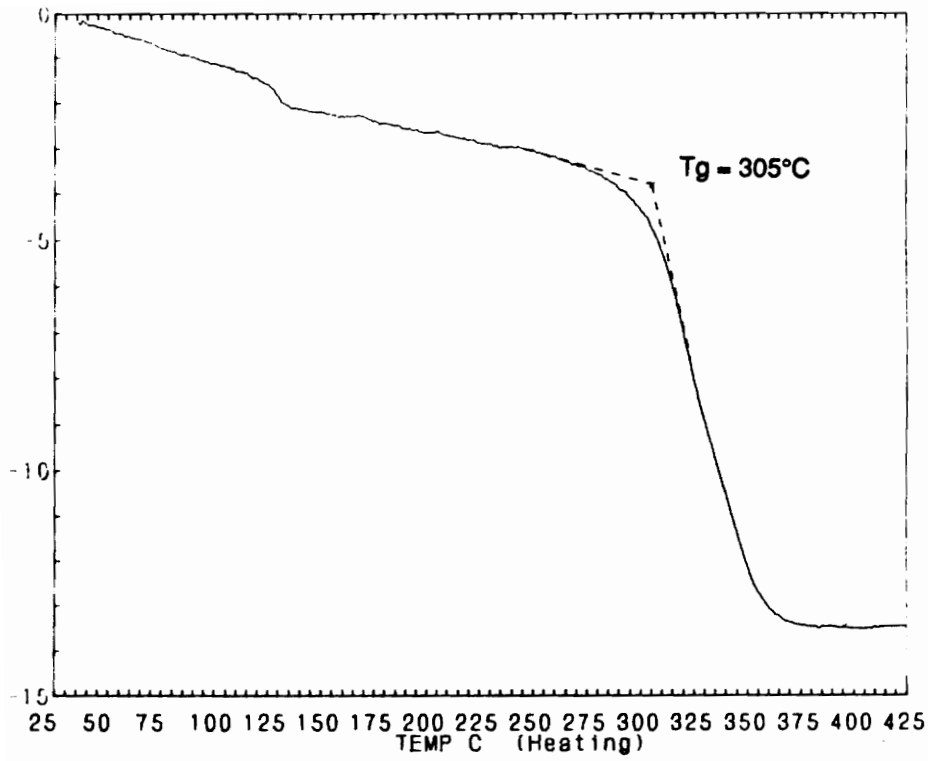

Figure 4.30: TMA Analysis of BDAF-PMDA-PA (30K) Polyimide

Table 4.12: Thermal Analysis Results of BDAF-6FDA/PMDA-PA (30K) Copolymers

BDAF (mol %)	6FDA (mol %)	PMDA (mol %)	Tg* (°C)	Tm** (°C)	5% Wt Loss‡ (°C)
100	0	100	306	472	538
100	20	80	276	440	547
100	30	70	274	---	562
100	40	60	268	---	530
100	60	40	260	---	545
100	80	20	254	---	541
100	100	0	251	---	534

Heating rate is 10°C/min for all experiments
*Second heat
**First Heat
‡In Air

endotherm was observed on both the first heat and the second heat after quick cooling from above the Tm (Figure 4.31). However, the area under the endotherm was reduced on the second heat suggesting that some crystallinity was lost when the sample was heated above the melt. Any significant amount of crystallinity disappeared upon incorporation of 30% or greater 6FDA .

Incorporation of the 3F diamine increased the glass transition temperature of the BDAF containing polyimides (Table 4.13). A Tg as high as 374°C was obtained for the BDAF containing polyimide with 70 mole % of the 3F diamine. However, as little as 20% incorporation of this comonomer eliminated any evidence of a crystalline phase. Interestingly, the copolyimides with 20-50 mole percent of the 3F diamine remained insoluble which may indicate that they are partially ordered.

Wide angle X-ray diffraction studies were conducted on a series of different controlled molecular weight BDAF-PMDA-PA homopolymers. To qualitatively evaluate the molecular weight of these polyimides, the inherent viscosities of the poly(amic acid)s were measured. Inherent viscosities of the poly(amic acid)s increased with increasing number average molecular weight. The 20K, 30K, and 40K homopolyimides display reflections at $2\theta = 18.8°$ (λ=4.71Å) and a broad amorphous halo centered at $2\theta = \sim16°$ (Figure 4.32). The low intensity diffraction peaks indicate some level of ordering in these materials. As the molecular weight was increased, the intensity of the reflections diminished which suggests that the degree of crystallinity was decreasing. This was an expected result because higher molecular weight polymers have higher melt viscosities; therefore, they have less mobility reducing the tendency to orient and crystallize. The uncontrolled molecular

Table 4.13: Thermal Analysis Results of BDAF/3FDAM-PMDA-PA (30K) Copolymers

BDAF (mol %)	3FDAM (mol %)	PMDA (mol %)	Tg* (°C)	Tm** (°C)	5% Wt Loss‡ (°C)
100	0	100	306	472	538
80	20	100	310	---	538
70	30	100	323	---	533
50	50	100	348	---	540
30	70	100	374	---	530
0	100	100	432	---	540

The heating rate is 10°C/min for all experiments.
*Second Heat
**First Heat
‡In Air

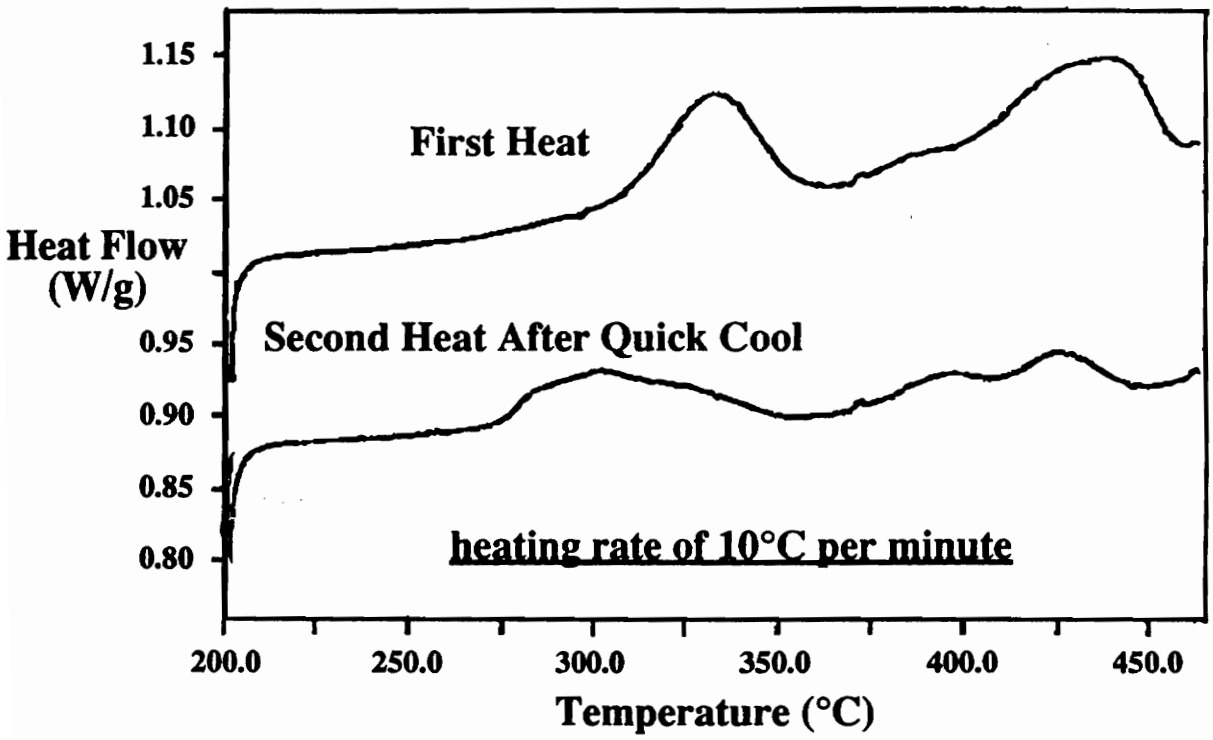

Figure 4.31: DSC Analysis of BDAF-20% 6FDA/ 80% PMDA-PA (30K)

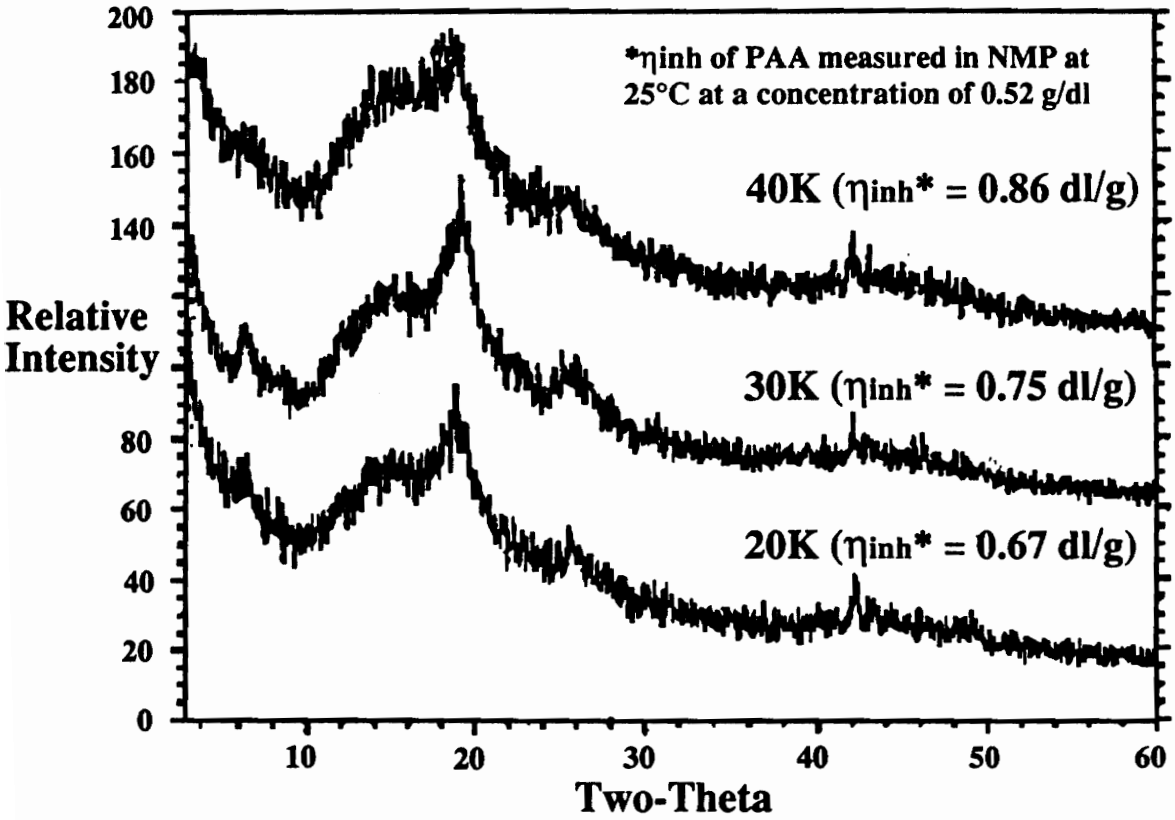

Figure 4.32: WAXS Analysis of BDAF-PMDA-PA Polyimides: The Effect of Molecular Weight on Crystalline Order

weight BDAF-PMDA polymer exhibited broad reflections superimposed on the amorphous halo which suggests a very low level of crystallinity is present at very high molecular weight (Figure 4.33). This result supports the DSC findings that the uncontrolled MW BDAF-PMDA polyimide does possess some crystallinity. The BDAF-20% 6FDA/80% PMDA-PA copolyimide displayed an endothermic transition at 440°C when analyzed by DSC. WAXS analysis showed a diffraction peak near 19° which provides evidence that the endothermic transition is due to melting.

4.2.4.3 Other Polyimides Derived From BDAF

BDAF-ODPA homo- and co-polymers were prepared and analyzed by TGA and DSC (Table 4.14). The BDAF-ODPA-PA (30K) polyimide had a Tg of 227°C which increased with increasing incorporation of PMDA. These materials appeared to be amorphous. However, the BDAF-BTDA polyimide showed an endotherm at 304°C on the first heat of the DSC thermogram and A Tg of 244°C.

4.2.4.4 Solvent Resistance of BDAF Polyimides

The semicrystalline fluorinated polyimides based on BDAF were insoluble in all common organic sovents, NMP, and m-cresol. The insolubility is attributed to the crystalline nature. The crystalline phase in polymers may behave similar to a physical crosslink in that the polymer-polymer interactions are stronger than the polymer-solvent interactions; thereby providing better solvent resistance. The copolymer solubility was a function of the comonomer concentration as shown in Table 4.15. Approximately 50 mole percent of the

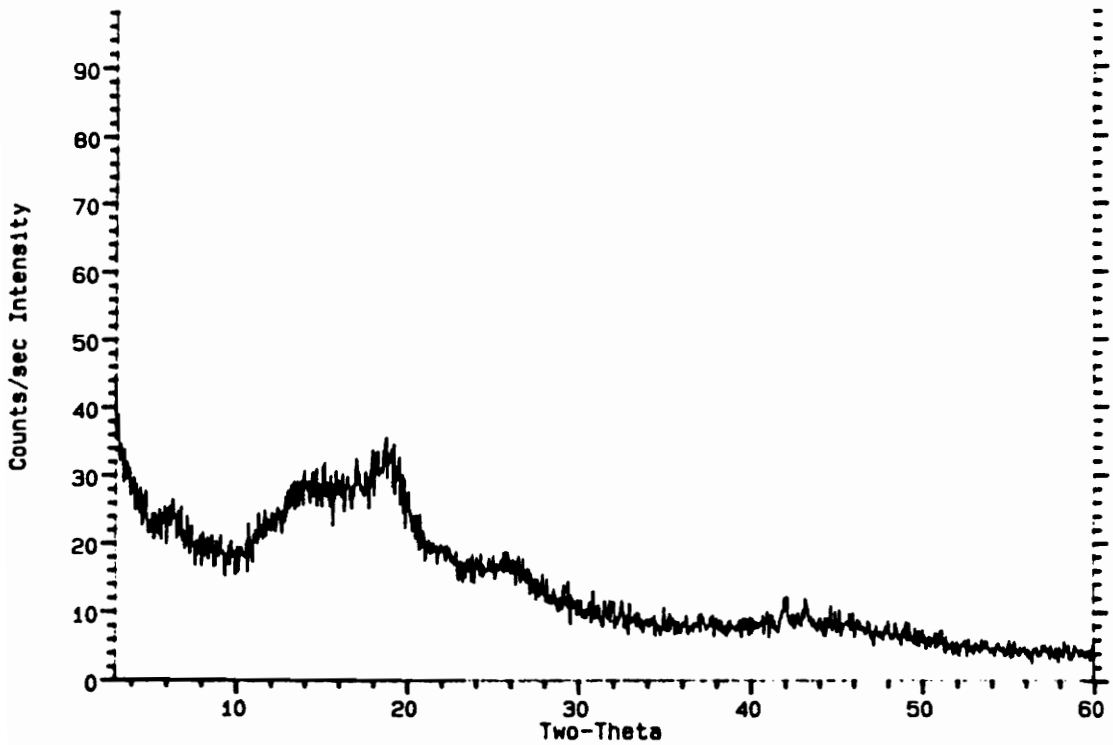

Figure 4.33: WAXS Analysis of Uncontrolled Molecular Weight BDAF-PMDA Polyimide

Table 4.14: Thermal Analysis Results of BDAF-PMDA/ODPA Polyimides

BDAF (mol %)	ODPA (mol %)	PMDA (mol %)	Tg* (°C)	5% Wt Loss‡ (°C)
100	100	0	227	546
100	70	30	237	541
100	50	50	243	542
100	30	70	261	548
100	0	100	306	538

*Second heat
‡In air at 10°C/min

Table 4.15: Solubility Study of BDAF Based Polyimides

BDAF	3FDAM	PMDA	Imid. Method	THF	CHCl3	NMP
100	0	100	Thermal	I	I	I
70	30	100	Thermal	I	I	I
50	50	100	Thermal	M	M	I
30	70	100	Soln	S	S	S
0	100	100	Soln	M	M	S
BDAF	6FDA	PMDA				
100	20	80	Thermal	I	I	I
100	40	60	Thermal	I	I	I
100	60	40	Soln	S	S	M
100	80	20	Soln	S	S	S

1% Solids, Room Temperature, Stirring, 24 Hours
S = Soluble, M = Marginally Soluble, I = Insoluble

comonomer, 6FDA or 3F diamine, was required to induce solubility. These polyimides were soluble in chloroform ($CHCl_3$), tetrahydrofuran (THF), and NMP.

4.2.4.5 Thermooxidative Stability of Polyimides

4.2.4.5.1 Short Term Thermooxidative Stability Studies of BDAF Polyimides

Dynamic thermogravimetric analysis (TGA) of the BDAF based polyimides given in Tables 4.12 and 4.13 demonstrate short term thermal stability above 450°C in air with 5% weight loss values of 530°C to 550°C. A typical dynamic TGA thermogram of a BDAF-PMDA-PA (30K) polyimide is presented in Figure 4.34. A better measure of a material's thermooxidative stability is obtained by isothermal TGA studies. An isothermal TGA of the 30,000 g/mole BDAF-PMDA-PA polyimide exhibited relatively little weight loss after 24 hours at 371°C (700°F) in air (Figure 4.35).

4.2.4.5.2 Long Term Thermooxidative Stability Studies of Polyimides

Long term thermooxidative stability studies of the BDAF-PMDA-PA (30K) and 3FEDAM-PMDA-PA (30K) polyimide films (similar film thickness) were conducted in a forced air Blue M oven. The first experiment was conducted at 316°C (600°F) for 250 hours (Figure 4.36) which is about 10°C above the Tg of the fluorinated, semicrystalline polyimides. At 316°C, a sample of Kapton (4,4' ODA-PMDA) was included in the experiment. The BDAF-PMDA-PA polyimide suffered approximately 8% weight loss within the first day of exposure at 316° but basically remained constant for the duration of the test. Kapton and 3FEDAM-PMDA-PA showed liittle weight loss until 140 hours where the

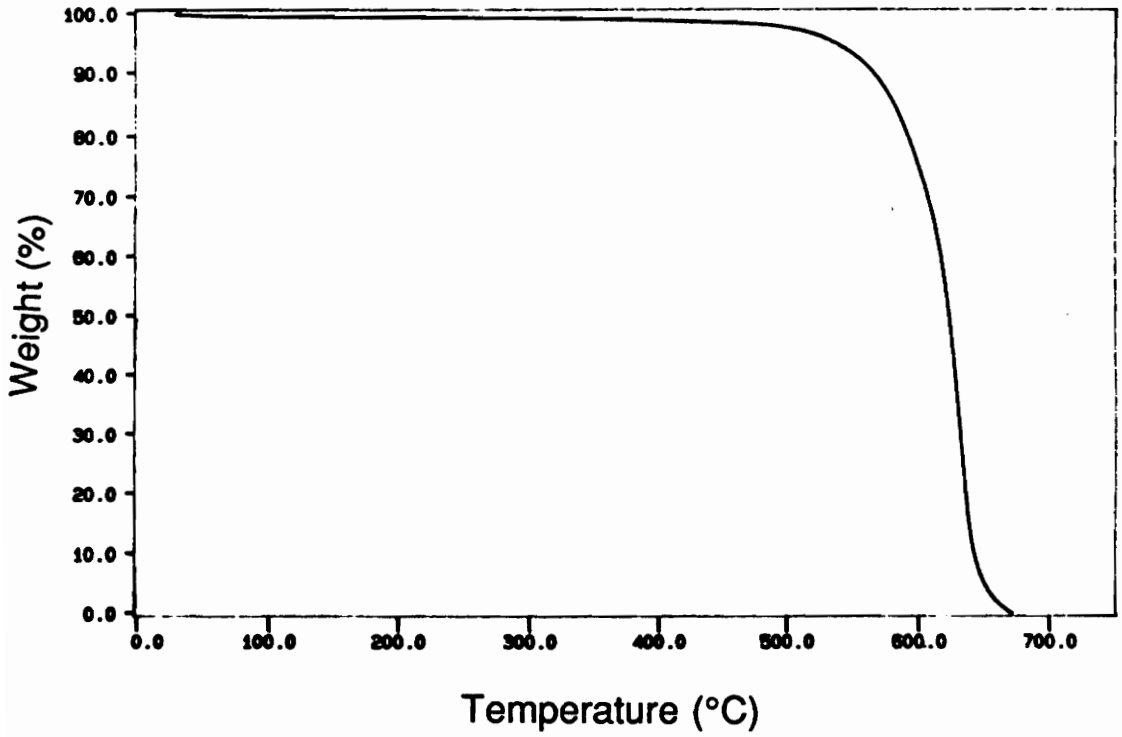

Figure 4.34: Typical Dynamic TGA of BDAF-PMDA-PA (30K) Polyimide

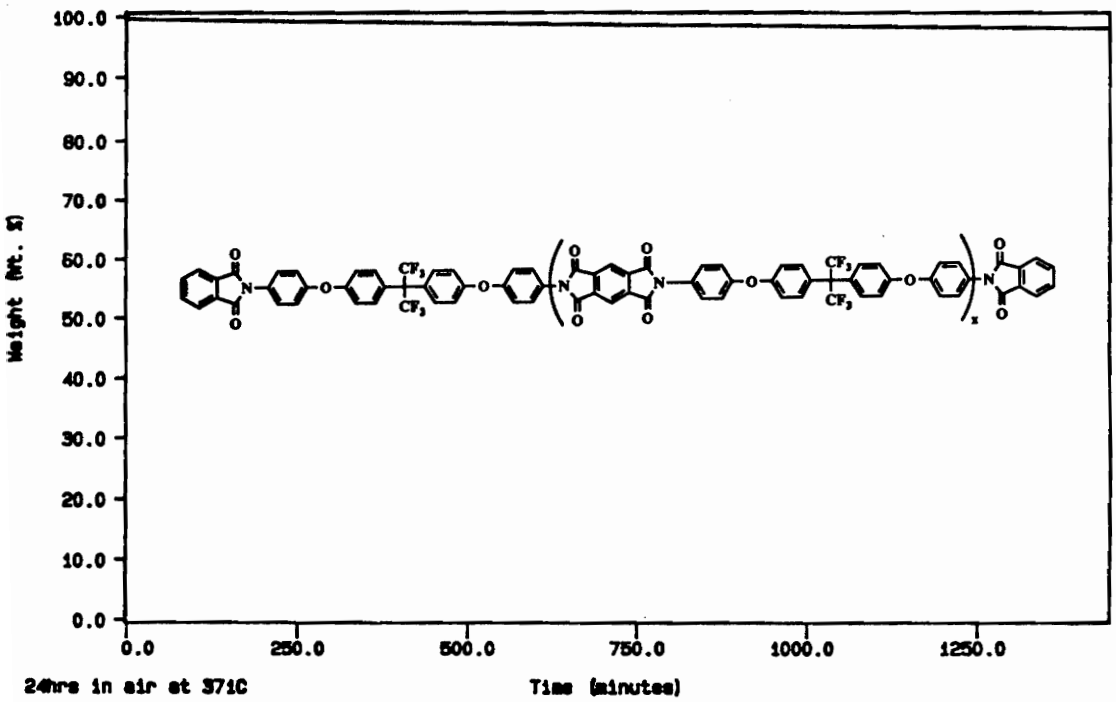

Figure 4.35: Isothermal TGA of BDAF-PMDA-PA (30K) Polyimide For 24 Hours at 371°C (700°F) In Air

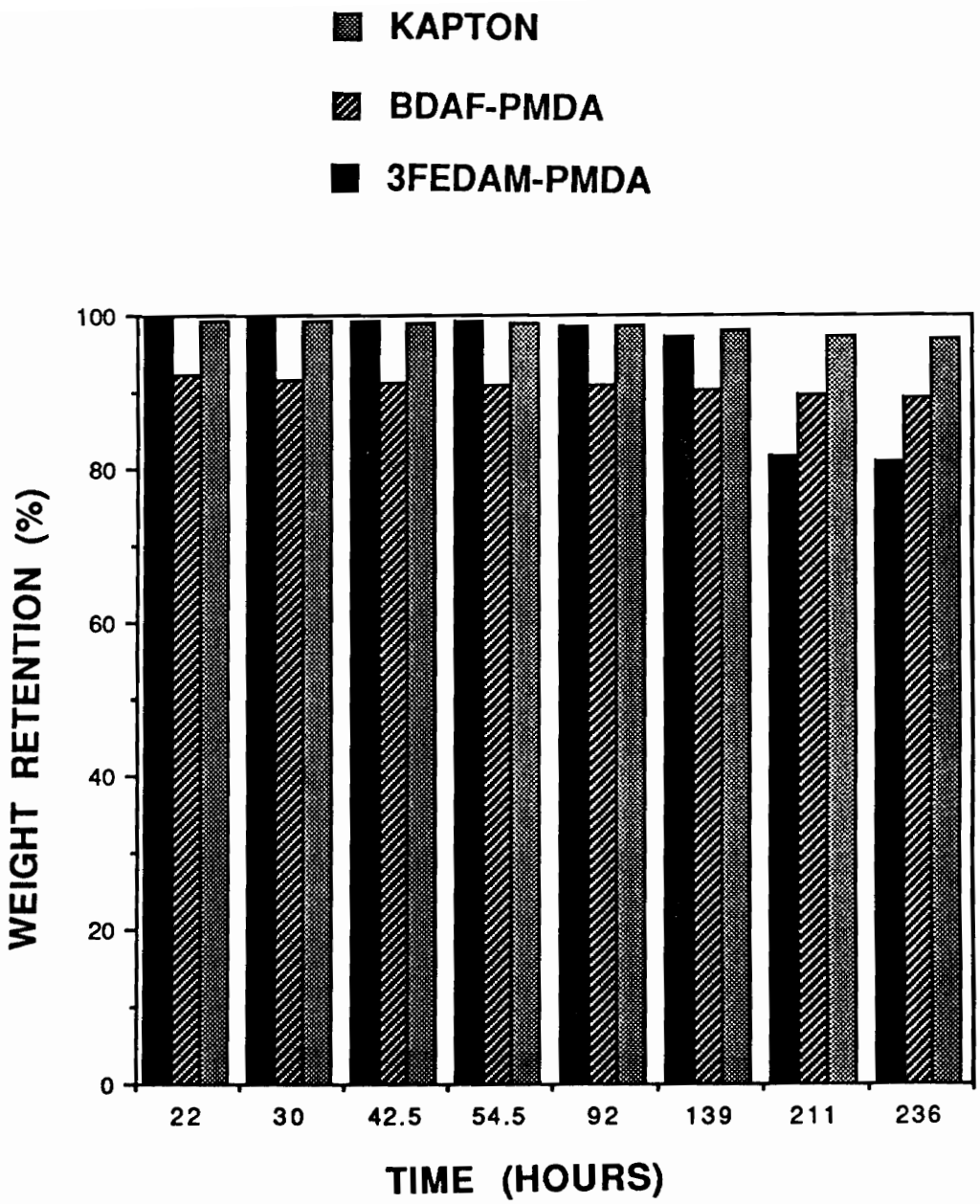

Figure 4.36: Thermooxidative Stability Study of Polyimides At 316°C (600°F)

3FEDAM-PMDA-PA sample suffered about 17% weight loss. After 250 hours, Kapton showed the lowest weight loss followed by BDAF-PMDA-PA.

The BDAF-PMDA-PA and 3FEDAM-PMDA-PA polyimides were also tested at 371°C (Figure 4.37) which is about 65°C above the Tg of these materials. These fluorinated, semicrystalline polyimides did not perform well at this elevated temperature. After 9 hours, BDAF-PMDA-PA polyimide showed a 20% weight loss but retained this weight for a total of 90 hours. After 90 hours, the BDAF-PMDA-PA polyimide showed a substantial weight loss maintaining only 30% of its original weight. The 3FEDAM-PMDA-PA sample continually lost weight with time and only retained about 20% of the total weight after 150 hours at 371°C.

4.2.5 TPEQ (1,4-bis(4-aminophenoxy)benzene) Based Polyimides

4.2.5.1 Various Homopolyimides Derived From TPEQ

The hydroquinone based diamine, 1,4-bis(4-aminophenoxy)benzene (TPEQ), is symmetrical and has two ether connecting linkages. Therefore, this diamine was expected to produce semicrystalline polyimides. Several polyimides controlled to Mn of 30,000 g/mol were prepared with TPEQ and various aromatic dianhydrides. Polyimides were synthesized by the bulk imidization method because these polymers precipitated from solution upon solution imidization. The resulting films were yellow to amber in color and all the films were opaque except for the TPEQ-PMDA film which was transparent. The polyimide films were analyzed by DSC showing that these materials were indeed semicrystalline (Table 4.16). The TPEQ-PMDA-PA polyimide did not exhibit any transitions up to 500°C by DSC analysis. The TPEQ-BPDA-PA

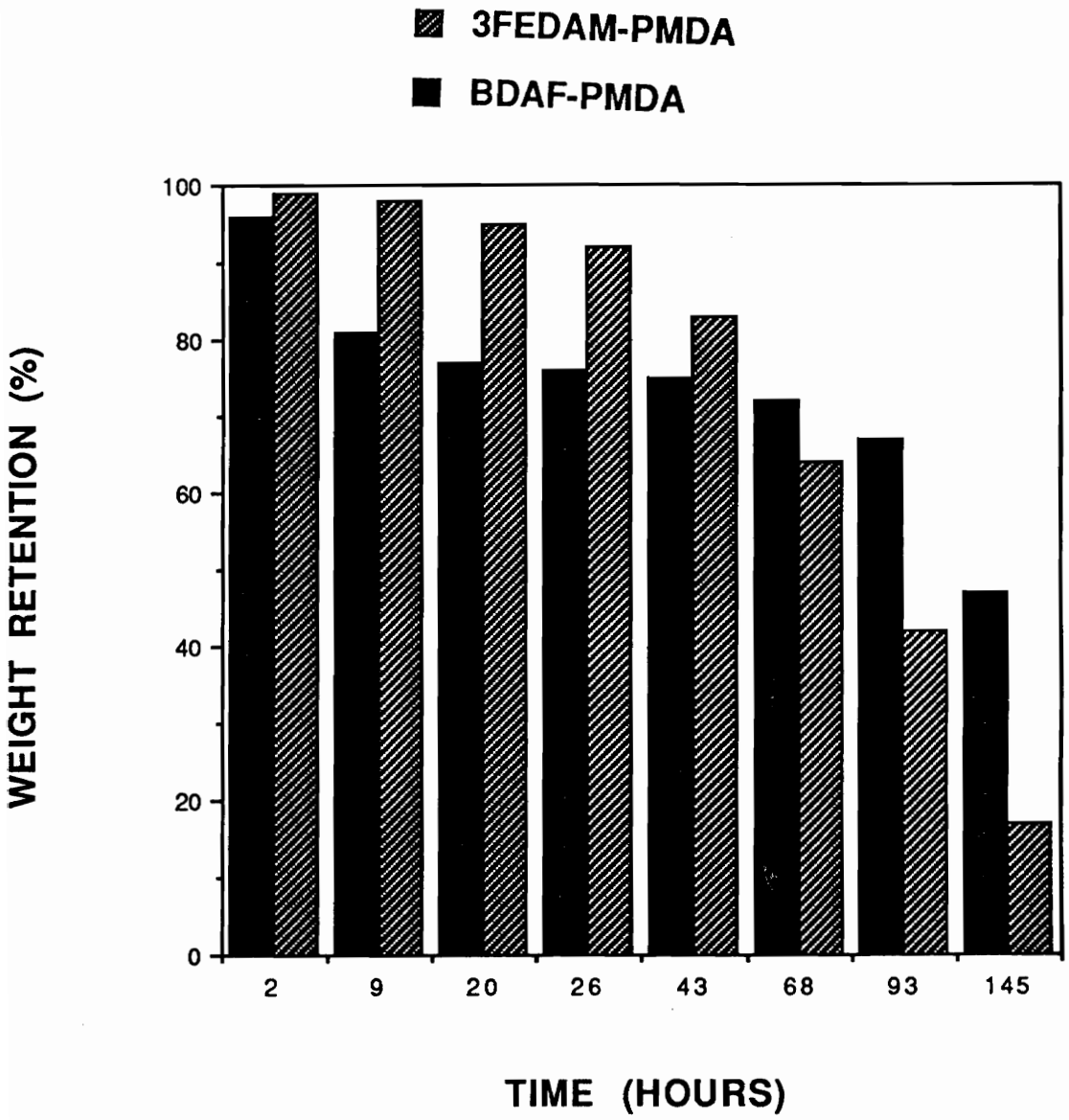

Figure 4.37: Thermooxidative Stability Study of Polyimides at 371°C (700°F)

Table 4.16: Thermal Analysis Results of TPEQ Based Polyimides

Polymer	Tg (°C)	Tm (°C)	5% Wt Loss* (°C)
TPEQ-BPDA-PA	255	453 (2)	573
TPEQ-BTDA-PA	251	468 (1)	548
TPEQ-ODPA-PA	239	411 (1)	590
TPEQ-PMDA-PA	?	?	594

The heating rate was 10°C/min for all experiments.
1: First Heat
2: Second Heat
*In Air

polyimide displayed the highest measurable Tg of 255°C and a melting endotherm on the first heat and the reminiscence of an endotherm on the second heat (Figure 4.38). The TPEQ-BTDA-PA polyimide had a Tg of 251°C and a Tm of 468°C which was only apparent on the first heat. The lowest Tg of 239°C was measured for the TPEQ-ODPA-PA polyimide; however, this polyimide showed a Tm at 411°C. This was encouraging because polymeric materials with melting transitions above 400°C are more difficult to process due to limitations of processing equipment at extremely high temperatures. Therefore, TPEQ-ODPA-PA polyimides have potential to be melt processed and were selected for further investigation.

4.2.5.2 TPEQ-ODPA-PA Polyimide

4.2.5.2.1 Influence of Molecular Weight on Properties

The Carother's equation was used to determine the correct stoichiometric amounts of the monomers to synthesize a series of molecular weights of the TPEQ-ODPA-PA polyimides. The number average molecular weight (Mn) was controlled from 7.5K to 30K and the intrinsic viscosities of the poly(amic acid)s were measured. The intrinsic viscosities ranged from 0.25 dL/g for the 7.5K polyimide and increased with increasing Mn to 0.42 dL/g corresponding to the 30K polyimide (Table 4.17). The thermal behavior of these polymers was evaluated by DSC analysis. The Tg was measured on the second heating scan in which the value of the Tg increased with the increase in Mn. The Tg values ranged from 214°C to 239°C for the lower MW (7.5K) material to the higher MW

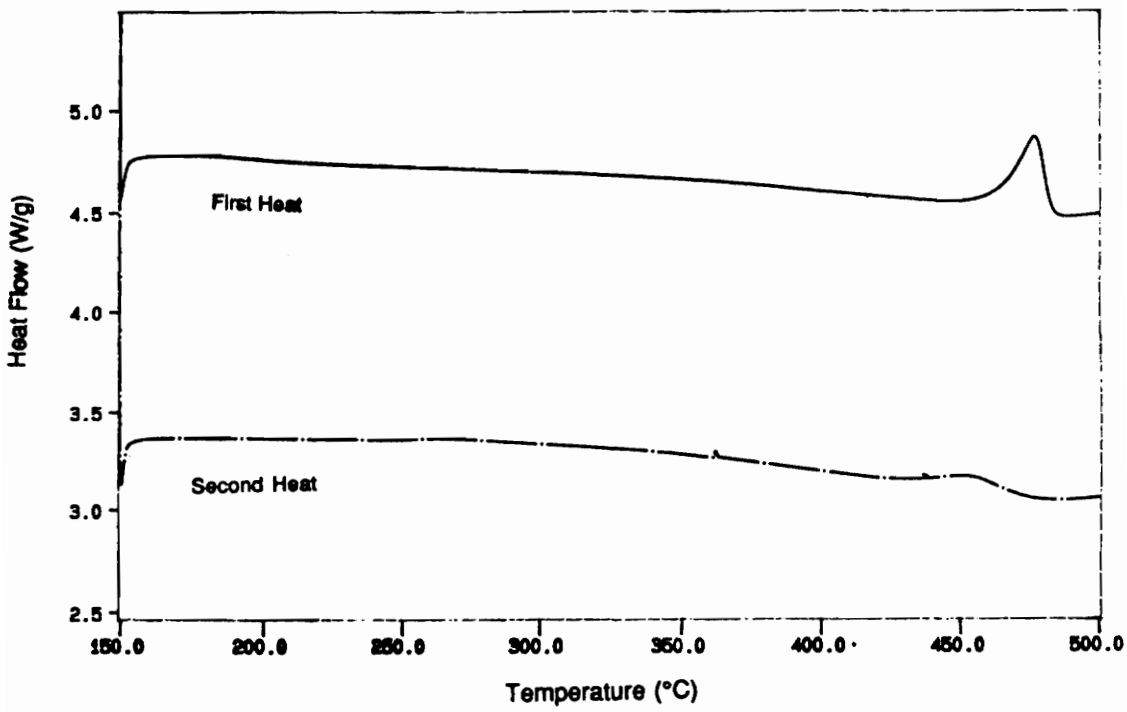

Figure 4.38: DSC Thermogram of TPEQ-BPDA-PA (30K) Polyimide

Table 4.17: Thermal Analysis Results of the TPEQ-ODPA-PA Polyimides-Second Heat Values

Mn theor (g/mol)	$[\eta]_{NMP}^{25°C}$ (dL/g)	Tg (°C)	Tc (°C)	ΔH_f (J/g)	Tm (°C)	ΔH_f (J/g)	5% Wt Loss (°C)
7.5K	0.25	214	282	-29	423	42	527
10K	0.29	222	306	-25	420	26	561
15K	0.32	226	335	-18	420	12	588
20K	0.34	231	---	---	~425	~0	573
30K	0.42	239	---	---	---	---	590

(30K) material, respectively. Upon heating in the second scan, the 7.5K, 10K, and the 15K polyimides displayed an exothermic crystallization transition (Figure 4.39). As the Mn increased, the Tc increased and the heat of fusion decreased. The 15K polyimide was analyzed by WAXS (Figure 4.40). The low intensity of the reflections suggest that this material has a low level of crystallinity. The 20K and 30K TPEQ-ODPA-PA polyimides did not show an exotherm in the second heat. The longer macromolecular chains have restricted mobility; therefore, it is more difficult for higher MW polymers to crystallize.

All the different MW TPEQ-ODPA-PA polyimides exhibited melting endotherms on the first heat in the DSC thermograms (Figure 4.41). The Tm was 430°C for the lowest MW polyimide and decreased with increasing Mn to 411°C for the 30K polyimide (Table 4.18). The heat of fusion values decrease with increasing MW which signifies that the level of crystallinity was lower with higher MW. All the MW samples, except the 30K polyimide, showed a melting endotherm on the second heat in which the Tm is approximately 420°C. The ΔH_f values also decrease with increasing MW as found for the trend in the first heat. As the molecular weight was increased, the relative percent crystallinity recovered decreased. After heating above the melt , 66% of the relative crystallinity remained for the 7.5K polyimide and only 33% of the relative crystallinity was retained for the 15K polyimide. This indicates that lower levels of crystallinity were achieved for higher MWs after being held at temperatures above the melt. Therefore, it is speculated from these results that the higher MW polyimides cannot crystallize as readily as the lower MW polyimides while in the melt due to higher viscosities.

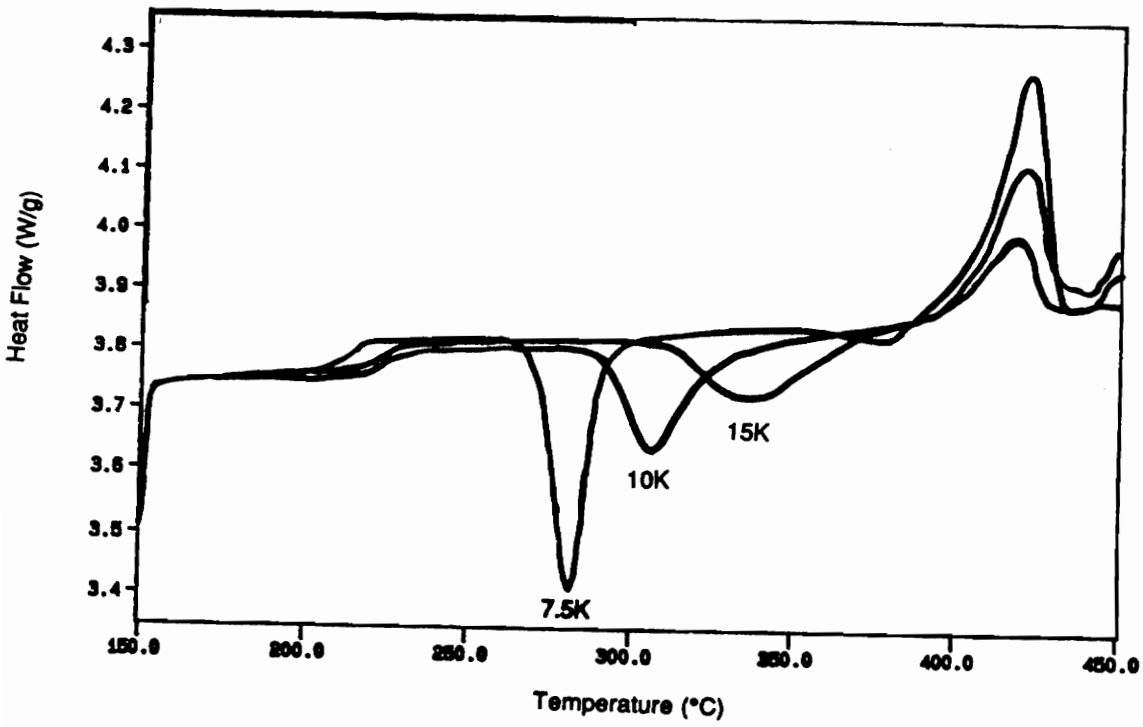

Figure 4.39: DSC Analysis of Three Lower Molecular Weight TPEQ-ODPA-PA Polyimides

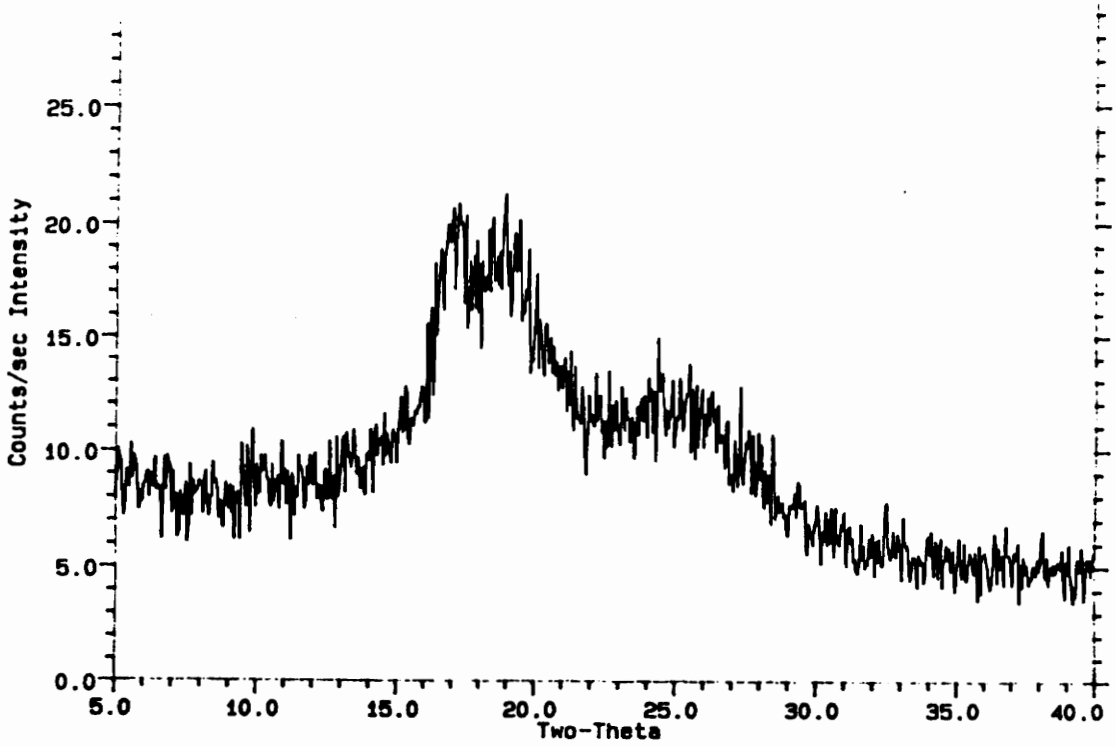

Figure 4.40: WAXS of 15K TPEQ-ODPA-PA Polyimide

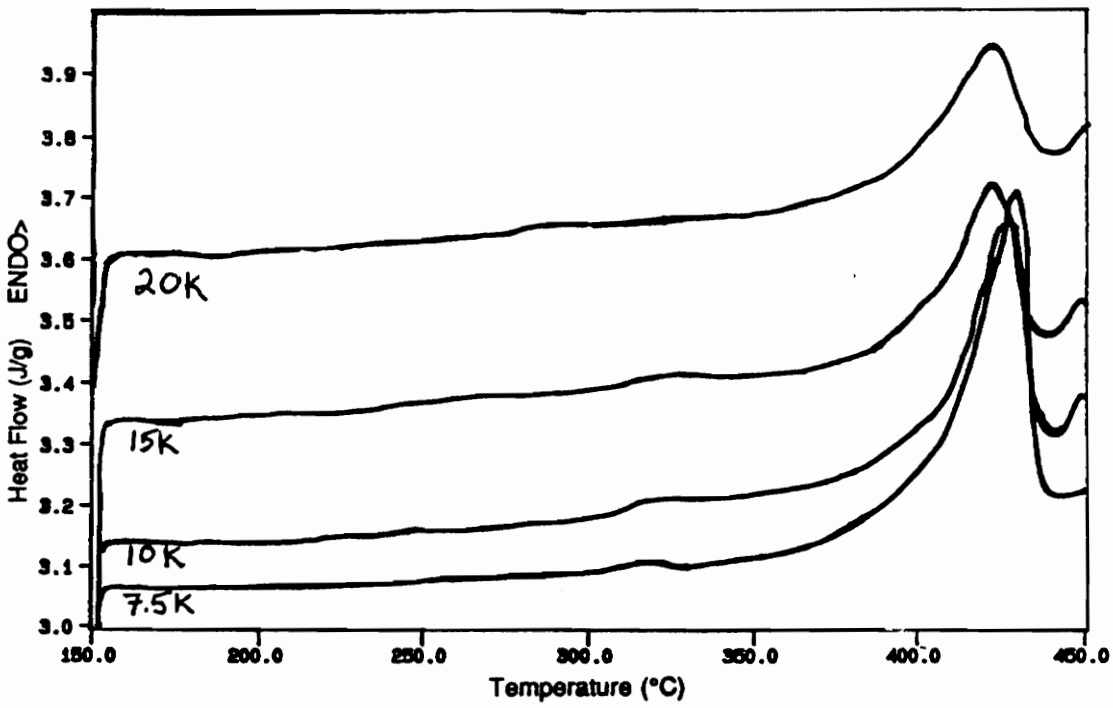

Figure 4.41: First Heat DSC Thermograms of TPEQ-ODPA-PA Polyimides

Table 4.18: Comparison of First and Second Heat Values for the Tm of TPEQ-ODPA-PA Polyimides

Mn theor (g/mol)	$[\eta]_{NMP}^{25°C}$ (dL/g)	First Heat Tm (°C)	Second Heat Tm (°C)	First Heat ΔH_f (J/g)	Second Heat ΔH_f (J/g)	Rel. Cryst. Recovered (%)
7.5K	0.25	430	423	63	42	66
10K	0.29	427	420	44	26	59
15K	0.32	425	420	36	12	33
20K	0.34	422	~425	33	~0	~0

The recrystallization behavior of the TPEQ-ODPA-PA systems were investigated. The goal was to ascertain the sensitivity of the 15K material to recrystallize after being held above the Tm. Each sample was heated at 40°C/min from ambient temperature to 440°C. The temperature of 440°C was selected because it was approximately 15°C above the peak melting point. The material was held for different periods of time, 0, 1, 5, and 10 minutes at 440°C. After the holding period, the samples were quenched by DSC. The second heating cycle was 10°C/min from 150°C to 450°C. The results are summarized in Table 4.19. The Tc and Tg values increased with hold time at 440°C (Figure 4.42). The Tm values decreased with increasing time above the melt indicating loss of nuclei and/or degradation. In addition, the ΔH_f decreased from 33 J/g for 0 minutes in the melt to 19 J/g for 5 minutes in the melt.

An experiment was conducted to determine whether the crystallinity could be enhanced by annealing. The 15K and 20K TPEQ-ODPA-PA polyimides underwent a first heat at 10°C/min from 150°C to 450°C, then were quenched. Each sample was heated at 200°C/min to 325°C, held for 30 minutes, and quenched. The polyimides were heated a second time to determine the transitions after thermal treatment.

The 15K polyimide showed a broad Tg and a Tm of 417°C. The heat of fusion for the melting could not be evaluated accurately because the baseline was not flat. Inspection of the thermogram seems to indicate that crystallization occurs. It appears to crystallize and then immediately melt.

The 20K polyimide displayed similar behavior to the 15K material except the baseline was better. This may suggest that the 20K material is more stable.

Table 4.19: The Relationship Between the Thermal Behavior of TPEQ-ODPA-PA (15K) Polyimide and Time in the Melt

Time (minutes)	Tg (°C)	Tc (°C)	Tm (°C)	ΔH_f (J/g)
0	224	282	423	33
1	226	297	421	27
5	228	315	417	19
10	~230	?	?	~0

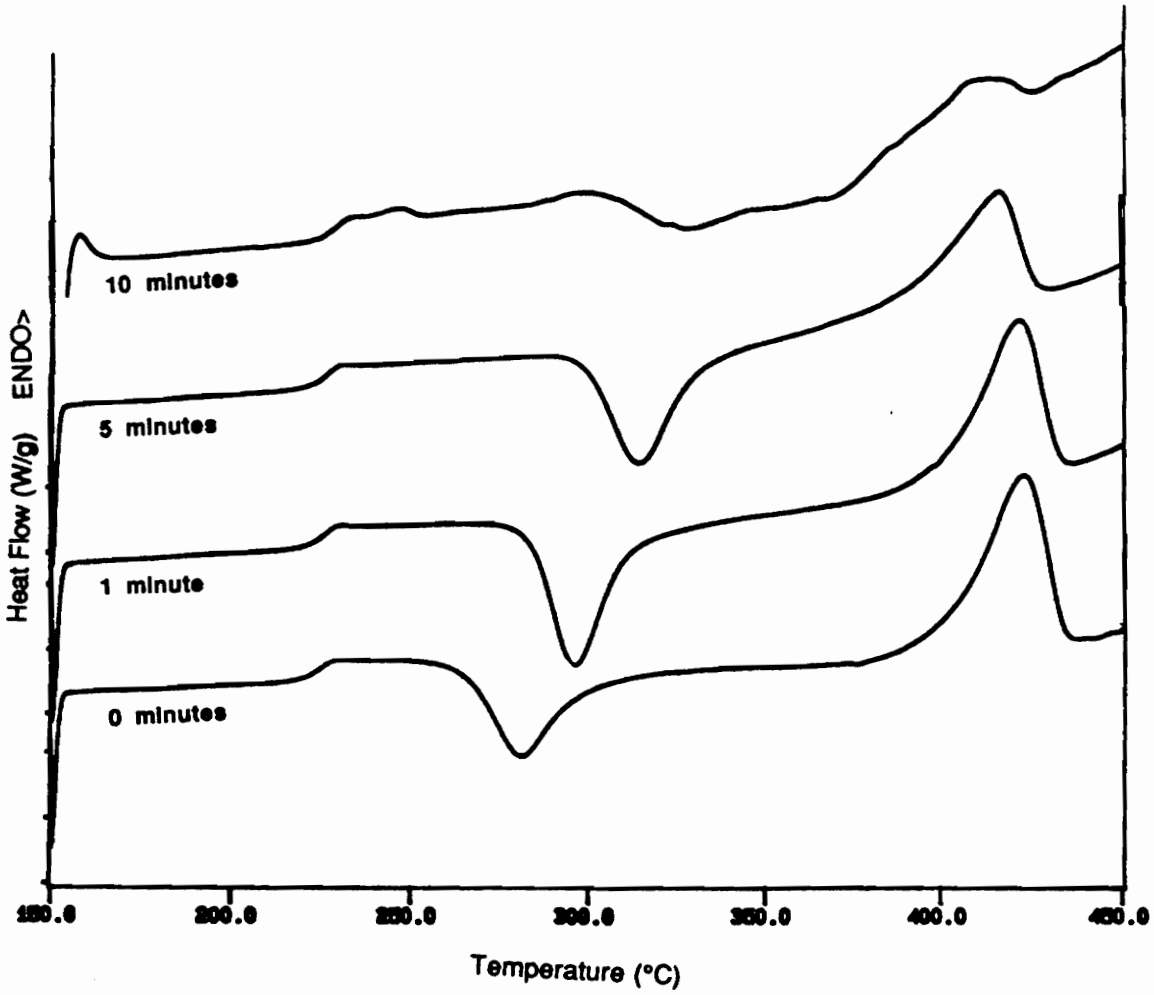

Figure 4.42: DSC Analysis of TPEQ-ODPA-PA (15K) Polyimide at Various Times in the Melt

The Tg was broad but the value was determined to be approximately 235°C. A broad endotherm was present with a peak value of 411°C. This is important because on the second heat this material does not show crystallinity due to the absence of an endotherm in the DSC analysis. Therefore, these results suggest that this material can be processed above the Tm (422°C, first heat) and then annealed to enhance the crystalline nature.

A study was conducted to determine the ability of the TPEQ-ODPA-PA (30K) polyimide to crystallize upon thermal treatment. Each sample was treated heated in the DSC at 10°C/min from 200°C to 450°C and held at 450°C for 2 minutes which completely erased any crystallinity. The samples were cooled at 10°C/min to the selected annealing temperature and held for the selected annealing time. After this thermal treatment, the samples were heated at 10°C/min to 450°C. Several annealing temperatures and times were investigated but showed that under these conditons the TPEQ-ODPA-PA (30K) polyimide does not crystalize from the melt (Table 4.20). Another sample was treated in the same manner as described for the samples crystallized from the melt but this sample was quenched after 2 minutes at 450°C, and then heated quickly to the annealing temperature and held for 30 minutes. This sample showed a small, broad endotherm at 405°C (ΔH_f = 5 J/g). This result suggests that this material crystallizes more readily from the glass than the melt.

4.3 Polyimide Powders

4.3.1 Preparation of Polyimide Powders

The objective of this research was to prepare polyimide particles by a facile, practical method and control the particle size. Secondary goals included

Table 4.20: Crystallization Behavior of TPEQ-ODPA-PA (30K) Polyimide Powders

Untreated Material: Tg = 232°C and Tm = 409°C (ΔH_f = 33 J/g)

Anneal Temperature (°C)	Anneal Time (minutes)	Tm (°C)
375	15	---
375	45	---
350	15	---
335	30	---
325*	30	405 (5 J/g)

*From the glass after exposure above Tm

characterization of the particles and evaluation of their potential as resins for composites via aqueous or electrostatic prepregging.

The polyimide particles were prepared by solution imidization. The first step was formation of the poly(amic acid) (PAA) and the second step was the cyclodehydration of the amic acid to the imide via solution imidization. Within a short period after the reaction flask was immersed in an oil bath controlled at 175°C, the solution became turbid indicating the polymer was precipitating from solution as the amic acid was converted to the imide. The temperature was maintained at 175°C for a total of two hours and the partially imidized particles were isolated.

4.3.2 Particle Size Analysis

4.3.2.1 Density Measurements

The density of the polymer and the density and viscosity of the solvent (in this case, water) were required for the particle size analysis. The density of the particles cannot be measured; therefore, the density of the corresponding film was utilized in the measurements. The bulk density of the BDAF-PMDA-PA film and the Kapton film were determined using the ASTM C373-88 method producing the values of 1.41 and 1.39, respectively. The reported densities (5) of the BDAF-PMDA and the Kapton film are 1.43 and 1.41; therefore, this was considered an excellent method for determining the bulk density of polymers. A density of 1.4 was used for all the polyimide particle size measurements.

4.3.2.2 Environmental Scanning Electron Microscopy (ESEM)

The particles were analyzed by ESEM to determine absolute particle size and compare these values with those obtained by PSA. Figure 4.43 shows an ESEM micrograph of the BDAF-PMDA-PA particles. As measured by PSA, the median particle diameter was 3.8 μm. The ESEM analysis showed particles with a relatively narrow distribution of particle sizes that ranged from about 0.7 μm to about 15 μm with the median of approximately 4 μm.

4.3.3 Parameters Influencing Polyimide Particle Size

4.3.3.1 Concentration of the Solution

Several experimental parameters were investigated to determine the effect on particle size. These were concentration of solution, temperature of imidization, molecular weight of polymer, stabilizer, and drying of the particles. The BDAF-PMDA-PA particles were synthesized and the concentration of the solution during imidization was systematically varied. All other conditions were held constant. As the concentration was decreased, the resultant size of BDAF-PMDA-PA particles decreased but appeared to level off at 10 wt % solution (Table 4.21). Thus, the 10 wt % concentration was chosen because it provides the smallest BDAF-PMDA-PA particles with the least solvent. The effect of solution imidization concentration on the size of TPEQ-ODPA-PA (30K) particles was also investigated. As the solution was diluted, the particle size decreased.

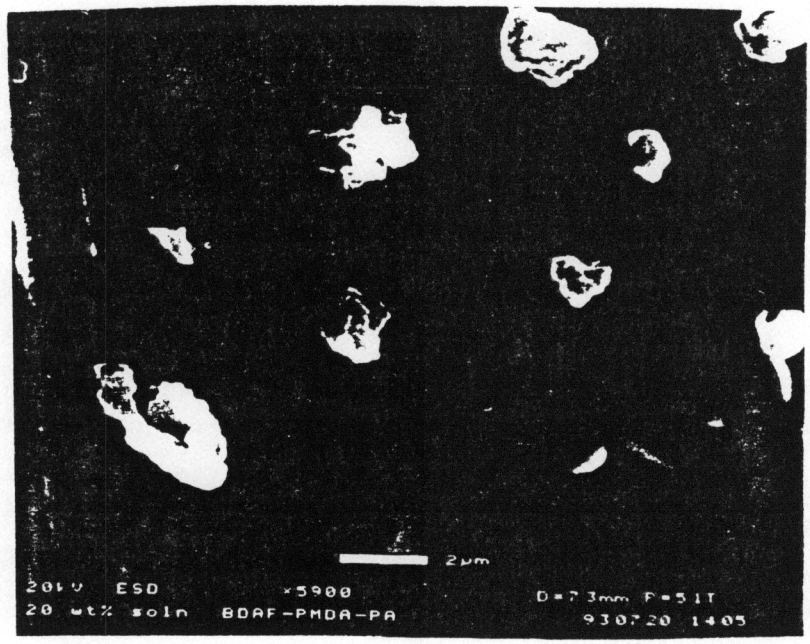

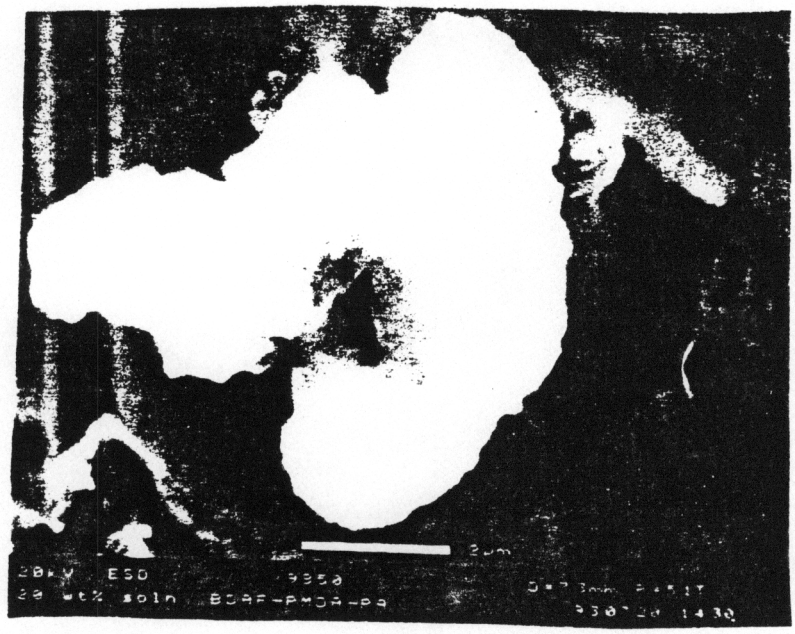

Median Particle Diameter By Particle Size Analyzer = 3.8 μm

Figure 4.43: ESEM of BDAF-PMDA-PA (30K) Polyimide Powder

4.3.3.2 Temperature

The influence of temperature during imidization on the particle size was evaluated (Table 4.22). To control the temperature of the solution, the thermocouple was immersed in the reaction solution. NMP was the solvent and the selected temperatures were 180°C, 165°C, and 155°C. As the temperature was increased, the particle size increased. These results may be explained by the lower rate of crystallization and increased solubility at higher temperatures.

4.3.3.3 Polymer Molecular Weight

A series of different molecular weight 4,4'-ODA-PMDA-PA polyimides were prepared. The other experimental conditions were held constant. The poly(amic acid) of each of these polymers were isolated by precipitation in cold water, filtered, and dried at room temperature in vacuo for 3 days. The intrinsic viscosity results showed little difference in the corresponding molecular weights. As the target Mn increased, the particle size increased as shown in Table 4.23.

The effect of MW on the particle size of the TPEQ-ODPA-PA system was investigated (Table 4.23). As the Mn increased, the particle size became smaller. This is the opposite trend observed for the 4,4'-ODA-PMDA-PA system.

Table 4.21: The Influence of the Solution Concentration on the Size of BDAF-PMDA-PA (30K) Polyimide Particles

CONCENTRATION (%)	PARTICLE SIZE (μm)
20	3.6
15	2.7
10	1.8
5	1.5

Table 4.22: The Effect of the Solution Imidization Temperature on the BDAF-PMDA-PA (30K) Particle Size

TEMPERATURE (°C)	PARTICLE SIZE (μm)
180	13.7
165	4.1
155	1.8

Table 4.23: The Relationship of Molecular Weight and Particle Size

POLYMER	Mn (g/mol)	[n]*	PARTICLE SIZE (μm)
ODA-PMDA-PA	10,000	0.34	0.4
ODA-PMDA-PA	20,000	0.35	0.3
ODA-PMDA-PA	30,000	0.34	1.60
ODA-PMDA-PA	40,000	0.32	1.90
TPEQ-ODPA-PA	15,000	0.32	33
TPEQ-ODPA-PA	20,000	0.34	27
TPEQ-ODPA-PA	30,000	0.42	17

*Intrinsic viscosities were measured on the poly(amic acid) in NMP at 25°C

4.3.3.4 Particle Stabilization

4.3.3.4.1 Self Stabilization

The particle stabilizer plays an important role in prepregging and the resulting composite properties. As discussed in the Literature Review, PEEK particles have been successfully stabilized by the ammonium hydroxide salt of LARC TPI poly(amic acid) and the poly(amic acid) salt stabilizer also serves as an effective binder for the particles to the fibers (117, 121). The isolated polyimide particles are not completely imidized; therefore, amic acid groups exist along the polymer backbone. Consequently, these particles may be able to SELF-STABILIZE. The ability of the partially imidized polyimide particles to self-stabilize due to the presence of the amic acid moiety along the backbone was investigated.

The control experiment was evaluation of the particle size without any stabilizer. Particles were prepared for the PSA as reported in the Experimental section except no stabilizer or base was added. The unstabilized particles flocculated and could not be measured.

In the first experiment to determine effect of pH on particle size (Table 4.24), the particles were isolated in NEUTRAL water and filtered. The PSA sample was prepared in the same fashion as described in Experimental section except that no Triton-X 100 was added. Instead, the pH of the solution was adjusted by addition of ammonium hydroxide. The particles were "partially stabilized" in that the median particle diameter was larger than in the presence of Triton-X 100 but they were still relatively small aggregates.

In the second experiment, the only variable that was altered was that the particles were isolated in BASIC water instead of neutral water. As shown in

Table 4.24: BDAF-PMDA-PA (30K) Particles Isolated in NEUTRAL Water

SOLN CONC	PH	PARTICLE SIZE (μm)
20%*	8-9	20.4
15%**	10	15.7
15%**	12	16.1

*20% with Triton X-100 stabilizer: 3.6 μm
**15% with Triton X-100 stabilizer: 2.7 μm

Table 4.25: BDAF-PMDA-PA (30K) Particles Isolated in BASIC Water

SOLN CONC	PH	PARTICLE SIZE (μm)
20%	8	6.8
20%	10	9.6
20%	12	5.3

20% with Triton X-100 stabilizer: 3.6 μm

Table 4.25, the particles were considerably smaller than for the experiment in which the particles were isolated in neutral water; however, the particles were not as small as the particles stabilized with Triton-X 100.

4.3.3.4.2 Particles Stabilized by Ammonium Salts of Poly(amic acid)

The tendency of the particles to be stabilized by the ammonium hydroxide salt of LARC TPI poly(amic acid) was studied. The ammonium hydroxide salt of LARC TPI poly(amic acid) and samples for PSA were prepared as described in the Experimental section except a solution of the poly(amic acid) salt was added as the stabilizer. Each sample was prepared under the same conditions such that 5 weight percent stabilizer was added to the particle suspension. The BDAF-PMDA-PA particles stabilized with the poly(amic acid) salt had a median diameter of 2.9 μm and the same particles stabilized with Triton X-100 had a median particle diameter of 2.4 μm. The effect of the stabilizer on particle size is summarized in Table 4.26.

Preparation of the ammonium hydroxide salt of the BDAF-PMDA poly(amic acid) was unsuccessful. A 25% excess of ammonium hydroxide per COOH group was added but the poly(amic acid) did not completely dissolve in water. This is believed to be a consequence of the crystallinity and the fluorine content. The crystalline polyimides were highly solvent resistant in highly polar solvents like NMP. As discussed in the literature review, water absorption decreases as fluorine content of a polymer increases; therefore, the solubility of this fluorine containing polyimide in water is very low.

Table 4.26: The Influence of the Stabilizer on the Size of BDAF-PMDA-PA (30K) Particles

Stabilizer	Median Particle Diameter (μm)
Triton X-100‡	2.4
Ammonium Salt of LaRC PAA	2.9
*Water pH = 7/ pH = 9	20.4
*Water pH = 8/ pH = 8	6.8
*Water pH = 10/ pH = 10	9.6

‡nonionic polyoxyethylene ether surfactant with a nominal MW of 646 g/mol
*pH of the water the particles were isolated in/ pH of the analyzed sample

4.3.3.5 Drying and Imidization of Particles

4.3.3.5.1 Percent Imidization of Particles

The particles begin to precipitate from solution during solution imidization after approximately 20 to 30 minutes. Studies have shown that many hours are required to produce completely cyclized polyimides by this technique (26, 52-57). Therefore, the particles are not completely imidized. A study was conducted to determine the percent imidization of the particles. There are many techniques available to follow conversion of an amic acid to an imide with each method having advantages as well as disadvantages over other techniques. The most common technique used to study imidization is FTIR (26, 31, 32, 38, 44) in which the main advantages of FTIR are that it is a relatively easy technique with well documented procedures. However, the 1778 and 725 cm^{-1} bands used in the FTIR analysis of imidization are insensitive to changes in the later stages of imidization that could be detected by thermal techniques (26). Navarre and coworkers (32) also stated that DSC and TGA analysis was more precise than FTIR analysis for evaluating the end of the imidization reaction providing a fully cured product. Therefore, TGA analysis was selected as the method to evaluate percent imidization.

The amount of imide cyclization and dehydro-condensation are stoichiometrically equal. Therefore, imidization can be followed by measuring the weight loss that accompanies the dehydro-condensation. However, it is very important to eliminate all the factors that might contribute to weight loss such as residual solvent and water absorbed upon isolation of the particles. Numata et al (33) developed a procedure to remove residual solvent and water.

A similar procedure was utilized for these studies as discussed in the Experimental section.

Three TPEQ-ODPA-PA (30K) samples were synthesized at various solution imidization temperatures to determine the effect of temperature on the percent imidization. Kim and coworkers (26) showed that maximum rehealing of the poly(amic acid) chain occurred at 180°C; therefore, it was believed that the higher temperatures would produce particles with higher percent imidization. The samples were analyzed by TGA (Figure 4.44) and the percent weight loss was measured at 200°C which was assumed to be equivalent to the amount of water lost upon cyclization. This value was divided by the weight loss for the completely unimidized polymer, the poly(amic acid), giving the value for the unimidized portion of the polymer. This value was subtracted from 100% to give the percent imidization of the particles. The particles prepared at 180°C were 57% imidized which was the highest percent imidization observed for the selected temperatures (Table 4.27).

4.3.3.5.2 Drying of Particles

The particles as isolated can be used for aqueous prepregging without further treatment. However, for electrostatic prepregging, the particles must be completely free of solvent and water. Therefore, the particles must be dried to remove solvent and water and quantitatively cyclized to ensure water is not evolved upon consolidation of the composite. The particle sizes of three different polyimide systems were evaluated with respect to the drying conditions (Table 4.28).

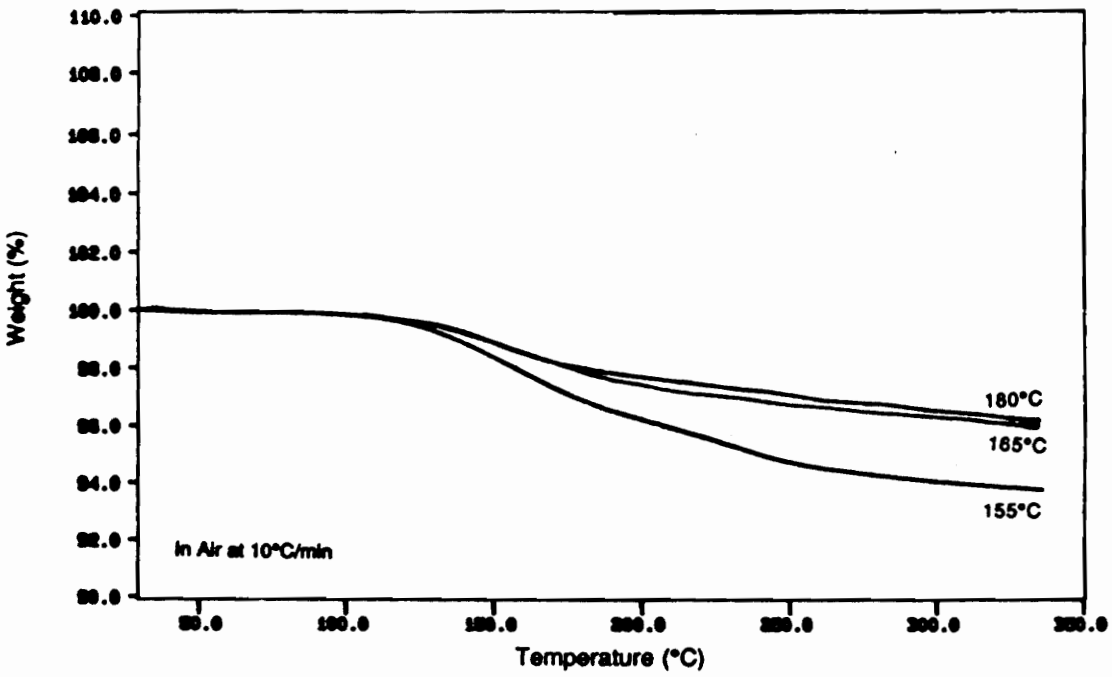

Figure 4.44: TGA Analysis of TPEQ-ODPA-PA (30K) Particles Synthesized At Different Temperatures

Table 4.27: The Effect of the Solution Imidization Temperature on the Percent Imidization of the TPEQ-ODPA-PA (30K) Powders

Temperature (°C)	% Wt Loss At 200°C*	% Imidization
155	3.82	36
165	2.74	54
180	2.51	57

*Weight loss measured by TGA-10°C/min and in air.

Table 4.28:The Effect of Drying on the Particle Size

Polymer	Drying Conditions	Particle Size (μm)
4,4'-ODA-PMDA-PA	none	8.3
4,4'-ODA-PMDA-PA	RT 3 days	5.3
4,4'-ODA-PMDA-PA	100°C 24 hours	---
4,4'-ODA-PMDA-PA	200°C 6 hours	12.5
BDAF-PMDA-PA	none	2.8
BDAF-PMDA-PA	RT 3 days	7.4
BDAF-PMDA-PA	100°C 24 hours	---
BDAF-PMDA-PA	200°C 6 hours	8.9
TPEQ-ODPA-PA	none	16.0
TPEQ-ODPA-PA	100°C, 200°C, 300°C 1 hour each	24.8
TPEQ-ODPA-PA	280°C 4 hours	45.1

The 4,4'-ODA-PMDA-PA (30K) particles were dried in vacuo for 3 days at room temperature. The particle size decreased from 8.3 μm to 5.3 μm which was an unexpected result. Usually upon drying, particles will aggregate. However, a reasonable explanation is that the wet particles were swollen with solvent causing a larger particle size. The 4,4'-ODA-PMDA-PA (30K) particles were heated slowly over a period of 4 hours to 100°C and held for 24 hours. The final step was 6 hours at 200°C which produced aggregated particles with a median diameter of 12.5 μm.

The BDAF-PMDA-PA (30K) particles underwent the same drying cycle as the 4,4'-ODA-PMDA-PA (30K) particles. The undried particles had a median particle diameter of 2.8 μm and increase to 8.9 μm after drying.

The undried TPEQ-ODPA-PA (30K) particles had a median diameter of 16 μm with a broad distribution ranging from 100 μm to 0.5 μm. The particles were dried in vacuo at room tempearture for 24 hours. The temperature was increased over two hours to 280°C and held for 4 hours. As expected, the particles aggregated displaying a median diameter of 45 μm.

Another series of particles were dried in a different manner. The first step was the particles were dried in vacuo at room temperature for 24 hours. Over the course of 4 hours, the temperature was increased to 100°C and held for 12 hours. Finally the temperature was held for 1 hour each at 200°C and 300°C. The median diameter of the particles was 25 μm.

4.3.3.6 Suspension Concentration

The two main variables controlling the volume fraction of fiber in a composite are the tow speed and the suspension concentration. Therefore, it is

necessary to determine the effect of suspension concentration on particle stabilization. The concentration of the stabilizer relative to the particles was held constant at 5 weight percent. The size of BDAF-PMDA-PA (30K) particles was measured as a function of suspension concentration (Table 4.29). The median particle diameter was 2.1 μm for the very dilute suspension concentration and increased by approximately 36% to 3.3 μm for a 20% suspension concentration. For aqueous or electrostatic prepregging, this change is inconsequential.

4.3.3.7 Suspension Shelf-Life

It is advantageous to form a suspension of the polyimide particles and have it remain stable until the time of prepregging. The time that the particle suspension remains stable is the "shelf-life" of the suspension. Suspensions of the BDAF-PMDA-PA (30K) particles with 5 weight percent of the stabilizer were prepared. Two stabilizers, Triton X-100 and the ammonium hydroxide salt of the LARC TPI poly(amic acid), were selected to determine the effect of stabilizer on shelf-life. Different suspension concentrations were prepared to determine the relationship of suspension concentration on shelf-life. The results are summarized in Tables 4.30 and 4.31. For the Triton X-100, the 0.5%, 2.5%, and the 10% suspension concentrations showed a 10% or less difference between the initial particle size and the particle size after 17 days, which is within instrumental error. However, the 5.0% and 20% suspension concentration showed a 13% and 20% decrease in the particle size after 17 days. One possible explanation for the decrease in particle size after extended periods is that the Triton X-100 may be slowly absorbing onto the surface of the particles

Table 4.29: The Influence of the Suspension concentration on the BDAF-PMDA-PA (30K) Particle Stabilization With Triton X-100

% Concentration of the Suspension	Median Particle Diameter (μm)
0.5	2.1
2.5	2.8
5.0	3.3
10	3.0
20	3.3

The concentration of the stabilizer to particles was held constant at 5 wt %.

Table 4.30: The Shelf-Life of BDAF-PMDA-PA (30K) Particles Stabilized With Triton X-100*

Time (days)	0.5%	2.5%	5.0%	10%	20%
0	2.10	2.78	3.27	3.02	3.31
3	2.19	2.83	2.82	2.59	3.41
10	2.35	2.86	3.81	2.58	2.53
17	2.34	2.90	2.86	2.86	2.65
Change‡	10	5	13	5	20

*The concentration of the stabilizer to particles was held constant for each sample at 5 wt %.
‡Values represent the % difference between the initial size with the size after 17 days.

Table 4.31: The Shelf-Life of BDAF-PMDA-PA (30K) Particles Stabilized With The Ammonium Salt of the LARC TPI Poly(amic acid)*

Time (days)	0.5%	2.5%	5.0%	10%	20%
0	2.90	3.17	3.8	3.4	3.39
10	3.03	4.16	3.69	3.56	3.41
Change‡	10	24	3	4	1

*The concentration of the stabilizer to the particles was held constant for each sample at 5 wt %.
‡The values reperesent the % difference between the initial size of the particles and the particle size after 10 days.

creating a more stable suspension. Using the poly(amic acid) salts, the median particle diameters are within instrumental error of the initial suspensions and the suspensions aged for 10 days except for the 2.5% suspension concentration sample. This sample showed a 24% increase in particle size after 10 days. This may be an anomaly or this sample aggregated due to an unstable suspension.

4.3.4 Sintering

Sintering experiments were conducted to examine processing conditions for the polyimide powders. Figure 4.45 is a schematic diagram displaying the steps involved in sintering and sample preparation for mechanical testing. Conditions for the sintering experiments are summarized in Table 4.32 and were selected based on the melting transition of the TPEQ-ODPA-PA (30K) powders. For experiments 1 and 2, the cold pressed disks were placed in the oven equilibrated at the desired temperature while the disks in experiments 3 and 4 were placed in the oven and heated slowly (5°C/min) to the desired temperature. Experiments 3 and 4 are more realistic conditions because the press heats at a rate of 5°C/min. The moduli values for the sintered TPEQ-ODPA-PA (30K) particles are presented in Table 4.33.

The sintered particles were analyzed by TGA (Table 4.34) and DSC (Table 4.35) to determine the influence of sintering on the thermal behavior of the polyimide. The sintered samples showed temperatures for 5 % weight loss 25°C to 40°C higher than the unsintered particle which may indicate that the sintered materials have slightly higher thermooxidative stability. The Tgs of the

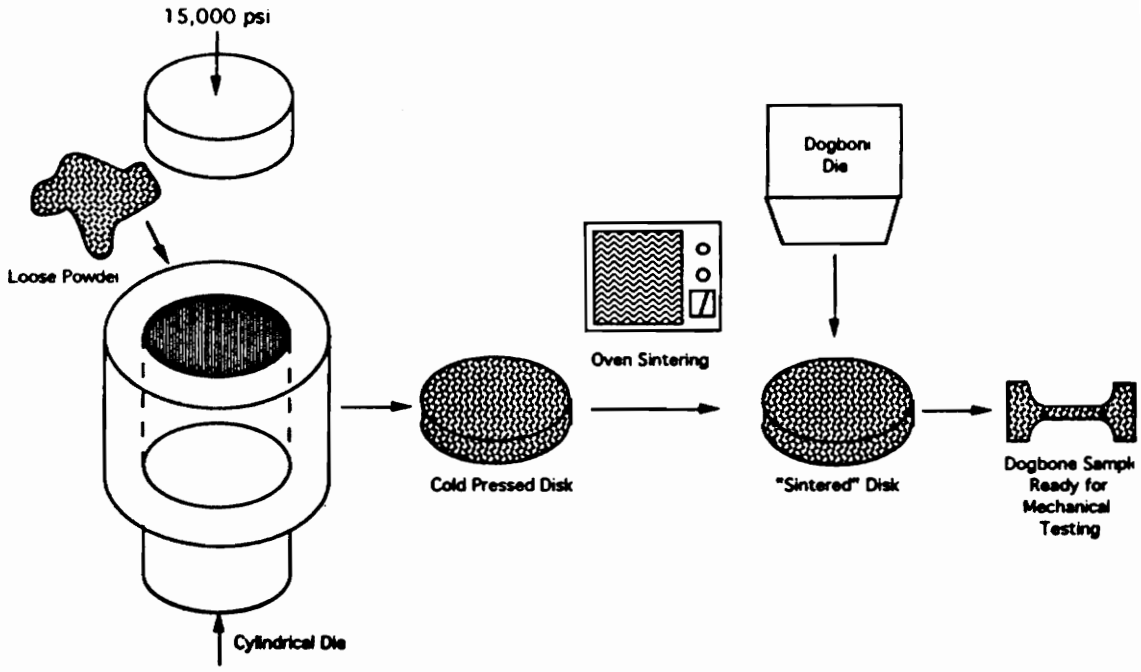

Figure 4.45: Sample Preparation For Sintering and Mechanical Testing

Table 4.32: Conditions for the Sintering Experiments of the TPEQ-ODPA-PA (30K) Particles

Experiment	Heating Rate	Temperature (°C)	Hold Time (min)
1	none	422	10
2	none	440	20
3	5°C/min	440	0
4	5°C/min	440	20

Table 4.33: The Moduli Values for the Sintered TPEQ-ODPA-PA (30K) Particles

Sintering Conditions	Ave. Secant Mod.* (MPa)	Ave. Max. Mod.‡ (MPa)	Ave. Strain‡ (%)
422°C 10 min	445 ± 52.8	892 ± 134	2.4
440°C 20 min	445 ± 24.6	937 ± 180	3.0
5°C/min 440°C 0 min	490 ± 99.9	953 ± 72	2.9
5°C/min 440°C 20 min	513 ± 91.2	880 ± 149	3.2

*Modulus at break from the collected data
‡Max value of derivative of the curve calculated using the Origin program

Table 4.34: TGA Results of the Sintered TPEQ-ODPA-PA (30K) Particles

Sintering Conditions	5% Wt Loss* (°C)
Unsintered Particles	552
422°C 10 min	573
5°C/min 440°C 0 min	592
5°C/min 440°C 20 min	577

*In air at 10°C/min

Table 4.35: DSC Analysis Results of the Sintered TPEQ-ODPA-PA (30K) Particles

Sintering Conditions	Tg (°C)	Tm * (°C)	ΔH_f (J/g)
Unsintered Particles	232	409	33
5°C/min 440°C 0 min	237	none	---
5°C/min 440°C 20 min	252	none	---

*Values were measured on the first heat.

sintered materials were higher than the unsintered sample and showed no evidence of crystallinity after the thermal treatment.

CHAPTER 5: CONCLUSIONS

A novel fluorinated ("3F") diamine, 1,1-bis[4-(4-aminophenoxy)phenyl]-1-phenyl-2,2,2-trifluoroethane (3FEDAM), has been prepared from trifluoroacetophenone. The 3FEDAM monomer was readily synthesized by two routes which one method was a novel two step procedure and the other pathway consisted of three steps that were analogous to the preparation of the 6F diamine, BDAF. The overall yields of the two step and the three step procedures were approximately 80% and 76%, respectively; therefore, the two step procedure is not significantly favorable over the three step procedure in terms of overall yield. However, the attractive characteristic of the two step procedure is it required less time to synthesize the product, 3FEDAM. The synthesis of 3FEDAM by the two step procedure has the potential to be scaled up to produce large amounts of the monomer for further studies.

Each intermediate in the synthesis of the 3FEDAM monomer was fully characterized by ^{1}H NMR, FTIR, melting point, and elemental analysis. The characteristic peaks in the^{1}H NMR of 3FEDAM combined with their integration values provided strong evidence that 3FEDAM had been synthesized. The results of the elemental analysis of the intermediates and 3FEDAM showed an excellent correlation between the theoretical and the experimental values. Potentiometric titration and HPLC analysis showed that the 3FEDAM monomer was pure. Intrinsic viscosity and GPC results showed that high molecular weight and controlled molecular weight polymer was obtained from this fluorinated monomer. Therefore, this new monomer was synthesized and purified to give monomer grade material.

A high molecular weight (MW) and a 30K controlled MW polyimide based on 3FEDAM and pyromellitic dianhydride (PMDA) were prepared. These materials exhibited high Tg's of 316°C and 308°C, respectively, and were semicrystalline in nature as determined by both DSC and WAXS. The 3FEDAM-PMDA-PA polyimide displayed a Tm of 476°C; however, the material degraded upon melting. Due to the high Tm and unstable melting transition, this material could not be melt processed. Therefore, several copolymers were investigated in hopes that the incorporation of the comonomer, 6FDA, would depress the Tm and provide a melt stable material. Indeed this was the case. Incorporation of 20 mole percent of 6FDA produced a melt stable endotherm at 440°C. However incorporation of more than 20% 6FDA destroyed the semicrystalline nature. Nevertheless, the 3FEDAM based polyimides studied were highly solvent resistant.

The BDAF-PMDA polyimide exhibited Tg of 305°C and a well defined high melting point via DSC near 470°C. Exothermic degradation was observed several degrees above this very high Tm. The melting point of the BDAF containing polyimides was lowered by the incorporation of the flexible comonomer 6FDA. Adding the 3F diamine to the BDAF containing polyimides significantly raised the Tg of the polyimides. However, the incorporation of 20 mole percent of 3F diamine completely eliminated the crystallinity.

The 3FEDAM and BDAF based polyimides demonstrated good thermooxidative stability under dynamic conditions and isothermal conditions for short time periods. Long term studies were initiated to further evaluate the thermooxidative stability of these fluorinated, semicrystalline polyimides. After 250 hours at 316°C, the 6F polyimide (BDAF-PMDA-PA) appeared to have

better thermooxidative stability than the corresponding 3F polyimide (3FEDAM-PMDA-PA). At 371°C (700°F), the difference in the thermooxidative stability of the 3F and the 6F polyimides was more significant. After 150 hours, the 3FEDAM-PMDA-PA (30K) polyimide only retained 20% of its original weight whereas the BDAF-PMDA-PA (30K) polyimide exhibited 45% weight retention. These fluorinated, semicrystalline polyimides performed better at 316°C than 371°C because 316°C is only slightly above the Tg (~306°C) of the polymers. Therefore, these materials have potential as matrix resins for aerospace applications for extended periods of time at 600°F. However, these fluorinated polyimides may be useful for short term applications at 700°F.

The 3FEDAM diamine is the 3F analog of the BDAF and is potentially more cost efficient to prepare than BDAF. The precursor to 3FEDAM, trifluoracetophenone, is less expensive and easier to handle than hexafluoroacetone. Since the 3FEDAM diamine is similar in structure to BDAF, it was proposed that this new monomer, 3FEDAM, would produce polyimides that possess similar characteristics inherent in the BDAF systems. The thermal analysis results of the BDAF and the 3FEDAM containing polyimides provided evidence supporting this prediction. Therefore, 3FEDAM polyimide systems could potentially replace the analogous BDAF polyimide systems.

The TPEQ based polyimides were semicrystalline in nature with Tm values in the range of 411°C to 468°C and Tgs in the range of 239°C to 255°C. The effect of molecular weight control was clearly demonstrated by the TPEQ-ODPA-PA polyimides. The apparent level of crystallinity showed a dependence on the molecular weight. In addition, the 7.5K, 10K, and 15K TPEQ-ODPA-PA polyimides exhibited a crystallization exotherm upon the second heat whereas

the higher molecular weight 20K and 30K samples did not exhibit a crystallization exotherm or a melting transition.

Fine polyimides powders in the range of 5 to 45 microns were directly synthesized via a 'dispersion-like' polymerization method utilizing solution imidization to affect cyclodehydration. This method is much more cost efficient than the current method to produce polyimide powders which is cryogenic grinding. Also this direct preparation of the powders allows control of particle size. Therefore, this procedure should be scaled up.

The polyimide powders are not completely imidized upon precipitation from solution. Therefore, poly(amic acid) moieties are present along the backbone and it has been shown that these partially imidized powders can self-stabilize. This may provide many advantages in preparing prepregs by the aqueous dispersion method. In addition, these polyimide powders show promise as resins for polymer matrix composites prepared via electrostatic prepregging because the powders can be completely dried with a small amount of aggregation.

CHAPTER 6: REFERENCES

1. C. Feger, M. M. Khojasteh, and J. E. McGrath, Editors, "Polyimides: Chemistry, Materials, and Characterization", Elsevier (1989).

2. D. Wilson, H. D. Stenzenberger, and P. M. Hergenrother, Editors "Polyimides", Chapman and Hall, New York (1990).

3. K. L. Mittal, Editor, "Polyimides: Synthesis, Characterization, and Applications", Plenum Press, New York, Volumes 1 and 2 (1984).

4. T. Takekoshi, Adv. Poly. Sci., 94, 1, (1990).

5. C. E. Sroog, Prog. Polym. Sci., 16, 561 (1991).

6. M. I Bessonov, M. M. Koton, V. V. Kudryavtsev, and L. A. Laius, "Polyimides: Thermally Stable Polymers", Consultants Bureau Div. Plenum Publishing Corp., New York (1987).

7. G. M Bower and L. W. Frost, J. Poly. Sci.: Part A, 1, 3135 (1963).

8. R. J. Boyce, T. P. Gannett, H. H. Gibbs, and A. R. Wedgewood, SAMPE, 32, 169 (1987).

9. T. M. Moy, C. D. DePorter, and J. E. McGrath, Polymer, 34(4), 819 (1993).

10. J. P. Critchley, R. A. Grattan, M. A. White, and J. S. Pippett, J. Poly. Sci.: Part A-1, 10, 1789 (1972).

11. M. Dorr and M. Levy, J. Polym. Sci. Polym. Chem. Ed., 13, 171 (1975).

12. W. F. Farrisey, J. S. Rose, and P. S. Carleton, Polym. Prepr., 9, 1581 (1968).

13. S. N. Kharkov, E. P. Krasnov, Z. N. Laurova, S. A. Baranova, U. P. Aksenova, and A. S. Chegola, J. Polym. Sci. USSR, 13(4), 940 (1971).

14. T. Takekoshi, J. G. Wirth, D. R. Heath, J. E. Kochanowski, J. S. Manello, and M. J. Webber, J. Polym. Sci. Polym. Chem. Ed., 18, 3069 (1980).

15. Y. Imai, Polymer Letters, 8, 555 (1970).

16. T. Takekoshi, J. L. Webb, P. P. Anderson, and C. E. Olson, IUPAC 32nd Inter.Symp. on Macromolecules, 464 (1988).

17. M. E. Rogers, PhD Dissertation, Virginia Tech (1993).

18. C. E. Sroog, A. L. Endrey, S. V. Abramo, C. E. Berr, W. M. Edwards, K. L. Olivier, J. Polym. Sci.: Part A, 3, 1373 (1965).

19. W. Volksen and P. M. Cotts in "Polyimides: Synthesis, Characterization, and Applications", K. L. Mittal, editor, Plenum Press, New York, 1, 163 (1984).

20. M. J. Brekner and C. Feger, J. Polym. Sci.: Part A: Polym. Chem., 25, 2005 (1987).

21. M. J. Brekner and C. Feger, J. Polym. Sci.: Part A: Polym. Chem., 25, 2479 (1987).

22. F. W. Harris in , "Polyimides", D. Wilson, H. D. Stenzenberger, and P. M. Hergenrother, editors, Chapman and Hall, New York, Chapter 1 (1990).

23. M. M. Koton, V. V. Kudriavtsev, and V. M. Svetlichny in "Polyimides: Synthesis, Characterization, and Applications", K. L. Mittal, editor, Plenum Press, New York, 1, 171 (1984).

24. V. M. Svetlichny, K. K. Kalnin'sh, V. V. Kudryavtsev, and M. M. Koton, Dokl. Akad. Nauk. USSR (Engl. Transl. 237 (3)), 693 (1977).

25. Y. J. Kim, T. E. Glass, G. D. Lyle, and J. E. McGrath, Macromolecules, 26, 1344 (1993).

26. S. Ando, T. Matsuura, and S. Nishi, Polymer, 33(14), 2934 (1992).

27. S. Ando, T. Matsuura, and S. Saski, J. Polym. Sci.: Part A: Polym. Chem., 30, 2285 (1992).

28. V. A. Zubkov, M. M. Koton, V. V. Kudryavtsev, and V. M. Svetlichny, Zh. Org. Khim. (Engl. Transl.) 17(8), 1501 (1982).

29. M. Hasegawa, Y. Shindo, T. Sugimura, K. Horie, R. Yokota, and I. Mita, J. Polym. Sci.: Part A: Polym. Chem., 29, 1515 (1991).

30. M. L. Bender, Y. L. Chow, F. Chloupek, J. Am. Chem. Soc., 80, 5380 (1958).

31. J. A. Kreuz, A. L. Endrey, F. P. Gay, and C. E. Sroog, J. Polym. Sci.: Part A-1, 2, 2607 (1966).

32. M. Navarre in "Polyimides: Synthesis, Characterization, and Applications", K. L. Mittal, editor, Plenum Press, New York, 1, 429 (1984).

33. S. Numata, K. Fujisaki, and N. Kinjo in "Polyimides: Synthesis, Characterization, and Applications", K. L. Mittal, editor, Plenum Press, New York, 1, 259 (1984).

34. C. E. Sroog, J. Polym. Sci. Macromol. Rev., 11, 161 (1976).

35. J. Preston and W. B. Black in "Man-made Fibers, Science, and Technology", H. F. Mark, S. M. Atlas, and E. Cernia, editors, Wiley, New York, vol. 2 (1968).

36. J. W. Verbicky, Jr. in "Encyclopedia of Polymer Science and Engineering", H. F. Mark, N. M. Bikales, C. G. Overberger, and G. Menges, editors, 2nd Edn., Wiley, New York, 12, 364 (1988).

37. V. L. Bell, B. L. Stump, and H. Gager, J. Polym. Sci., Polym. Chem. Ed., 14, 2275 (1976).

38. D. E. Kranbuehl, S. E. Delos, P. K. Jue, and R. K. Schellenberg in "Polyimides: Synthesis, Characterization, and Applications", K. L. Mittal, editor, Plenum Press, New York, 1, 207 (1984).

39. E. Pyun, R. J. Mathisen, And C. S. P. Sung, Macromolecules, 22, 1174 (1989).

40. D. R. Day And S. D. Senturia in "Polyimides: Synthesis, Characterization, and Applications", K. L. Mittal, editor, Plenum Press, New York, 1, 249 (1984).

41. M. F. Grenier-Loustalot, F. Joubert, and P. Grenier, J. Polym. Sci.: Part A: Polym. Chem., 29, 1649 (1991).

42. C. Johnson and S. L. Wunder, J. Polym. Sci.: Part B: Polym. Phys., 31, 677 (1993).

43. L. A. Laius and M. I. Tsapovetsky in "Polyimides: Synthesis, Characterization, and Applications", K. L. Mittal, editor, Plenum Press, New York, 1, 295 (1984).

44. R. Ginsburg and J. R. Susko in "Polyimides: Synthesis, Characterization, and Applications", K. L. Mittal, editor, Plenum Press, New York, 1, 237 (1984).

45. L. A. Laius, M. I. Bessonov, F. S. Florinski, Vysokomol. Soyed., A13 (9), 2006 (1971).

46. R. W. Snyder, B. Thomson, B. Bartges,D. Czerniawski, and P. C. Painter, Macromolecules, 22, 4166 (1989).

47. E. J. Sacher, Macromol. Sci. Phys., B25, 405 (1986).

48. P. H. Hermans and J. W. Streef, Die Makromol. Chemie, 74, 133 (1964).

49. G. A. Bernier and D. E. Kline, J. Appl. Polym. Sci., 12, 593 (1968).

50. R. A. Dine-Hart, Makromol. Chem., 143, 189 (1971).

51. S. V. Vingradova, V. V. Korshak, and Y. S. Vygodski, Vysokomol. Soedin., 8, 809 (1966).

52. J. E. McGrath, M. E. Rogers, C. A. Arnold, Y. J. Kim, and J. C. Hedrick, Makromol. Chem., Macromol. Symp., 51, 103 (1991).

53. J. D. Summers, PhD Dissertation, Virginia Tech (1988).

54. B. C. Johnson, PhD Dissertation, Virginia Tech (1984).

55. C. A. Arnold, J. D. Summers, Y. P. Chen, R. H. Bott, D. Chen, and J. E. McGrath, Polymer, 30, 986 (1989).

56. D. L. Wilkens, C. A. Arnold, M. J. Jurek, M. E. Rogers, and J. E. McGrath, J. Thermoplas. Compos. Mater., 3(1), 4 (1990).

57. R. O. Waldbauer, M. E. Rogers, C. A. Arnold, G. A. York, Y. Kim, and J. E. McGrath, Am. Chem. Soc. Div. Polym. Chem. Polym. Prepr., 31(2), 432 (1990).

58. G. Odian, "Principles of Polymerization", 3rd Edn., Wiley Interscience, New York (1991).

59. W. D. Weber and M. R. Gupta in "Recent Advances in Polyimide Science and Technology", W. D. Weber and M. R. Gupta, editors, 214 (1987).

60. A. Rudin, "The Elements of Polymer Science And Engineering", Academic Press, Orlando (1992).

61. D. A. Scola, R. A. Pike, J. H. Vontelli, and C. M. Brunette, High Performance Polymers, 1(1), 17 (1989).

62. M. E. Rogers, M. H. Brink, A. Brennan, and J. E. McGrath, Polymer, 34(4), 849 (1993).

63. P. J. Flory, "Principles of Polymer Chemistry", Cornell University Press, Ithaca (1953).

64. M. J. Jurek and J. E. McGrath, Polymer, 30, 1552 (1989).

65. F. W. Mercer and T. D. Goodman, High Performance Polymers, 3(4), 297 (1991).

66. T. L. St. Clair in "Polyimides", D. Wilson, H. D. Stenzenberger, and P. M. Hergenrother, editors, Chapman and Hall, New York, Chapter 3 (1990).

67. C. E. Sroog, Macromolecular Reviews, 11, 161 (1976).

68. J. P. Critchley, G. J. Knight, and W. W. Wright, "Heat Resistant Polymers", Plenum (1983).

69. P. E. Cassidy, "Thermally Stable Polymers", Marcel Dekker (1980).

70. F. E. Rogers (E. I. du Pont de Nemours and Co.), US Patent 3,356,648 (December 1967).

71. The Interdisciplinary Symposium on Recent Advances in Polyimides, Reno, Nevado, July 13-16, 1987.

72. P. E. Cassidy, T. M. Aminabhavi, J. M. Farley, JMS-Rev. Macromol. Chem. Phys., C29 (2 & 3), 365 (1989).

73. T. L. St. Clair, A. K. St. Clair, and E. N. Smith in "Structure-Solubility Relationships in Polymers", F. W. Harris and R. B. Seymour, editors, Academic Press, 199 (1977).

74. A. K. St. Clair, T. L. St. Clair, and W. S. Slemp in "Recent Advances in Polyimide Science and Technology", W. D. Weber and M. R. Gupta, editors, 16 (1987).

75. Y. S. Negi, Y. I. Suzuki, T. Hagiwara, Y. Takahashi, M. Iijima, M. A. Kakimoto, and Y. Imai, J. Poly. Sci.: Part A: Poly. Chem., 30, 2281 (1992).

76. R. J. Jones, G. E. Chang, S. H. Powell, And H. E. Green in "Polyimides: Synthesis, Characterization, and Applications", K. L. Mittal, editor, Plenum Press, New York, 2, 1117 (1984).

77. H. H. Gibbs, J. Appl. Poly. Sci. (Applied Polymer Symp: Long-Term Prop. of Polymers and Polymeric Materials), 35, 207 (1979).

78. T. Matsuura, Y. Hasuda, S. Nishi, and N. Yamada, Macromolecules, 24, 5001 (1991).

79. A. K. St. Clair, T. L. St. Clair, K. I. Shevket, Am. Chem. Soc. PMSE Proceedings, 51, 62 (1984).

80. L. M. Ruiz, Int. SAMPE Electron. Conf., 3, 209 (1989).

81. T. Ichino, S. Sasaki, T. Matsuura, and s. Nishi, J. Poly. Sci.: Part A: Poly Chem., 28, 323 (1990).

82. S. D. Senturia, "Polyimides in Microelectronics", Proc. of the ACS Div. of Poly. Mater. Sci. Eng., 55, 385 (1988).

83. J. Economy, Contemporary Topics in Poly. Sci., 5, 351 (1992).

84. A. K. St. Clair, T. L. St. Clair, and W. P. Winfree, Am. Chem. Soc. Mater. Sci. Eng., 59, 28 (1988).

85. A. C. Misra, G. Tesoro, G. Hougham, and S. M. Pendhackar, Polymer, 33(5), 1078 (1992).

86. D. M. Stoakley, A. K. St. Clair, and R. M. Baucom, Int. SAMPE Electron. Conf., 3, 224 (1989).

87. D. A. Scola, J. Poly. Sci.: Part A: Poly Chem., 30, 1997 (1993).

88. M. K. Gerber, J. R. Pratt, A. K. St. Clair, and T. L. St. Clair, Am. Chem. Soc. Div. Polym. Chem. Polym. Prepr., 31(1), 340 (1990).

89. F. W. Harris, S. L. Hsu, C. C. Tso, Am. Chem. Soc. Div. Polym. Chem. Polym. Prepr., 31, 342 (199).

90. J. Wang, A. T. DiBenedetto, J. F. Johnson, S. J. Huang, and J. L. Cercena, Polymer, 30, 719 (1989).

91. A. J. Waddon and F. E. Karasz, Polymer, 33(18), 3783 (1992).

92. A. J. Waddon, M. J. Hill, A. keller, and D. J. Blundell, J. Mater. Sci., 22, 1773 (1987).

93. A. J. Lovinger and D. D. Davis, Macromolecules, 19, 1861 (1986).

94. T. L. St. Clair, H. D. Burks, N. T. Wakelyn, and T. H. Hou, Am. Chem. Soc. Div. Polym. Chem. Polym. Prepr., 28(1), 90 (1987).

95. T. H. Hou, N. T. Wakelyn, and T. L. St. Clair, J. Appl. Poly. Sci., 36, 1731 (1988).

96. C. Arnold, J. Polym. Sci. Macromol. Rev., 14, 265 (1979).

97. P. M. Hergenrother, N. T. Wakelyn, and S. J. Havens, J. Poly. Sci.: Part A: Poly Chem., 25, 1093 (1987).

98. P. M. Hergenrother and S. J. Havens, J. Poly. Sci., 27, 1161 (1989).

99. F. W. Harris, S. O. Norris, B. A. Reihardt, R. D. Case, S. Varaprath, S. M. Dakaki, M. Tories, W. A. Feld, and L. H. Lanier, in "Polyimides: Synthesis, Characterization, and Applications", K. L. Mittal, editor, Plenum Press, New York, 1, 3 (1984).

100. W. J. Jackson, Jr., Br. Polym. J., 12, 154 (1980).

101. W. J. Jackson, Jr., Macromolecules, 16, 1027 (1983).

102. P. P. Huo, J. B. Friler, And P. Cebe, Polymer, 34(21), 4387 (1993).

103. D. P. Heberer, S. Z. D. Cheng, J. S. Barley, S. H. Lien, R. G. Bryant, and F. W. Harris, Macromolecules, 24(8), 1890 (1991).

104. S. Z. D. Cheng, D. P. Heberer, J. J. Janimak, S. H. Lien, F. W. Harris, Polymer, 32(11), 2053 (1991).

105. S. Z. D. Cheng, D. P. Heberer, H. S. Lien, and F. W. Harris, J. Polym. Sci.: Part B: Polym. Phys., 28, 655 (1990).

106. S. Z. D. Cheng, M. Y. Cao, and B. Wunderlich, Macromolecules, 19, 1868 (1986).

107. S. Z. D. Cheng, and B. Wunderlich, Macromolecules, 21, 879 (1988).

108. S. Z. D. Cheng, D. P. Heberer, S. H. Lien, F. W. Harris, J. Polym. Sci., Polym. Phys. Ed., 28, 655 (1990).

109. S. Z. D. Cheng, M. L. Mittleman, J. J. Janimak, D. Shen, T. M. Chalmers, H. Lien, C. C. Tso, P. A. Gabori, and F. W. Harris, Polymer International, 29, 201 (1992).

110. C. A. Arnold, P. M. Hergenrother, and J. E. McGrath in "Composite Applications: The Role of Matrix, Fiber, and Interface", T. L. Vigo and B. J. Kinzig, editors, VCH Publishers, New York, 3, (1992).

111. I. Y. Chang, Int. SAMPE Symp., 37, 1276 (1992).

112. J. C. Seferis and K. J. Ahn, Int. SAMPE Symp., 34, 63 (1989).

113. D. Lesser and T. Hartness, SAMPE Q., 20(4), 38 (1989).

114. K. E. Goodman and A. C. Loos, J. Thermoplastic Comp., 3, 34 (1990).

115. D. E. Hirt, J. M. Marchello, and R. M.Raucom, Int. SAMPE Symp., 22, 360 (1990).

116. R. M. Baucom and J. M. Marchello, Int. SAMPE Symp., 36, 175 (1990).

117. T. M. Towell, D. E. Hirt, and N. J. Johnston, Int. SAMPE Symp., 22, 1156 (1990).

118. M. Ohta, S. Tamai, T. W. Towell, N. J. Johnston, and T. L. St. Clair, Int. SAMPE Symp., 35, 1030 (1990).

119. D. F. Hiscock and D. M. Bigg, Polym Comp., 10, 3 (1989).

120. J. Muzzy, B. Varughese, and P. H. Yang, Int. SAMPE Symp., 36, 1523 (1991).

121. A. Texier, R. M. Davis, K. R. Lyon, A. Gungor, J. E. McGrath, H. Marand, and J. S. Riffle, Polymer, 34(4), 896 (1993).

122. K. W. Rausch, Jr. and W. J. Farrissey, Soc. of Plastics Engineers Annual Tech. Conf., 34, 644 (1976).

123. J. W. Tom and P. G. DeBenedetti, J. Aerosol. Sci., 22 (5), 555, (1991).

124. A. E. Brink, S. Gutzeit, T. Lin, H. Marand, K. Lyon, T. Hua, R. Davis, and J. S. Riffle, Polymer, 34(4), 825 (1993).

125. H. J. Grubbs, PhD Dissertation, Virginia Tech, 1994.

126. W. H. Carothers, Trans. Faraday Soc., 32, 39 (1936).

127. T. Provder, Editor, "Particle Size Distribution: Assessment and Characterization: ACS Symp. Series No. 332, Washington, D. C. (1987).

130. J. March, "Advanced Organic Chemistry", 3rd Ed., John Wiley and Sons, New York, 493 (1985).

131. G. Olah, "Friedel-Crafts and Related Reactions", Interscience, New York (1964).

132. J. E. Jansen, US Patent, 2,468,982 (1949).

133. A. K. St. Clair, T. L. St. Clair, and E. N. Smith, Am. Chem. Soc. Div. Polym. Chem. Polym. Prepr., 17, 359 (1976).

134. P. N. Rylander, "Catalytic Hydrogenation Over Platinum Metals", Academic Press, New York, 168 (1967).

135. M. E. Rogers and B. A. Averill, J. Org. Chem., 51 (17), 3312 (1986).

136. M. Nakano and Y. Sate, J. Org. Chem., 52, 1844 (1987).

137. A. N. K. Lau and L. P. Vo, PMSE, 66, 24 (1992).

138. V. N. Sekharipuram, G. D. Lyle, and J. E. McGrath, Am. Chem. Soc. Div. Polym. Chem. Polym. Prepr., 34(1), 618 (1993).

139. J. D. Summers et al, Polym. Eng. Sci., 29(20), 1413 (1989).

140. W. B. Alston and R. F. Gratz, "Proceedings from the Second International Conference on Polyimides", Ellenville, New York, 1 (1985).

141. H. D. Burks and T. L. St. Clair in "Polyimides: Synthesis, Characterization, and Applications", K. L. Mittal, editor, Plenum Press, New York, 1, 117 (1984).

142. P. R. Young and N. T. Wakelyn, "Proceedings from the Second International Conference on Polyimides", Ellenville, New York, 414 (1985).

143. J. P. Critchly and M. A. White, J. Polym. Sci., Polym. Chem. Edn., 10, 1809 (1972).

VITA

Heather Brink was born in Syracuse, New York on April 20, 1968 and grew up in upstate New York. During her high school career, she became very interested in chemistry and after graduating third in her class from Victor Central High School in June 1986, she joined the University of Florida to pursue a career in chemistry. She began undergraduate research after her first year at the University of Florida and each summer she participated in research programs at University of Florida (1987), Colgate University (1988), and University of Tennessee (1989). The last year and a half of her undergraduate education, she had the wonderful opportunity to work with Professor K. B. Wagener and investigate thermally reversible covalent crosslinks in polymer systems. Heather graduated with a Bachelor of Science degree from the University of Florida in May 1990 with honors and a thesis option.

Before attending graduate school, the author gained industrial experience during the summer of 1990 where she was an intern at Hoechst Celanese in Charlotte, North Carolina. In August 1990, she entered the PhD program at Virginia Polytechnic Institute & State University where she obtained her doctoral degree in Polymer Chemistry in May 1994. As a graduate student, she presented papers in polymer chemistry at regional and national meetings. She has coauthored six papers and one patent disclosure. In her third year, she was awarded the Department of Defense Augmentation Award for Science and Engineering Fellowship.

On August 8, 1992, she married Andrew Brink in Blacksburg, Virginia. She and her husband will begin work as Advanced Research Chemists at Eastman Chemical Company in Kingsport, Tennessee on June 13, 1994.

Mary Heather Brink